ROLES OF ADHESION G PROTEIN-COUPLED RECEPTORS DURING ZEBRAFISH GASTRULATION AND NEURONAL MIGRATION

By

XIN LI

Dissertation

Submitted to the Faculty of the

Graduate School of Vanderbilt University

in partial fulfillment of the requirements

for the degree of

DOCTOR OF PHILOSOPHY

in

Neuroscience

August, 2013

Nashville, Tennessee

Approved:

Professor Joshua T. Gamse, Chair

Professor Christopher J. Janetopoulos

Professor Heidi E. Hamm

Professor Lilianna Solnica-Krezel, Advisor

ACKNOWLEDGEMENTS

First, I would like to thank my wonderful mentors, Lilianna Solnica-Krezel, Florence Marlow and Heidi Hamm. Lila, you are a true science mom to me (hope you don't mind). You gave me strength when I faced challenges and you made sure for me to shine when there were opportunities. I will take perseverance with me to conquer whatever obstacles I might encounter in the future. Then, Flo, you have to be my science sister (and I have always felt that way in our interactions). Thanks for being such an amazing role model for me. I will always remember to believe in myself as a scientist, mom and whoever I want to become in the future. Heidi, thank you for supporting all my crazy moves and advising me to be patient with science.

I would also like to thank all the members of the Solnica-Krezel and Marlow labs for your help and friendship. My fellow graduate students, Xinxin, Dan, Christina, Haiting, Yinzi, Jade, Phil, Odelya and Meredyth, you are all so talented in science and many other things. I feel so lucky to be among you guys and I'm confident that you will be great success in your career. Adi, and Sophie, thank you for your friendship, encouragements and help! Fang, Simon, Diane, Atsushi and Seok-Hyung, thank you for everything you taught me about research. Isa, we were bonded by our project and the status as new moms. I truly enjoyed the great collaboration we had on our project and I wish you best of luck with the continuation on this wonderful project. Sara, Amy, Heidi and Spartak, thank you for excellent fish care!

My committee, thank you for all the time and support you gave me over the years! Josh, you set such a great example for me to learn how scientist should help each other. Thank you for being such an awesome chair! Chris, I appreciate the efforts you made to participate in my committee while working on gazillions of other things as a young faculty member.

I am also deeply in debt to my moms, dads and grandmas. I'm grateful for my parents-in-law. You are just mom and dad to me as to Mingwei. I appreciate all your love and wisdom. Dad, I hope you are proud of what we have achieved as a family. Mom and dad, thank you so much for your help with Ailin. I know you will always be there when I ask for help. My grandmas, you are so dear to me. I'm so sorry for making you miss me so much.

Finally I would like to acknowledge my sweet husband and our precious daughter. You gave me the most genuine love and you made everything worth it. Mingwei, thank you for infusing me with you great altitude towards food, challenges and dream. We have had quite a spectacular journey and I can't wait to experience with you the road ahead of us. Ailin, my dear, I can't help wondering how your life will be when you are at my age, and I know you will have your real fabulous version of it if you have a dream and a will to reach it.

TABLE OF CONTENTS

LIST OF TABLES

LIST OF FIGURES

LIST OF ABBREVIATIONS

µg	microgram
µl	microliter
µm	micrometer
AP	anterior-posterior
AV	animal-vegetal
Bb	Balbiani body
BMP	Bone Morphogenetic Protein
C&E	convergence and extension
Celsr	Cadherin EGF LAG seven-pass G-type receptor
Cdh	cadherin
D	dorsal
Daam1	Dvl associated activator of morphogenesis 1
DEP domain	Dishevelled, Egl-10 and Pleckstrin domain
DIX domain	Dishevelled and Axin domain
dpf	days post fertilization
DV	dorsal-ventral
Dvl	Dishevelled
FBMN	facial branchiomotor neuron
Fmi	Flamingo
Fz	Frizzled
GDP	guanosine diphosphate

GOF	gain-of-function
GPCR	G protein-coupled receptor
GPS	GPCR proteolysis site
GTP	guanosine triphosphate
GFP	green fluorescence protein
hpf	hours post fertilization
Kny	Knypek
LOF	loss-of-function
LWR	length-to-width ratio
ML	mediolateral
MLC	Myosin light chain
MO	morpholino oligonucleotides
MZ	maternal-zygotic
ng	nanogram
Papc	Protocadherin
PBS	phosphate buffered saline
PCP	planar cell polarity
PDZBM	PDZ-biding motif
PDZ domain	PSD95, Dishevelled and ZO-1 domain
PGC	primordial germ cell
Pk	Prickle
r	rhombomere
RFP	red fluorescent protein

RT-PCR	reverse transcription-polymerase chain reaction
Ryk	Receptor tyrosine related protein
Scrb1	Scribble 1
Tri	Trilobite
WT	wild-type
V	ventral
Vang	Van gogh
Syn4	Syndecan-4

CHAPTER I

INTRODUCTION

Gastrulation is the first morphogenetic event occurring during animal embryonic development. During gastrulation the three germ layers, ectoderm, mesoderm and endoderm, form, the body axes are established, and the organ rudiments are positioned along the body axes. These defining features of gastrulation are achieved through a combination of patterning events and morphogenetic movements that transform a radially symmetric blastula into a polarized gastrula with defined anterior-posterior (AP), and dorsal-ventral (DV) axes. AP axis lies along the animal-vegetal (AV) axis, which is specified during oogenesis and marks the first polarity of the future embryo. In oocytes, the transiently present Balbiani body (Bb) is the earliest indicator of the AV axis (Figure 1A). The Bb forms adjacent to the nucleus as a collection of organelles including mitochondria and endoplasmic reticulum membranes, proteins and RNAs. It subsequently translocates to the vegetal pole, delivers its cargo and disperses. The molecular mechanisms underlying AV axis formation and its relationship to the Bb are largely unknown (Marlow 2010).

The mature zebrafish oocyte is radially symmetric about the animal-vegetal axis, and no DV asymmetry is evident prior to fertilization. In amphibian and zebrafish, the Canonical Wnt pathway plays a pivotal role in dorsal specification (De Robertis 2006; De Robertis & Kuroda 2004; Schier & Talbot

2005). Dorsal determinants such as the transcript of Wnt8a, the ligand of the canonical Wnt pathway, and RNAs encoding its transporting machinery such as Syntabulin localize to the Bb and are transported during oogenesis to the vegetal pole (Lu et al 2011; Nojima et al 2010). Subsequently, they move along the microtubule array to the prospective dorsal side where they activate the canonical Wnt pathway (Figure 1B) (Lu et al 2011; Nojima et al 2010). Activation of the canonical Wnt pathway at the dorsal side of the embryo is demarcated by β-catenin accumulation in nuclei of blastomeres close to the blastoderm-yolk margin as early as the 128-cell stage and later in the nuclei of the yolk syncytial layer after its formation at 500-1,000 cell stage (Figure 1C) (Lu et al 2011; Schneider et al 1996). Upon initiation of zygotic transcription at the mid-blastula transition (1000-cell stage; 3 hours post fertilization, hpf), β-catenin activates the transcription of genes whose protein products antagonize the action of ventralizing Bone Morphogenetic Protein (BMP) secreted factors or repress their expression on the dorsal side (Gonzalez et al 2000; Goutel et al 2000; Langdon & Mullins 2011; Little & Mullins 2006; Marlow 2010; Reim & Brand 2006; Schier & Talbot 2005).

At late blastula stage, the progenitors of the three germ layers are specified in the blastoderm along the AV axis, with ectodermal progenitors located within the first several tiers from the animal pole, endodermal progenitors in the marginal tier right above the yolk and mesodermal progenitors intermingled with endodermal progenitors in the marginal tier and tiers next to the margin (Figure 1D). Members of the Nodal family of TGFβ signals play essential roles in

mesoendodermal induction and patterning (Schier & Talbot 2005). Both Nodal ligands Cyclops (Cyc) and Squint (Sqt) are expressed in the first three tiers of blastomeres at the margin and Sqt is also expressed in the yolk syncytial layer (Erter et al 1998; Feldman et al 1998). Cyc acts locally while the morphogen Sqt can travel efficiently to induce mesoendodermal cell fates at a distance from the source and in a concentration dependent manner (Chen & Schier 2001; Muller et al 2012). The extent of Nodal signaling is refined by the expression of their feedback antagonists, including Lefty1 & 2, to ensure proper induction of progenitors giving rise to the future three germ layers (Chen & Schier 2002; Feldman et al 2002; Muller et al 2012). Despite these significant inductive events that specify embryonic axes and germ layers during blastula stages, the embryo remains as a semi-sphere of morphologically indistinguishable blastomeres sitting on top of the yolk.

During gastrulation, embryonic cells engage in concerted morphogenetic movements to generate morphologically evident DV and AP body axes and to place organ progenitors at specific DV and AP positions. Gastrulation movements include epiboly, internalization, convergence and extension (Figure 1D-F) (Roszko et al 2009; Solnica-Krezel 2005; Yin et al 2009). In zebrafish, epiboly starts at the late blastula stage (*i.e.* after 4 hpf). It is characterized by the spreading of cells over the yolk, and movement of the yolk syncytial nuclei within the yolk cell, from the animal pole towards the vegetal pole (Figure 1D and E). Epiboly proceeds until the yolk cell is entirely engulfed by the embryonic cells. At 5.25 hpf, endodermal and then mesodermal progenitor cells at the blastoderm

margin begin to internalize via synchronized ingression of individual cells,creating a ring-like structure around the equator of the embryos, known as the germ ring (Figure 1D). Internalization marks the onset of the gastrula period. Cells that are

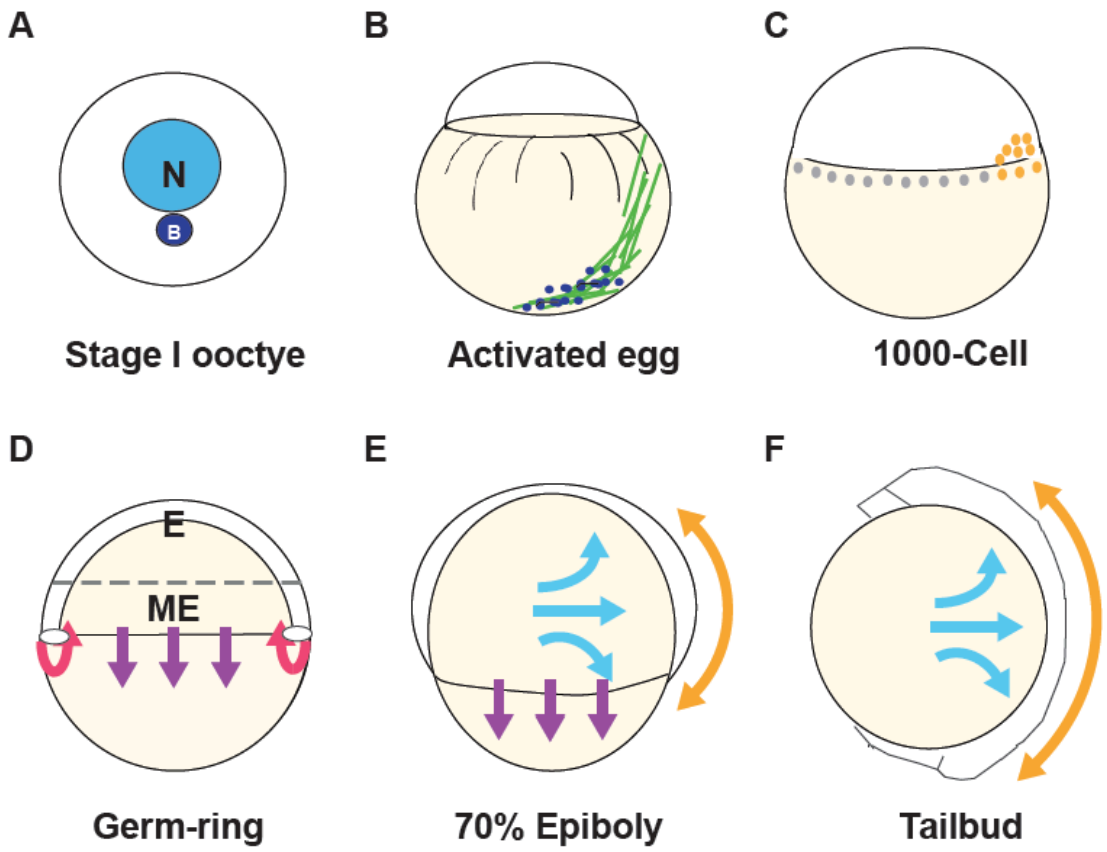

Figure 1. Stages of zebrafish oogenesis and early embryogenesis. Animal pole up. Lateral views in (B-F), dorsal right. Blue dots in (B) represent dorsal determinant and green lines represent microtubule network. Orange dots in (C) represent nuclear β-Catenin and grey dots represent yolk syncytial layer nuclei. Purple arrows in (D) and (E) mark epiboly, magenta arrows in (D) mark internalization, blue arrows in (E) and (F) mark convergence, and orange arrows in (E) and (F) mark extension movements. N, nucleus; B, Balbiani body; E, ectoderm; ME, mesoendoderm.

not internalized form the definitive ectoderm. Convergence movements are characterized as the dorsal-ward movement of cells from lateral positions, resulting in DV, or mediolateral (ML) narrowing of all germ layers (Figure 1E and F). Convergence starts locally in the dorsal, thick portion of the germ ring known as the embryonic shield, the zebrafish equivalent of the Spemann-Mangold dorsal gastrula organizer. Subsequently, convergence spreads to lateral regions and causes the embryo to narrow mediolaterally (Figure 1E and F) (Sepich & Solnica-Krezel 2005). Cells in the ventral-most gastrula region do not engage in convergence. Instead they undergo epibolic migration towards the vegetal pole, where they contribute to tail morphogenesis (Myers et al 2002a). As cells show bias towards dorsal or vegetal, depending on their AP location, during dorsal-ward migration the converging cell population fans out anterio-posteriorly, which contributes to the lengthening of the tissue (extension) (Figure 1D) (Sepich et al 2005). When cells approach the dorsal side of the embryo, they undergo dramatic changes in behaviors and engage in polarized cell intercalations that drive efficient convergence and extension movements to elongate the embryo anterio-posteriorly (Figure 1F). The gastrula period ends when the embryonic tissue covers the entire yolk, marking 100% epiboly. However, extensive C&E movements persist into segmentation stages (Gonzalez et al 2000; Little & Mullins 2006; Schier & Talbot 2005; Solnica-Krezel 2005; Westerfield 2000).

A remarkable feature of gastrulation is that cells are concurrently undergoing complex morphogenetic movements as their fates are being specified, which raises the question of how these seemingly distinct processes

are integrated within individual cells and coordinated throughout the whole embryo. Interestingly, in the last decade the major morphogens that pattern the embryo have been discovered to simultaneously instruct cell fate specification and control cell movements during gastrulation (Branford & Yost 2002; Carmany-Rampey & Schier 2001; Ciruna & Rossant 2001; Feldman et al 2002; Myers et al 2002b; von der Hardt et al 2007). It was recently discovered that BMP signaling specifies cell fates in an anterior-to-posterior sequence. Cell fates in the anterior region are specified at the onset of gastrulation, whereas those in more caudal region are patterned at progressively later stages during gastrulation (Tucker et al 2008). In parallel to instructing cell fates during gastrulation, the ventral to dorsal BMP gradient regulates cell movements, limiting convergence and extension movements to dorsolateral gastrula regions (Myers et al 2002a; von der Hardt et al 2007).

Gastrulation is highly conserved across vertebrate species, including humans. In human embryos, gastrulation occurs during the third and fourth weeks of gestation. As is the case for zebrafish gastrulation, this evolutionarily conserved morphogenetic process also produces the three germ layers, establishes the body axes, AP, DV, and left–right, and specifies the cell fates of various organs such as the brain and eye anlagen of the human embryo (Sadler 2010). During the gastrula period, embryos are highly sensitive to teratogenic insults. For example, high doses of alcohol during this stage can kill cells in the anterior midline of the germ disc, producing a deficiency of midline cells that normally give rise to craniofacial structures resulting in holoprosencephaly

(Cohen & Shiota 2002). Children with viable forms of holoprosencephaly, have a small forebrain, medially merged lateral ventricles, and eyes that are close together. Mutations or functional disruption of genes with critical functions during gastrulation could thus lead to similar devastating consequences to the developing embryo. On the other hand, disruption of genes regulating posterior mesoderm formation during gastrulation cause caudal dysgenesis (Sadler 2010). Because caudal mesoderm contributes to the formation of the lower limbs, urogenital system and lumbosacral vertebrae, affected individuals exhibit a variable range of defects, including hypoplasia and fusion of the lower limbs, vertebral abnormalities, renal agenesis, imperforate anus, and anomalies of the genital organs. In addition, abnormal function of genes regulating establishment of the left-right axis results in *situs inversus*, a condition in which the major visceral organs are reversed from left to right as a mirror image of the normal condition, or *situs ambiguous*, which is the randomization of the organs with respect to their normal positions (Levin 2004). The abnormal persistence of primitive streak in the sacrococcygeal region or abnormal migration of primordial germ cells during gastrulation can also cause tumor growth in children (Rescorla 2012). Sacrococcygeal teratomas, which commonly contain tissues derived from all three germ layers are the most common tumors diagnosed in newborns, occurring with a frequency of one in 37,000 (Sadler 2010). As gastrulation is critical for normal vertebrate embryonic development, including humans, studying the conserved cell behaviors and signaling pathways regulating gastrulation shall greatly aid our understanding about normal gastrulation process and developing

preventive and therapeutic innovations to treat gastrulation-related congenital anomalies in humans.

Cell behaviors driving gastrulation movements and their underlying molecular mechanisms

At the cellular level, epiboly is the result of intense radial intercalation of cells positioned in deeper regions into more superficial layers, resulting in a thinning and spreading of the embryonic tissue over the yolk (Figure 2A) (Solnica-Krezel & Driever 1994; Warga & Kimmel 1990). The bias of intercalation towards superficial layers has been attributed to the differential adhesion properties between cell layers based on the studies of E-cadherin or Cadherin 1 (Cdh1) function during zebrafish gastrulation (Kane et al 1996; Kane et al 2005). Kane et al. reported a gradual increase of *cdh1* transcript levels progressing from deep to superficial layers of zebrafish gastrula at the shield stage. They reasoned that higher E-cadherin/Cdh1 levels were required to maintain cells in the exterior layer after radial intercalation, since in *half baked/E-cadherin/cdh1* mutant embryos, the rate of radial intercalation was not changed, but cells were more likely to fall back into deeper layers after intercalation (Kane et al 2005). By contrast, Montero et al. argued that embryos, injected with *E-cadherin/cdh1* antisense morpholino oligonucleotides (MO) to block E-cadherin/Cdh1 function, had reduced radial intercalation at 65% epiboly (Montero et al 2005). Although these two reports fail to reach a unified conclusion, they both suggest that an E-cadherin/Cdh1 gradient could provide directionality for biased cell

rearrangement. Furthermore, the heterotrimeric G proteins, $G_{12/13,}$ have been reported to regulate epiboly by binding to the intracellular domain of E-cadherin/Cdh1 and inhibiting its activity in mediating adhesion (Lin et al 2008). Another cadherin-repeat containing protein family, the Celsr (Cadherin EGF LAG seven-pass G-type receptors, vertebrate homologues of *Drosophila* Flamingo ,Fmi) adhesion GPCRs have also been shown to contribute to epiboly (Carreira-Barbosa et al 2009). Interestingly, although Celsr/Fmi proteins are better known as core components of the planar cell polarity (PCP) pathway, these molecules are thought to regulate epiboly independent of the PCP pathway. Instead, Celsrs are predicted to function in epiboly as modulators of cellular adhesion via homophilic interaction (Carreira-Barbosa et al 2009).

At the beginning of the gastrula period, mesoendodermal precursors at the blastoderm margin internalize and migrate beneath the surface ectodermal cells towards the animal pole (Figure 1C) (Sepich et al 2005). The tight association between internalization and induction of mesoendoderm is evident in embryos lacking Nodal signaling in which this movement is blocked and mesoendodermal cells are largely absent. Conversely, in embryos with elevated Nodal signaling, internalization is prolonged and mesoendoderm is expanded (Carmany-Rampey & Schier 2001; Feldman et al 2002; Feldman et al 2000). Synchronized ingression from exterior to interior positions as individual cells is likely the mechanism cells employ during internalization (Fig. 1.2 B) (Adams & Kimmel 2004; Carmany-Rampey & Schier 2001; Keller et al 2008; Montero et al 2005; Schier & Talbot 2005). Signal transducer and activator of transcription 3 (Stat3)

plays an important role during gastrulation. Beside its non-cell autonomous role in regulating C&E of the lateral mesoderm, Stat3 regulates the anterior migration of gastrula organizer cells cell-autonomously by activating its downstream target Liv1. The activation of Liv1 is essential for the nuclear localization of the zinc-finger protein Snail, an evolutionarily conserved negative regulator of *E-cadherin /cdh1* gene transcription and consequently of cell delamination and directed migration (Barrallo-Gimeno & Nieto 2005; Yamashita et al 2002; Yamashita et al 2004). Snail1 can also be stabilized by Prostaglandin E(2) (PGE2) signal and consequently negatively regulates *E-cadherin/Cdh1* transcript abundance (Speirs et al). PGE2 also regulates E-Cadherin/Cdh1 protein levels independent of Snail by an unknown mechanism. Together, regulation of E-Cadherin/Cdh1 RNA and protein enable the precise and rapid regulation of cell adhesion that is required for the dynamic cell behaviors driving various gastrulation movements, including internalization (Speirs et al).

While epiboly and the directed migration of internalized cells toward the animal pole help to spread the cells along the AP axis, C&E serves as the main mechanism to narrow the embryo from back to belly and lengthen it from head to tail. Although precursors of all three germ layers participate in C&E, the specific cell behaviors utilized by cells within each germ layer and in different regions of the gastrula can vary (Concha & Adams 1998; Nair & Schilling 2008; Pezeron et al 2008; Yin et al 2009). For mesoderm in particular, cells in distinct DV zones adopt different behaviors to accomplish C&E (Jessen et al 2002; Myers et al 2002a; Solnica-Krezel 2006; Yin et al 2009). Cells in a 20-30° arc of the ventral

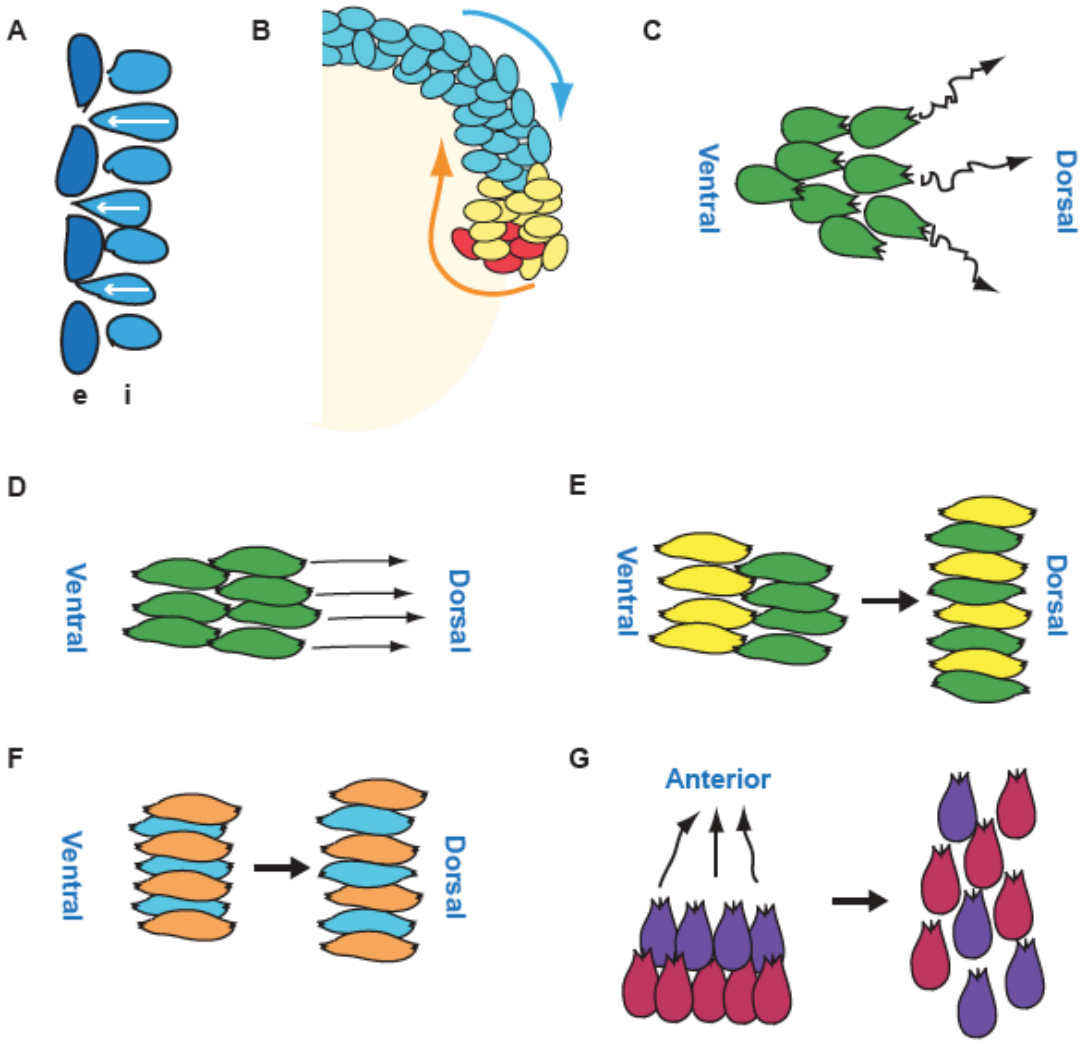

Figure 2. Cell behaviors driving zebrafish gastrulation movements. (A) Polarized radial intercalation from interior (i) layers to exterior (e) layers driving epiboly movement. (B) Ingression of cells at the marginal layers resulting in internalization of mesoendoderm, whereas ectoderm cells do not undergo internalization, but engage in epiboly. Red, endodermal cells; yellow, mesodermal cells; and blue, ectodermal cells. Orange arrow represents the trajectory of internalized cells and blue arrow depicts epibolic movements. (C) Slow dorsal-directed migration. (D) Fast dorsal-directed migration. (E) Mediolateral intercalation. (F) Anterior-posterior-directed radial intercalation. (G) Anterior-directed migration.

margin constitute the no convergence no extension zone. Upon internalization, they initially spread over the yolk and later move toward the vegetal pole (Myers et al 2002a). In the lateral mesoderm, dorsally directed cell migration is the main behavior contributing to C&E. At midgastrulation or around 70% epiboly (7.7hpf), these laterally localized cells start to migrate in a dorsal direction with either an animal or vegetal bias according to their position along the AP axis. They often change directions and thereby the net dorsal speed is very slow (Figure 2C). This fanning out effect leads to modest net C&E movements (Sepich et al 2005). At late gastrulation, the lateral mesodermal cells approaching the midline become mediolaterally elongated and undergo dorsal migration along straight paths, achieving a high net speed (Jessen et al 2002; Marlow et al 2002) and therefore fast convergence (Figure 2D). In the medial presomitic mesoderm, adjacent to the midline, cells become highly elongated, align parallel to the ML equator and intercalate preferentially in this direction to lengthen the embryo anterio-posteriorly (Figure 2E) (Jessen et al 2002; Marlow et al 2002; Schier & Talbot 2005; Solnica-Krezel 2006; Topczewski et al 2001). In addition, polarized radial intercalation of cells preferentially separating anterior and posterior neighboring cells in the paraxial mesoderm also contributes to lengthening of the embryo (Yin et al 2008) (Figure 2F). In the axial mesoderm, the prechordal plate precursors migrate directly toward the animal pole, contributing to anterior extension of the axial tissue (Figure 2G) (Heisenberg et al 2000; Yamashita et al 2002; Yamashita et al 2004). In contrast, cells from the trunk axial mesoderm are mediolaterally elongated and aligned and undergo mediolateral intercalation, resulting in

modest convergence and rapid extension (Figure 2E) (Glickman et al 2003; Lin et al 2005; Warga & Kimmel 1990).

C&E movements are highly coordinated along the embryonic axes. To achieve such highly ordered large-scale directed cell movements, cells likely rely on mechanisms, such as direct contacts with their neighbors and other extracellular cues, as they move according to their coordinates with respect to the DV and AP axes. Gradients formed by differential adhesion or secreted extracellular cues have been widely used in biological processes to fulfill such requirements and these mechanisms have also been proposed to instruct C&E movements. (Rohde & Heisenberg 2007; Sepich et al 2005; Solnica-Krezel 2006; Yin et al 2009). How differential adhesion might contribute to C&E is evident from studies of BMP signaling during gastrulation. Specifically, BMP signaling was proposed to regulate C&E movements by negatively regulating adhesion through a mechanism independent from its role in fate specification (Myers et al 2002a; von der Hardt et al 2007). Since BMP signaling forms an activity gradient that declines from the ventral to dorsal gastrula regions, it was hypothesized that a reciprocal increase in cell adhesion from ventral to dorsal regions mediates convergence of lateral mesodermal cells. On the other hand, cells could be attracted by a gradient formed by a secreted signal from the dorsal region of the embryo. However, these potential mechanisms are not mutually exclusive. An intriguing line of evidence supporting the existence of a molecule(s) secreted from the dorsal midline comes from the identification of Stat3 as a C&E regulator. Activation of Stat3 in the dorsal gastrula region has been hypothesized to

activate transcription of a secreted factor(s), which non-cell autonomously regulates convergence of lateral mesoderm cells (Miyagi et al 2004; Yamashita et al 2002). However, so far, the hypothetical secreted factor(s) has not been identified. Through forward genetic approaches and other functional analyses, components of the Wnt/planar cell polarity (PCP) pathway have been uncovered as regulators of C&E movements, rendering the Wnt/PCP pathway the best studied pathway regulating C&E movements in all vertebrates from fish to mammals (Gray et al 2011; Tada & Kai 2009; Yin et al 2009). The contribution of this and other signaling pathways to C&E will be discussed in detail in the following sections.

PCP signaling regulates C&E movements

The vertebrate Wnt/PCP pathway is the equivalent of the *Drosophila* PCP pathway, which orients structures such as wing hairs and ommatidia in the plane of epithelia (Adler et al 1997; Feiguin et al 2001; Krasnow & Adler 1994; Krasnow et al 1995; Simons & Mlodzik 2008; Strutt 2001; Strutt et al 1997; Usui et al 1999). As suggested by its name, the PCP pathway mainly regulates polarized features across the plane of tissues, which in epithelial tissues is perpendicular to the apico-basal axis of the cells comprising the tissue. However, in vertebrates, Wnt/PCP pathway dependent processes are not restricted to epithelial tissues (Goodrich & Strutt 2011; Gray et al 2011). As an example, during gastrulation, Wnt/PCP pathway regulates planar polarity of mesenchymal cell populations (Gray et al 2011; Roszko et al 2009; Tada & Kai 2009).

In zebrafish, the Wnt/PCP pathway is required for C&E gastrulation movements, caudal migration of facial branchiomotor neurons (FBMNs) and polarized distribution of the microtubule organizing center and cilia (Borovina et al ; Roszko et al 2009; Sepich et al 2011; Tada & Kai 2009; Wada & Okamoto 2009). The vertebrate Wnt/PCP pathway is composed of extracellular ligands, *i.e.* Wnts, membrane and intracellular components (Figure 3) (Gray et al 2011; Roszko et al 2009; Tada & Kai 2009). A hallmark of genes controlling planar cell polarity is that both loss and gain of their activity cause similar cell polarity defects and impair processes such as C&E that depend on polarized cell behaviors (Bastock et al 2003; Carreira-Barbosa et al 2009; Heisenberg et al 2000; Jessen et al 2002; Krasnow & Adler 1994; Krasnow et al 1995; Marlow et al 2002; Usui et al 1999). In the process of zebrafish C&E movements, Wnt5 and Wnt11 are the key ligands as both gain- and loss-of-function (LOF and GOF) of these Wnts lead to C&E defects. They likely function in a partially redundant fashion in regulating zebrafish C&E movements (Heisenberg et al 2000; Kilian et al 2003). In *Drosophila* the core PCP membrane components include the receptor Frizzled (Fz), and four-pass transmembrane protein Van gogh (Vang) /Strabismus and another seven-pass transmembrane protocadherin Flamingo (Fmi)/Starry Night. The current view is that the activity of Fz receptor determines PCP pathway activity, but the molecular mechanism of Fz activation in this process remains unclear (Goodrich & Strutt 2011). Aggregation experiments in S2 cells as well as cultured zebrafish embryonic cells suggest that Fmi can

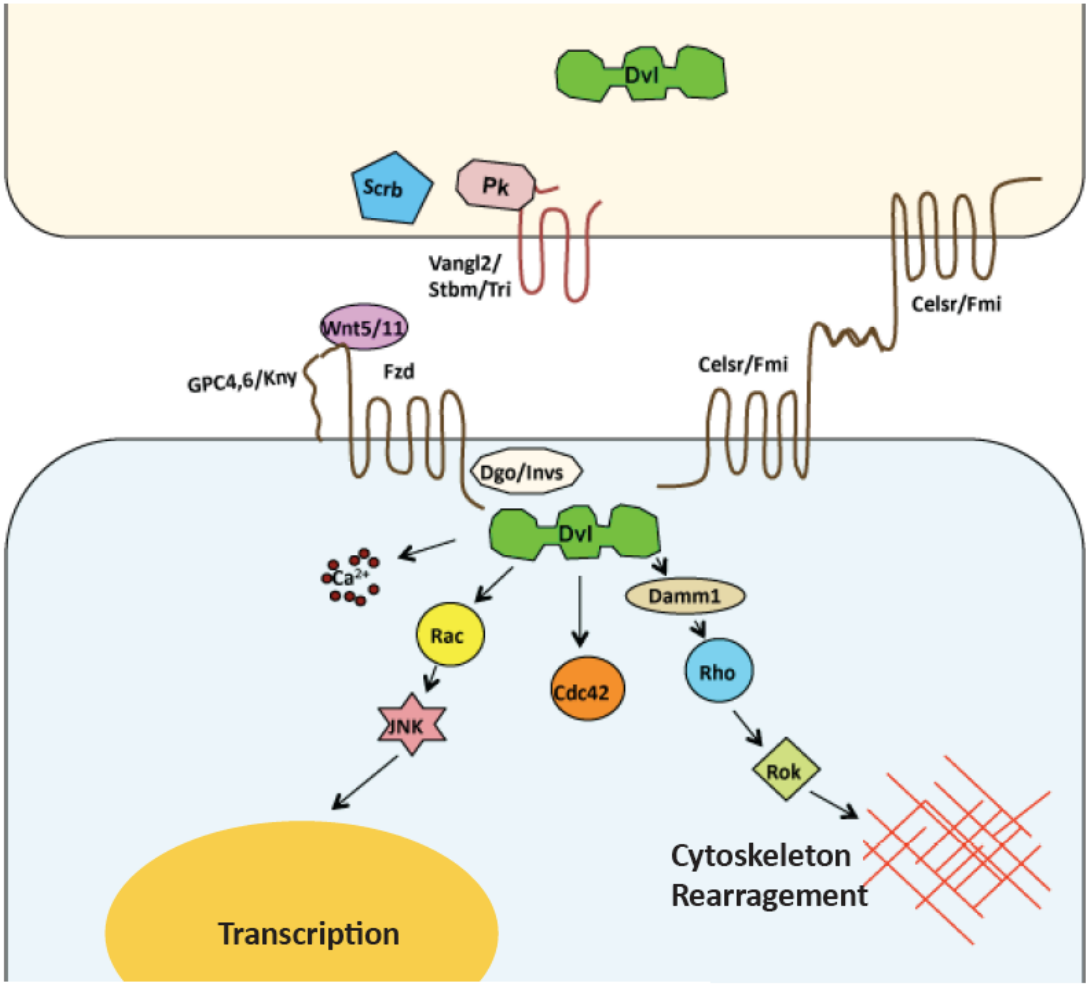

Figure 1.3. Simplified vertebrate Wnt/PCP pathway.

interact homophilically via its extracellular cadherin repeats (Carreira-Barbosa et al 2009; Usui et al 1999). In addition, it has also been hypothesized to interact with Fz and Vang to form asymmetric complexes on juxtaposed cell membranes (Strutt et al 2011). The functions of these three proteins are conserved in vertebrates, as multiple vertebrate homologues, Fz2 and Fz7, Trilobite/Vang gogh-like 2 (Tri/Vangl2) and Celsr1a, 1b and 2 (Vertebrate homologues of Fmi) have been shown to function during C&E (Carreira-Barbosa et al 2009; Formstone & Mason 2005; Jessen et al 2002; Kilian et al 2003; Park & Moon 2002). Interestingly, vertebrate PCP signaling employs additional factors, including membrane-associated proteins to modulate C&E. A role for the GPI-anchored extracellular heparan sulfate proteoglycan Knypek/Glypican4 (Kny/Gpc4) in potentiating Wnt/PCP signaling has been identified in zebrafish mutagenesis screens (Topczewski et al 2001). In addition, a receptor related to tyrosine kinase (Ryk) has been proposed to function downstream of Wnt5b to provide directionality to cells undergoing C&E (Lin et al). However, other studies do not support an instructive role for Wnt/PCP signaling in directing dorsal migration (reviewed in (Gray et al 2011)). In *Xenopus*, the cell-surface transmembrane heparan sulfate proteoglycan xSyndecan-4 interacts functionally and biochemically with Fz7 and Dishevelled (Dvl). It can recruit Dvl to the membrane upon binding to Fibronectin (Munoz et al 2006).

Upon binding to Wnt, Fz recruits Dvl, the intracellular signal transducer of Wnt/PCP signaling, to the cell membrane. Dvl membrane translocation is thought to be a prerequisite for the activation of PCP signaling (Wallingford et al 2000).

Three functional domains have been defined in Dvl, the N-terminal DIX (Dishevelled and Axin) domain, the middle PDZ (PSD95, Dishevelled and ZO-1) domain and the C-terminal DEP (Dishevelled, Egl-10 and Pleckstrin) domain (Gao & Chen). DIX is not required for PCP signaling, as a N-terminally truncated Dvl, which lacks the DIX domain, can suppress the defects resulting from disruption of Wnt11 function in both zebrafish and *Xenopus* (Heisenberg et al 2000; Tada & Smith 2000). In contrast, both PDZ and DEP domains are required for PCP signaling (Pan et al 2004; Sokol 1996; Wallingford et al 2000). Besides Dvl, Diego (Diversin and Inversin in vertebrates) and Prickle (Pk) are two additional cytoplasmic core PCP components (Simons & Mlodzik 2008) and their conserved function in vertebrates has been confirmed in a number of studies (Carreira-Barbosa et al 2003; Moeller et al 2006; Simons et al 2005). Prickle forms a complex with Vang, whereas Diego interacts with Fz and Fmi (Feiguin et al 2001; Jenny et al 2003a). Interestingly, Diego, Vang and Prickle can all interact with Dvl. Moreover, Prickle competes with Diego for Dvl binding, likely promoting Dvl degradation (Carreira-Barbosa et al 2003; Jenny et al 2005). Additional cytoplasmic proteins have also been reported to interact with Dvl. Casein kinase alpha and I epsilon positively regulate planar cell polarity via Dvl phosphorylation (Klein et al 2006). An essential function of Protein kinase C δ for Dvl membrane translocation and function in Wnt/PCP signaling has been demonstrated during *Xenopus* convergent extension movements (Kinoshita et al 2003).

As the molecular hub of the Wnt/PCP pathway, Dvl mediates PCP

signaling by activating multiple small GTPases, which cycle between their inactive GDP-bound and active GTP-bound form to regulate diverse cellular processes including cytoskeletal rearrangement, cell adhesion and transcription (Hall & Nobes 2000; Kaibuchi et al 1999; Van Aelst & Symons 2002). Rho and its downstream kinase Rok/Rock are well characterized downstream effectors of Dvl in multiple model systems (Habas et al 2001; Marlow et al 2002; Nishimura et al 2012; Winter et al 2001; Zhu et al 2006). In zebrafish, interference with RhoA or Rok/Rock functions lead to C&E defects and moderate overexpression of these proteins is able to suppress the defects in *slb/wnt11* or *pipetail/wnt5* mutants (Marlow et al 2002; Zhu et al 2006). In *Xenopus* and recently in mouse, Dvl associated activator of morphogenesis 1 (Daam1), a Formin homology protein, has been shown to mediate RhoA pathway activation downstream of Fz and Dvl (Habas et al 2001; Nishimura et al 2012). Activated Rok can activate myosin light chain (MLC) via phosphorylation and activated MLC has been implicated in the contraction of various actin-based structures (Hartman et al 2011). Dvl can also form a Wnt-induced complex with Rac, another regulator of the cytoskeleton, via its DEP domain. Moreover, a truncated Dvl with only its DEP domain can activate C-Jun kinase (JNK) through Rac (Habas et al 2003). Consistently, depletion or inhibition of Rac as well as JNK perturbs *Xenopus* gastrulation (Habas et al 2003; Yamanaka et al 2002). JNK, once activated by Cdc42, has been reported to promote expression of paraxial protocadherin (PAPC) (Schambony & Wedlich 2007). In another study, Cdc42 was shown to regulate cell adhesion during

Xenopus gastrulation (Choi & Han 2002). In summary, the core PCP components identified in *Drosophila* are conserved in vertebrates, where they regulate C&E gastrulation movements along with additional vertebrate specific Wnt/PCP pathway components.

Polarized distribution of PCP components

Asymmetric localization of subsets of PCP pathway components to opposing cell membranes correlates with planar polarity of the tissues in both *Drosophila* and in vertebrates. However, whether this is a cause or consequence of cell polarization and the functional significance of these polarized localization patterns remains unsettled. Adult fly wing is composed of two layers of hexagonally shaped epithelial cells, which are positioned in parallel with two vertices pointing in the proximal-distal direction. Wing hairs are assembled at the distal-most cell vertex and grow distally, demarcating the planar asymmetry of the epithelia (Figure 4A). Prior to this asymmetrical hair growth, Fz together with Dsh (Dvl in vertebrates) and Diego localize to the distal, whereas Vang/Strabismus and Prickle localize to the proximal membrane of cells in (Figure 4B) (Goodrich & Strutt 2011; Gray et al 2011). Significantly, stereotyped asymmetric localization of Pk and Dvl on the respective anterior and posterior membranes has also been observed in neural keel and dorsal mesodermal cells undergoing C&E in zebrafish (Ciruna et al 2006; Yin et al 2008) (Figure 4D), and in the cells of the organs that generate the left-right asymmetry, *i.e.* the gastrocoel roof plate in *Xenopus* and the node in mouse (Antic et al 2010).

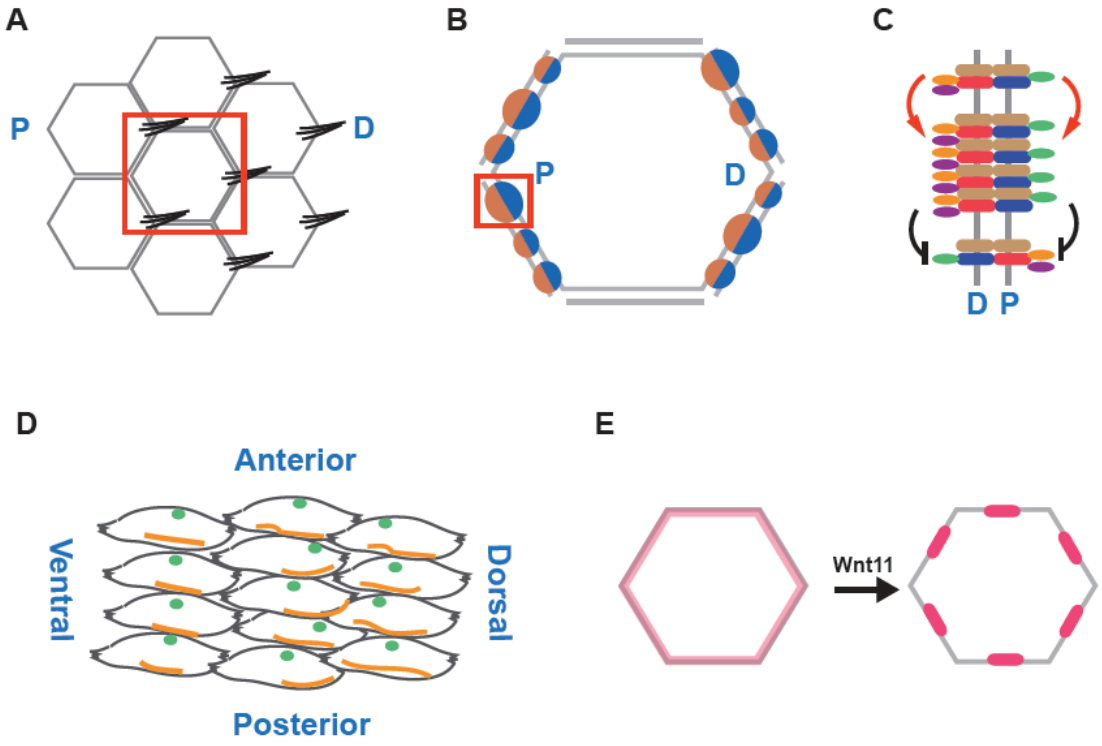

Figure 4. Polarized distribution of PCP components in *Drosophila* and zebrafish. (A) A portion of *Drosophila* wing epithelia with wing hair pointing toward the distal tip of the wing. P, proximal; D, distal. (B) The enlarged view of boxed area in (A). Orange colored hemispheres represent the distal PCP supramolecular complex and blue colored hemispheres represent the proximal PCP supramolecular complex. (C) The enlarged view of boxed area in (B). Fmi in light brown, Fz in brown, Stbm in Blue, Dsh in green, Dgo in purple and Pk in light purple. Red arrows indicate recruitment and black blunted arrows indicate exclusion. (D) A portion of the dorsal mesoderm of zebrafish gastrula. Pk dots in light purple are preferentially localized anterior edges and Dvl patches in green in the posterior edges of the cells. (E) Wnt11 induces the accumulation of Fzd7 and Dvl complexes (together in magenta) into membrane patches in later blastula stage zebrafish embryos.

Asymmetric localization of PCP components in polarized *Drosophila* epithelia and protein interaction studies supports a model whereby PCP components interact in asymmetric membrane complexes spanning the juxtaposed cells to generate planar polarization (Goodrich & Strutt 2011; McNeill 2010). Intriguingly, core PCP components have been observed to localize to discrete domains (puncta) on or close to the membrane in flies and zebrafish (Ciruna et al 2006; Strutt & Strutt 2008; Yin et al 2008). In *Drosophila* pupal wing epithelia, these puncta are regarded as stable asymmetric junctional complexes, thought to possibly protect PCP components from rapid endocytic trafficking and degradation. Together with directional trafficking of PCP components along apically localized microtubules (Shimada et al 2006), the stable junctional complexes are thought to mediate establishment of planar cellular asymmetry (Strutt & Strutt 2008). In addition, a recent study in the fly wing revealed that membrane and cytoplasmic core PCP components play different roles in the formation of these membrane puncta. Whereas the transmembrane core proteins, Fz, Fmi and Vang, are required to localize core proteins to junctions, the cytoplasmic core proteins are essential for clustering localized proteins into prominent membrane puncta (Figure 4C) (Strutt et al 2011). In zebrafish, Witzel et al adapted an “animal cap assay” originally developed in *Xenopus* to visualize PCP pathway components in a simple cellular context that does not manifest inherent planar polarization (Green 1999; Park & Moon 2002). Witzel and colleagues injected fusion constructs encoding Wnt11, Fz7 and Dvl into one-cell–stage embryos and analyzed the localization of the proteins in animal-pole

blastoderm cells at late blastula stages (30% epiboly; 4.5 hpf) (Witzel et al 2006). They found that in the absence of Wnt11, Fz7-YFP localizes uniformly at the plasma membrane and to cytoplasmic aggregates or “puncta”, while in the presence of low amounts of Wnt11, Fz-YFP accumulates as patches on the plasma membrane. Utilizing a transplantation approach, they went on to show that the ability of Wnt11 to induce Fz accumulation involves both cell autonomous and non-cell autonomous activities. Even more intriguing was the location of Dvl in this context, as Dvl translocation to the membrane is essential for PCP pathway activation. When coexpressed with Fz7, Dvl-YFP localized uniformly to the plasma membrane. However, when Dvl-CFP was coexpressed with Fz7-YFP and Wnt11, it colocalized with Fz7-YFP at the resulting membrane accumulations (Figure 4E) (Witzel et al 2006). These studies support the notion that the formation of PCP component membrane puncta might reflect the activation of this pathway. Furthermore, *Xenopus* Vangl2 and *Drosophila* Prickle have been observed in patch-like subdomains on the membrane when co-expressed in frog animal cap (Jenny et al 2003a). These observations elicit questions regarding how membrane puncta are assembled and whether they play a significant role during C&E movements and other PCP dependent processes in vertebrates.

PCP signaling and polarized cytoskeletal organization

One of the major outcomes of PCP signaling is the polarized rearrangement of cytoskeletal structures. In *Drosophila*, Fz localized on the distal

membrane of the wing epithelial cells directs the accumulation of actin at the distal cell vertex where microtubules are also densely distributed. Actin filaments and microtubules then elongate distally to form the trichome (wing hair) (Eaton et al 1996; Strutt 2001). In vertebrates, Celsr1 has recently been reported to concentrate in the medial hinge point of the chick neural plate, a region densely populated with adherens junctions along the mediolateral axes of the neural plate. At these adherens junctions, Celsr1 cooperates with Dvl, DAAM1, and the PDZ-RhoGEF to upregulate Rho kinase activity, causing actomyosin-dependent contraction in a planar-polarized manner. This planar-polarized contraction promotes simultaneous apical constriction and midline convergence of neuroepithelial cells (Nishimura et al 2012). In the case of C&E movements, posteriorly or laterally biased orientation of microtubule organizing centers has been reported at late gastrulation and depends on PCP signaling components, including Kny/Gpc4 and Dvl (Sepich et al 2011). In contrast, polarized distribution of the actin cytoskeleton has not been reported. One major obstacle to study actin cytoskeleton in cells undergoing C&E is that in contrast to the relatively stationary wing or neural epithelial cells, these mesenchymal cells are highly motile and often change neighbors. Therefore the changes of actin cytoskeleton are likely highly dynamic and difficult to track. Tools that allow simultaneous recording of the dynamic changes of cytoskeleton and cell position in live embryos will aid our understanding of this process. Kim et al. investigated the contribution of F-actin dynamics to convergent extension movements by using

Actin binding domain of Meosin tagged GFP as a reporter for F-actin localization live cells. Their study revealed that punctuated actin contractions within converging and extending mesoderm and uncovered a permissive role for non-canonical Wnt-signaling, myosin contractility and F-actin polymerization in regulating these dynamics (Kim & Davidson 2011). Indirectly, cell shape and orientation of the cell body, and protrusive activities have been used as readouts of changes of membrane properties and/or cytoskeleton of mesodermal cells undergoing C&E. During gastrulation, mesoendodermal cells migrate using a combination of different types of protrusions, e.g. membrane blebbing, lamellipodia and filopodia (Diz-Munoz et al 2010; Montero et al 2003; Ulrich et al 2003; Weiser et al 2007). Notably, the directionality and protrusive activities highly correlate with the bulk cell movements underlying C&E. Before initiation of C&E, the lateral mesodermal cells exhibit round and nonpolarized morphology and extend both short bleb-like and longer lamelliform protrusions in a random fashion as they meander in all directions (Sepich et al 2005). By mid- to late gastrulation, cells become more polarized and migrate in a highly dorsally biased manner (Myers et al 2002b; Yin et al 2009). Once they approach dorsal midline, they shut down protrusive activity, such as the bleb-like protrusions mediated by the Rho/ROCK/Myosin II pathway and become more adherent to each other at stages when mediolateral intercalation is taking place (Weiser et al 2007).

More detailed studies have been carried out to analyze the protrusive activities of prechordal plate cells, which migrate anteriorly during gastrulation.

Several signaling pathways, including PDGF/PI3K and Wnt/PCP signaling, have been suggested to control protrusion formation and migration of prechordal plate cells (Montero et al 2003; Ulrich et al 2003). More recently, Diz-Munoz et al have used the combined expression of membrane-anchored red fluorescent protein (RFP) and Lifeact-green fluorescent protein (GFP) to monitor the protrusions of prechordal plate cells. Three types of cellular protrusions were found, including blebs, which are spherical protrusions initially devoid of actin, lamellipodia, which are sheet-like protrusions containing actin throughout their extent, and long, thin actin-containing filopodia. They further elucidated that reducing membrane-to-cortex attachment increases the proportion of blebs and reduces the net movement speed and directionality of these cells (Diz-Munoz et al 2010). The use of such reagents to characterize cellular protrusions of cells in other gastrula regions during C&E in WT as well as PCP mutant embryos should provide meaningful insights into the molecular mechanisms by which PCP signaling regulates C&E movements and underlying polarized cell behaviors.

PCP signaling regulates neuronal migration

Another well-characterized PCP-regulated process in zebrafish is the tangential migration of facial branchiomotor neurons (FBMNs) in the hindbrain. In mammals and zebrafish, FBMNs are born in rhombomere 4 (r4) and then migrate tangentially and caudally through r5 into r6, where they form the facial motor nuclei (Figure 5) (Chandrasekhar 2004; Chandrasekhar et al 1997; Gilland & Baker 2005; Song 2007; Wada & Okamoto 2009). In contrast, FBMNs in chick

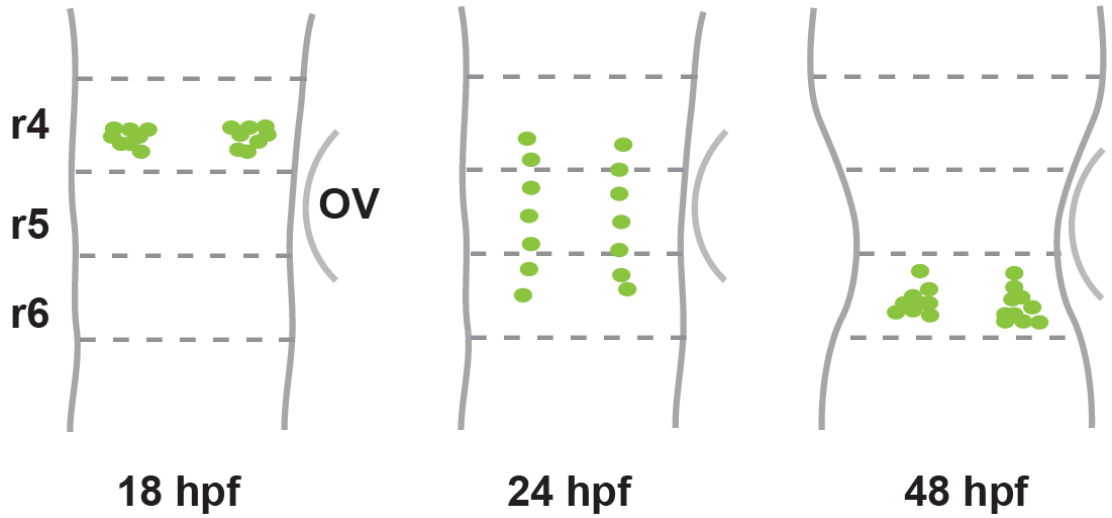

Figure 5. FBMN migration in the hindbrain of zebrafish embryo. Dorsal views of zebrafish hindbrain at three time points. FBMNs are labeled in green. r, rhombomere, OV, otic vesicle.

embryos do not migrate caudally but remain in r4 (Chandrasekhar 2004; Gilland & Baker 2005; Song 2007; Wada & Okamoto 2009). Interestingly, when a chick r4 is homotopically transplanted in mouse r4, the chick FBMNs migrate caudally into mouse r5 and r6 and conversely, mouse FBMNs fail to migrate when transplanted into the chick hindbrain, suggesting the FBMNs move according to environmental cue from the surrounding neuroepithelia (Studer 2001).

Tri/Vangl2 was the first PCP pathway component identified to regulate caudal migration of FBMNs in zebrafish (Bingham et al 2002; Jessen et al 2002).

Subsequently, it was shown that Pk1a, the binding partner of Tri/Vangl2 is also required for FBMN migration (Carreira-Barbosa et al 2003). In 2000, Okamoto's group published a transgenic zebrafish line that expresses GFP in the cranial motor neurons under the control of *islet*-1 promoter. They used this line to perform a mutagenesis screen for genes regulating FBMN migration (Higashijima et al 2000). In this screen, Off-limits (Olt)/Fz3a, Off-road (Ord)/Celsr2 and Landlocked (LlK)/Scribble 1(scrb1) were identified as essential regulators of FBMN migration, strongly arguing that FBMN migration is a PCP regulated event (Wada et al 2005; Wada et al 2006). However, several PCP components, including Wnt ligands, Kny and possibly Dvl are not required for FBMN migration, suggesting the pathway regulating FBMN migration deviates from a typical PCP pathway, like the one regulating gastrulation (Bingham et al 2002; Chandrasekhar 2004; Chandrasekhar et al 1997; Jessen et al 2002; Topczewski et al 2001; Wada & Okamoto 2009).

PCP signaling likely acts both in the FMBNs and in their surrounding neuroepithelium to regulate FBMN migration, as transplanting WT FBMNs into PCP mutant embryos or vice versa revealed cell autonomous and non-cell autonomous requirement for PCP components (Jessen et al 2002; Wada et al 2005; Wada et al 2006). Interestingly, neuroepithelia also possess polarized features along the AP axis. Pk has been demonstrated to localize preferentially to the anterior membrane of neural keel cells and this asymmetric localization is lost in maternal-zygotic (MZ) *tri/vangl2* and MZ*slb/wnt11*; MZ*pipetail/wnt5*; *wnt4*-morphant embryos (Ciruna et al 2006). In addition, *Tri/Vangl2* and *Llk/scrb1* have

been shown to control the posterior tilting of primary motile cilia lining the neurocoel and the asymmetric localization of cilia to the posterior apical membrane of neuroepithelial cells (Borovina et al ; Walsh et al 2011). Thus, it is hypothesized that the anterior-posterior polarity of neuroepithelia may provide a positional cue(s) for FBMN migration (Wada & Okamoto 2009; Walsh et al 2011). On the other hand, PCP signaling plays an important role in maintaining the integrity of the neuroepithelium. Cohesion between neuroepithelial cells is postulated to block FBMNs from sending processes towards the ventricle prior to their radial migration to the dorsomedial part of the hindbrain (Wada et al 2006). Indeed, a recent report demonstrated that reducing neuroepithelial cohesion by interfering with Cadherin 2 (Cdh2) activity causes FBMNs positioned at the basal side of the neuroepithelium to move apically towards the neural tube midline, instead of tangentially towards r6/7 (Stockinger et al 2011). On the other hand, how PCP components act cell-autonomously in FBMNs is less clear. The study of Pk1b indicates that it acts at least partially independent of the core PCP signaling, as contrary to its function in the cytosol in PCP signaling, its nuclear localization is required during FBMN migration (Mapp et al 2011; Rohrschneider et al 2007).

Despite sharing several common molecular components, the mechanisms by which PCP pathway regulates FBMN migration and C&E movements could be rather divergent, as mutants for Wnt5, Wnt11 and Kyn/Gpc4 do not exhibit FBMN migration defects and overexpression of a dominant-negative version of Dvl (Xdd1) causes strong C&E defects without affecting FBMN migration

(Chandrasekhar 2004; Jessen et al 2002).

Cell adhesion and C&E movements

Although cells in different mediolateral zones of zebrafish embryos exhibit different cell behaviors during C&E, the common feature of these cell behaviors is their dorsal-ward bias. Analogous to the adhesion gradient increasing from interior to exterior to drive outward radial intercalation during epiboly, a ventral-to-dorsal gradient of increasing adhesion could drive the movement of cells toward dorsal. It was first reported in *Xenopus* that Bmp4 overexpression blocks Activin-induced convergent extension of animal cap explants, while inhibition of BMP4 signaling by overexpressing a dominant negative form of its receptor can instigate convergent extension of ventral marginal zone explants (Graff et al 1994; Jones et al 1992). As described earlier in this Introduction, the effect of BMP signaling on C&E was studied in dorsalized zebrafish embryos with deficient BMP signaling or ventralized embryos characterized by increased and dorsally expanded BMP signaling (Myers et al 2002a; von der Hardt et al 2007). Morphometric and individual cell analyses indicate that low Bmp activity in dorsal regions allows C&E by promoting mediolateral elongation and alignment and dorsally biased intercalation while moderate BMP levels in lateral regions are compatible with dorsal-directed migration. Interestingly, dorsal migration of lateral cells is impaired in both dorsalized and ventralized embryos (Myers et al 2002a). This suggests that a BMP gradient across the DV axis is required to provide a directional cue or driving force for dorsal-directed migration. Further work done

by von der Hardt et al. demonstrated that the Bmp gradient determines the direction of lateral mesodermal cell migration during dorsal convergence in zebrafish gastrulae by negatively regulating Ca^{2+}/Cadherin-dependent cell-cell adhesiveness to form an adhesion gradient (von der Hardt et al 2007). However, despite the fact that E-cadherin/Cdh1 is also required for C&E (Babb & Marrs 2004; Montero et al 2005; Shimizu et al 2005), it is not an obvious candidate for regulation by BMP signaling, as neither its transcript nor protein forms a detectable dorsoventral gradient. The same is true for N-cadherin (Cdh2) as well as Protocadherin C (Papc), which in *Xenopus* is required for C&E movements (Chen & Gumbiner 2006; von der Hardt et al 2007) However, recent work has revealed that $G_{12/13}$ can regulate E-cadherin/Cdh1 activity without affecting its protein level or localization during epiboly, and Wnt11 and Fz7 can modulate C-cadherin mediated adhesion by promoting its clustering during convergent extension in *Xenopus* (Kraft et al 2012; Lin et al 2008). Analogously, instead of regulating a concentration gradient of an adhesion molecule, the BMP pathway can possibly work by establishing an activity gradient of these formerly-investigated adhesion molecules or other adhesion molecule(s). However, the mechanism via which BMP regulates C&E movements is not limited to its effects on cell adhesion. It has been demonstrated that high BMP activity inhibits expression of Wnt11 and Wnt5a encoding genes during zebrafish gastrulation. This negative regulation of essential PCP ligands by BMP affords another mechanism via which ventral to dorsal BMP gradient limits C&E behaviors to the dorsolateral regions of zebrafish gastrula (Myers et al 2002a).

Notably, other cadherin repeat-containing molecules, Celsr proteins, have also been found to regulate C&E movements and their relationship with respect to the BMP gradient has yet to be determined (Carreira-Barbosa et al 2009; Chen & Gumbiner 2006; Kim et al 1998). Although it is evident that Celsrs likely function by modulating cellular adhesion via homophilic interaction to regulate epiboly, it is unclear whether this aspect of Celsr function is required during C&E (Carreira-Barbosa et al 2009).

In addition to cadherin repeat-containing molecules, *Xenopus* Syndecan-4 (Syn4), a cell-surface transmembrane heparan sulphate proteoglycan was also discovered to regulate C&E by cooperating with the extracellular matrix protein, Fibronectin (Munoz et al 2006). Interestingly, a similar interaction is essential for focal adhesion formation in cell culture (Couchman et al 2001) and triggers recruitment of Dvl to cell membranes in *Xenopus* animal cap explants (Munoz et al 2006). In addition, xSyn4 was shown to interact with Fz7 in co-immunoprecipitation experiments, further supporting its role as a new component of the PCP pathway. It is very intriguing how Syn4 acts in this pathway. Since Syn4 is a key component of focal adhesions, it could recruit Dvl to focal adhesion sites and because Dvl is able to cluster other PCP components, the Syn4-mediated Dvl recruitment could lead to formation of stable PCP complexes in focal adhesion sites. Alternatively, Syn4 could work as a co-receptor for Fz7 and facilitate Dvl recruitment by Fz7. It is noteworthy that Fibronectin fibrils are assembled along outer interfaces surrounding the mesoderm and such polarized deposition is necessary for the subsequent mediolateral polarization of dorsal

mesodermal cells. Furthermore, polarized Fibronectin distribution depends on the Wnt/PCP pathway (Goto et al 2005). Therefore, Syn4 could function as a downstream effector of the Wnt/PCP pathway to regulate polarized deposition of Fibronectin fibrils.

GPCR, G proteins and C&E movements

The key C&E regulator, Celsr, not only function as a core Wnt/PCP pathway component and an adhesion protocadherin, but it also belongs to G protein-coupled receptor (GPCR) family (Fredriksson & Schioth 2005). The potential roles of GPCRs during C&E has been speculated and gradually discovered during recent years (Sepich et al 2005; Solnica-Krezel 2006; Yin et al 2009). GPCRs constitute a diverse superfamily of seven-pass transmembrane receptors. With their wide range of physiological roles, GPCRs represent the most targeted gene family by modern medicinal drugs (Overington et al 2006). Based on the sequence similarities between the transmembrane region, GPCRs are grouped into five families, namely, glutamate, rhodopsin, adhesion, frizzled and secretin according to the GRAFS classification system (Fredriksson et al 2003). GPCRs are activated by extracellular ligands ranging from light-sensitive compounds, odors, pheromones, hormones, and neurotransmitters, which vary in size from small molecules to peptides to large proteins. After activation, GPCRs in turn catalyze GDP to GTP exchange on the G protein alpha-subunit ($G\alpha$) of heterotrimeric G proteins within the cell. GTP binding leads to conformational changes in $G\alpha$, allowing it to dissociate from $G\beta\gamma$ subunits. The dissociation

exposes binding sites for their downstream effectors consequently leading to the activation of downstream signaling cascades. There are four types of heterotrimeric Gα proteins, namely G_s, $G_{i/o}$, $G_{q/11}$ and $G_{12/13}$. Each Gα activates or inactivates its own downstream effectors, hence causing distinct cellular responses (Oldham & Hamm 2008). In contrast to numerous reports about the crucial roles of GPCRs and G proteins in many biological processes in adults, the reports about their roles during development remain surprisingly limited. Excitingly, in recent years, several studies have uncovered functions for GPCRs and G proteins during C&E gastrulation movements, endoderm migration and myelin formation (Cha et al 2006; Formstone & Mason 2005; Gray et al 2011; Kai et al 2008; Lin et al 2005; Nair & Schilling 2008; Scott et al 2007; Solnica-Krezel 2006; Speirs et al ; Tada & Kai 2009; Zeng et al 2007), warranting further studies of G-Protein mediated signaling pathways during C&E.

Earlier described studies of the function of Stat3 during dorsal convergence movements of the lateral mesoderm cells suggested that it regulates a secreted cue(s) to instruct cell behaviors. Phosphorylation and activation of Stat3 is only evident in the dorsal mesoderm and transplantation experiments revealed that Stat3 is required in the axial mesoderm to regulate dorsal convergence of lateral mesoderm in a non-cell autonomous manner (Yamashita et al 2002). During *Drosophila* eye morphogenesis, ommatidia seem to sense a local gradient of a secreted signal controlled by the JAK/STAT3 pathway (Zeidler et al 1999). Analogously, a secreted signal downstream of Stat3 emanating from the axial mesoderm could serve as an attractive cue for lateral

mesodermal cells. Evidence for the existence of such an attractive cue comes from measurements of cell behaviors in the lateral mesoderm during C&E movements. Sepich et al. showed these cells exhibit a directional preference, directionally-regulated speed, and turn toward dorsal when off-course (Sepich et al 2005). Using mathematical modeling, they posited that directional preference is sufficient to account for mesoderm convergence and extension, and that a minimum of two sources of guidance cues emanating from the dorsal midline would be sufficient to orient cell paths (Sepich et al 2005). In chick embryos, FGF4 produced in the forming notochord was proposed to serve as a chemoattractant to guide convergence movements of internalized mesoderm cells toward the midline (Yang et al 2002). However, a similar role of Fgfs for C&E movements in zebrafish or other vertebrates has not been reported. Alternatively, GPCRs and their ligands could fulfill such a requirement, as a subset of GPCRs are known to regulate chemotaxis toward the gradients of their cognate ligands in the social amoeba *Dictyostelium discoideum* and in the mammalian immune system (Devreotes & Janetopoulos 2003). During gastrulation, Sdf1a/Cxcl12a and its receptor Cxcr4b regulate primordial germ cell (PGC) migration in a classic chemotaxis fashion. During gastrulation stages, *sdf1a* transcript is expressed in a highly dynamic fashion along the migratory path of PGCs. PGCs expressing Cxcr4b perceive Sdf1a/Cxcl12a and migrate towards the highest level of Sdf1a/Cxcl12a. In addition, another Sdf1a/Cxcl12a receptor Cxcr7 is also required for proper PGC migration. However this receptor is expressed in the somatic cells, which show enhanced internalization of Sdf1,

suggesting Cxcr7 acts as a sink for Sdf1a/Cxcl12a and therefore promotes the dynamic distribution of Sdf1a/Cxcl12a protein (Boldajipour et al 2008; Doitsidou et al 2002). In contrast to the role of Cxcl12a in PGC migration, Cxcl12b along with its receptor, Cxcr4a, restricts the migration of endodermal cells. Depletion of gene product of either the liand or the receptor causes untethering of endodermal cells from mesodermal cells and excessive anterior migration of endodermal cells. By the end of gastrulation, these mismigrated cells fail to reach their destination near the midline, leading to bilateral endodermal organs rather than a single midline array of endodermal organs (Nair & Schilling 2008).

Besides Cxcl12s and their receptors, several other ligand-receptor pairs have also been demonstrated to regulate cell movements during gastrulation. Apelin and Sphingosin-1-phospate together with their respective receptors are specifically involved in migration of cardiac precursors, which reside in the anterior lateral plate mesoderm and converge toward dorsal to form bilateral heart fields flanking the dorsal midline at late gastrulation (Keegan et al 2004). During segmentation, the two heart fields converge towards the midline, where they fuse to form a single heart tube (Auman & Yelon 2004; Moorman & Christoffels 2003; Yelon et al 1999). Consistent with their role as ligand and receptor in cardiac precursor migration, *agtrl1b* is expressed in the anterior lateral plate mesoderm and *apelin* transcripts are confined to the dorsal midline during gastrulation. Heart field formation is impaired both when Agtrl1b or Apelin function is disrupted, and when Apelin is globally overexpressed (Scott et al 2007; Zeng et al 2007). Whether Apelin expression in under the control of Stat3

remains to be tested. Furthermore, as cardiac precursors stop before reaching the midline, where Apelin concentration is assumed to be the highest, the mechanism of their action might not be a simple chemotaxis. Alternatively, additional counteracting factors might exist to prevent cardiac precursors from moving into the field of cells that are the source of Apelin. In addition, evidence suggests Edg5 and its ligand sphingosin-1-phospate regulate cardiac precursor migration by generating an environment permissive for their migration (Kupperman et al 2000). This same ligand/receptor pair also plays a role in the migration of the prechordal plate cells (Kai et al 2008).

Unlike the aforementioned GPCRs, which appear to regulate C&E movements of selective tissues, Prostaglandin 2 (PGE_2) regulates global C&E movements and epiboly through its EP4 receptor by promoting cell protrusive activity and limiting cell adhesion by modulating E-cadherin/Cdh1 transcript and protein (Cha et al 2006; Speirs et al). Notably, Fz receptors for both canonical and non-canonical Wnt signaling, are seven-pass transmembrane proteins, and have been proposed to couple to multiple G proteins in the context of canonical Wnt signaling (Ahumada et al 2002; Liu et al 2001; Liu et al 1999a; Liu et al 1999b) and recently to act in the context of both PCP and canonical branches in *Drosophila* (Katanaev et al 2005).

As the main signal transducers downstream of GPCRs, the $G\alpha$ subunits of heterotrimeric G proteins have been hypothesized to play a role during gastrulation. In cell culture, the $G\alpha$12/13 G protein family has been implicated in numerous cellular processes to regulate Rho-mediated cytoskeletal

rearrangements, thereby affecting cell shape and migration (Aittaleb et al 2010). Three zebrafish genes encoding G_{12} and G_{13} are ubiquitously expressed during gastrulation and their function is required in all germ layers for epiboly, convergence and extension. Their function as global gastrulation regulators is carried out in part by inhibiting E-cadherin/Cdh1 activity and modulating Actin cytoskeleton (Kane et al 2005; Lin et al 2008; Lin et al 2005). The other $G\alpha$ subfamily of particular relevance to C&E movements is Gi/o. Since Gi/o mediates the chemotactic migration of immune cells downstream of chemokine receptors (Devreotes & Janetopoulos 2003), it is reasonable to hypothesize that a similar role of Gi/o might contribute to directed migration of mesoderm cells during C&E movements. So far the evidence supporting this hypothesis is limited. In *Xenopus* embryos treated with pertussis toxin, a Gi/o inhibitor, mesodermal tissues fail to separate from ectodermal cells, thus causing secondary defects of gastrulation. Epistasis analyses indicate Gi/o regulates this process via a Wnt/PCP independent pathway downstream of Fz7 and upstream of PKC (Winklbauer et al 2001). In a heterologous system, Gi/o has shown to be activated by Apelin via Agtrl1b (Scott et al 2007). However, whether it acts downstream of Agtrl1b to impact cardiac precursor migration has not been confirmed.

Findings and hypotheses resulting from this work

Gastrulation is the fundamental process during embryogenesis when the germ layers and shape of the animal are generated. Although the major cell

movements during gastrulation have been well characterized, the underlying cellular and molecular mechanisms are only beginning to be understood. Identifying new molecules involved in gastrulation and studying their interactions with known gastrulation regulators will bring us closer to a full mechanistic understanding of gastrulation.

In this study, I focused on the adhesion GPCR family, the most recently described of the five GRAFS GPCR families (Bjarnadottir et al 2007; Fredriksson et al 2003). By conducting BLAST searches of the zebrafish genome database with the peptide sequences of human adhesion GPCRs and searching for GPS domain-containing proteins encoded in the zebrafish genome, I found 30 annotated or partially annotated adhesion GPCRs in the sequenced zebrafish genome. They represent members from all seven groups of adhesion GPCRs found in humans. By RT-PCR, I determined that the transcripts of seven adhesion GPCR genes are expressed during zebrafish gastrulation stages and eight adhesion GPCR genes are maternally deposited.

Focusing on the Group IV adhesion GPCR subfamily members, I analyzed their spatiotemporal expression profiles by *in-situ* hybridization and found that four members of this family exhibit distinct and dynamic expression patterns during the early stages of embryogenesis. In the subsequent functional analyses, I uncovered distinct functions of Gpr124 and Gpr125 during early embryogenesis.

Interfering with the function of Gpr124 resulted in defects in multiple tissues in the caudal region of the embryo, including the notochord and

vasculature. While we have yet to further pursue the mechanism of Gpr124 function, we focused on functional studies of Gpr125 during gastrulation and FBMN migration to gain insights into the molecular mechanism of its action. Consistent with a potential role during gastrulation, I showed *gpr125* is expressed maternally and zygotically at blastula and gastrula stages. Since gastrulation movements are sensitive to both elevated and reduced levels of their regulators (Jessen et al 2002; Lin et al 2005; Marlow et al 2002; Zeng et al 2007), we investigated the potential roles of Gpr125 utilizing gain- and loss-of-function approaches. Excess Gpr125 in WT embryos impaired C&E movements, resulting in shortening of the AP axis and synophthalmia or cyclopia. On the cellular level, Gpr125 overexpression impaired mediolateral cell elongation and alignment as well as anterior Pk localization.

In LOF experiments, *gpr125* interacted with PCP genes to promote PCP mediated processes. Although injection of *gpr125*-specific MO (MO-*gpr125*) did not affect WT embryos, it significantly exacerbated the defects of PCP homozygous mutants, causing further reduction of the AP axis and more severe cyclopia in *llk/scrb1*, *tri/Vvangl2* and *slb/wnt11* homozygotes. Moreover, MO-*gpr125*, but not control morpholinos, led to significant shortening of the AP axis of normally aphenotypic PCP heterozygotes, and injection of synthetic *gpr125* RNA lacking the MO-targeting sequence was able to partially rescue such defects. I determined that these exacerbated defects arose from enhanced C&E defects by examining tissue-specific markers and cell morphology in late gastrulae. In addition, a subset of PCP genes (*e.g. vangl2/tri* and *scrb1/llk*) also regulate

FBMN migration in zebrafish and mouse (Bingham et al 2002; Carreira-Barbosa et al 2003; Chandrasekhar 2004; Jessen et al 2002; Wada et al 2005; Wada & Okamoto 2009; Wada et al 2006). Interestingly, *gpr125* also interacted with this class of PCP genes to promote FBMN migration.

At the molecular level, when co-expressed with Gpr125, Dvl-GFP was recruited to cell membranes, where it became clustered in discrete subdomains of cells in late blastulae. This was striking in light of previous reports that Fz7, a PCP pathway receptor, recruits Dvl uniformly to the cell membrane at the blastula stages, but only promotes Dvl accumulation in discrete membrane subdomains when co-expressed with a PCP ligand, Wnt11 (Witzel et al 2006).

Through structure-function analyses, I identified the domains of Gpr125 required to modulate Dvl localization. Gpr125 lacking the entire intracellular domain (ICD) did not promote Dvl-GFP translocation, nor could affect C&E movements when overexpressed, suggesting that the intracellular domain is essential for Dvl recruitment and its function during gastrulation. Moreover, deletion of the PDZ-biding motif (PDZBM) resulted in less efficient Dvl recruitment, smaller Dvl clusters on the membrane and lower activity in affecting C&E movements upon overexpression. Corroborating the localization studies, in biochemical experiments GST-Gpr125ICD could pull down Dvl-GFP, strongly arguing for a direct interaction, while the ΔPDZBM form pulled down less Dvl-GFP. Thus, the PDZB motif likely mediates Dvl binding with contributions from additional motifs.

In an independent line of investigation, I found that a Gpr125 fluorescent fusion protein was uniformly distributed along the membrane when expressed alone in zebrafish blastulae. However, in striking contrast, Gpr125 colocalized with Dvl-GFP in membrane subdomains when the proteins were coexpressed. Similarly, Dvl also clustered Kny/Gpc4 into membrane subdomains. These observations resonate with a recent report in *Drosophila*, proposing essential roles for Dvl in the formation of PCP supramolecular complexes (Strutt et al 2011). In addition, Gpr125 and Dvl were able to recruit Fzd7 and Kny/Gpc4 but not Tri/Vangl2 into membrane subdomains.

Based on these observations, we propose Gpr125 acts as a novel Wnt/PCP signaling component in zebrafish. We hypothesize that Gpr125 facilitates formation of asymmetric PCP supramolecular complexes, which are thought to mediate PCP signaling between neighboring cells (Jenny et al 2003b; Strutt et al 2011; Witzel et al 2006). Our discovery of a function for Gpr125 in C&E during gastrulation, a processes where all known PCP components act, and later during FBMN migration, where only a subset of PCP genes are required, opens up exciting avenues for further studies of Gpr125 function, in particular towards understanding how Gpr125 and Wnt/PCP signaling operate to regulate cell and tissue polarity in these unique developmental contexts.

CHAPTER II

SURVEY FOR ADHESION GPCRS DURING EARLY ZEBRAFISH DEVELOPMENT

Introduction

Structural basis of adhesion GPCRs

Adhesion GPCRs are natural chimeras of adhesion molecules and generic GPCRs (Figure 6A). Some adhesion GPCRs were formally known as LN-TM7 or EGF- TM7 receptors. Since they have comparatively higher sequence similarity to the secretin-receptor family (B1), these receptors were classified as the B2 GPCR family (Harmar 2001). In 2002, Fredriksson et al. proposed a new GPCR classification system, GRAFS, based on the phylogenetic analysis of the entire repertoire of the seven transmembrane (TM7) regions of human GPCRs. In GRAFS, 33 human GPCRs were for the first time grouped into a distinct family and named as adhesion GPCRs (Fredriksson et al 2003).

Based on sequence similarity within the TM7 region, adhesion GPCRs can be further divided into seven groups and the receptors within the same group also share similar extracellular domains (Figure 6B). Group I adhesion GPCRs share Thrombospondin repeats, Group III share EGF repeats, Group IV share leucine-rich regions and Group V share cadherin repeats (Yona et al 2008). Another unique feature of adhesion GPCRs is the presence of a GPCR proteolysis site (GPS), which is conserved in all but one human adhesion GPCRs and five human polycystic kidney disease (PKD) proteins (Arac et al 2012;

Bjarnadottir et al 2007; Fredriksson et al 2002; Ponting et al 1999; Yona et al 2008). The GPS motif is always localized at the end of the long extracellular region immediately before the first transmembrane helix of the GPCR subunit (Figure 6A). GPS mediated cleavage has been reported for the CD97 antigen receptor (CD97), the EGF-TM7-latrophilin-related receptor (ETL), the EGF-like module containing receptor 2 (EMR2), EMR4, the calcium independent receptor of α-latrotoxin 1 (CIRL1) and GPR56 (Bjarnadottir et al 2007; Ke et al 2008; Krasnoperov et al 2002; Kwakkenbos et al 2002; Stacey et al 2002). The proteolytic reaction occurs in the endoplasmic reticulum via a self-catalyzed cis-proteolysis mechanism often between a conserved aliphatic residue (usually a leucine) and a threonine, serine or cysteine residue (Krasnoperov et al 2002; Lin et al 2004). A recent study of GPCR protein structures indicates that the GPS motif is not an autonomously folded unit but rather part of a much larger evolutionally conserved GPCR-autoproteolysis inducing (GAIN) domain required and sufficient for autoproteolysis (Arac et al 2012). After cleavage, the two parts form a heterodimer via a non-covalent interaction involving an extensive network of conserved interstrand hydrogen bonds and primarily hydrophobic side-chain interactions (Arac et al 2012; Lin et al 2004). It was shown that cleavage is essential for surface expression of CIRL1 and GPR56 (Ke et al 2008; Krasnoperov et al 2002). However, a recent study of Lat-1/Latrophilin function in *C. elegans* suggests that activity of this receptor does not require cleavage but relies on the presence of the GPS motif (Promel et al 2012).

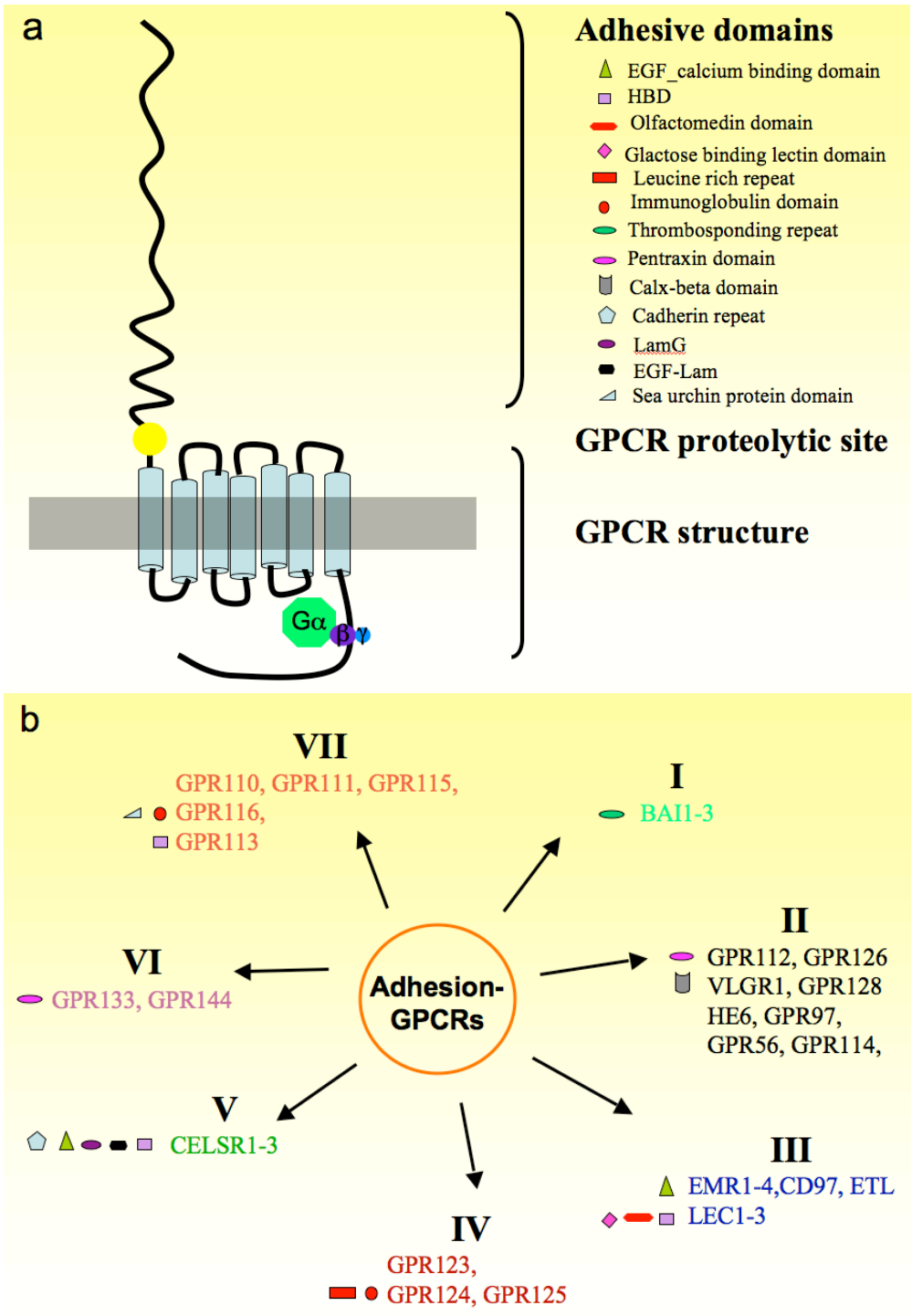

Figure 6. Adhesion GPCRs are chimeras of adhesion molecules and GPCRs. (A) The schematic representation of adhesion GPCR protein domains. GPCR proteolytic site (GPS) is marked by a yellow circle. (B) Adhesion GPCR subgroups.

Adhesion GPCRs and development

The majority of adhesion GPCR genes have been discovered recently; thus, little is known about their functions in adult organisms and especially during development. Exceptions include the Group V Celsr proteins, which are well-known regulators of developmental processes. As discussed previously, the *Drosophila* homology of Celsr, named Flamingo, was first discovered to regulate planar cell polarity in *Drosophila*. As a conserved component of the PCP pathway in vertebrates, Celsr proteins have been reported to regulate FBMN migration in zebrafish (Wada et al 2006) and a recent study indicated that Celsr1a, 1b and Celsr2 function redundantly during zebrafish gastrulation (Carreira-Barbosa et al 2009). In mammals, homozygous *celsr1* mutant mouse embryos fail to initiate neural tube closure and have severe defects in planar cell polarity mediated orientation of hair cells within the organ of corti (Curtin et al 2003). A gene-silencing study with small hairpin RNAs in postnatal day 4 rat cortical slices revealed that Celsr2 and Celsr3 regulate neurite growth in opposing manners. Whereas Celsr2 enhances, Celsr3 suppresses neurite growth (Shima et al 2007). Another group reported that Celsr3 is required for axonal tract formation, as *Celsr3* mutant brain lacks anterior commissure and internal capsule, shows a reduction of fibers in the cortical intermediate zone and abnormal small radial fascicles in the upper cortical tier (Tissir et al 2005).

In the last decades, genetic studies have provided substantial evidence regarding the pivotal roles of additional adhesion GPCRs in various developmental processes. Mutations associated with human congenital

diseases have been mapped to adhesion GPCRs and deletion of adhesion GPCRs lead to developmental defects in animal models. Mutations in human *GPR56* cause a brain cortical malformation called bilateral frontoparietal polymicrogyria, and knockout of Gpr56 in mice results in a similar cobblestone like cortical malformation (Li et al 2008; Piao et al 2004). Mutations disrupting the very large G protein-coupled receptor (*VLGR1)* have been linked to Usher's syndrome, a genetic disorder characterized by blindness, deafness, and audiogenic seizures in mice (McGee et al 2006; Sun et al 2012; Weston et al 2004). In addition, knockout mouse models have uncovered an essential role of GPR124 in CNS-specific angiogenesis while GPR64/HE4 is required for male fertility (Davies et al 2004; Kuhnert et al). Moreover, zebrafish mutagenesis studies have revealed an essential role for Gpr126 in Schwann cells myelination (Monk et al 2009), and the murine Gpr126 homolog was subsequently shown to have a conserved function in myelination (Monk et al 2011). Expression analyses have revealed diverse expression patterns among many additional adhesion GPCRs during development (Homma et al 2008; Moriguchi et al 2004), warranting further investigation of the function of this class of proteins during development. In addition to the mounting evidence indicating important functions of adhesion GPCRs during normal development, aberrant expression of several adhesion GPCRs has been reported in various human cancers (reviewed in (Lin 2012). In this context, GPCRs are thought to be involved in tumorigenesis by affecting tumor cell growth, migration, or tumor angiogenesis.

Adhesion GPCRs and transmembrane signaling

GPCRs are thought to interact with their extracellular ligands and initiate intracellular signal transduction by coupling to and activating heterotrimeric G proteins. However, most adhesion GPCRs currently are classified as orphan receptors, meaning their ligands have not yet been identified (Gupte et al 2012; Paavola & Hall 2012; Tang et al 2012). Therefore, substantial ongoing efforts are directed towards deorphanizing these receptors and identifying their prospective downstream heterotrimeric G proteins. Progress towards this end has been made for CD97, Celsr and Gpr56 adhesion GPCRs. CD97 was shown to bind the SCR repeat of CD55 via its first two EGF-like domains, and chondroitin sulphate via its fourth EGF-like domain (Hamann et al 1996; Lin et al 2001; Stacey et al 2003). Homophilic interactions have been documented for the Celsr adhesion GPCRs (Carreira-Barbosa et al 2009; Shima et al 2007; Usui et al 1999). Recently, Latrophilin 1 (LPH1) has been reported to form a high-affinity transsynaptic receptor pair with Lasso/teneurin-2. The C-terminal fragment of Lasso interacts with LPH1 and induces Ca^{2+} signals in presynaptic boutons of hippocampal neurons and in neuroblastoma cells expressing LPH1 (Silva et al 2011). Moreover, Collagen type III alpha-1 (Col3a1) has been identified as the ligand of GPR56 through an *in vitro* biotinylation/proteomics approach. Similar to the phenotypes seen in Gpr56 null mutant mice, Col3a1 null mutant mice show a cobblestone-like cortical malformation associated with migration of mutant neurons through the pial basement membrane. Functional studies suggest that the interaction between Collagen III and GPR56 is required to inhibit neural

migration. Four mutations in Col3a1 that completely abolish the ligand binding ability of GPR56 have been associated with human disease (Luo et al 2011; Luo et al 2012).

Though knowledge of adhesion GPCR ligands is limited, even less is known about the ability of adhesion GPCRs to couple to G proteins. Based on *in vitro* studies, GPR56 couples to the $G\alpha_{12/13}$ family of G proteins to activate the RhoA pathway upon ligand binding (Iguchi et al 2008; Luo et al 2011). The ability of cAMP to rescue the myelination defects of *gpr126* mutants suggests that $G\alpha s$ might function downstream of Gpr126 (Monk et al 2009). The homophilic interaction of Celsr2 and Celsr3 is able to elevate intracellular calcium concentration. Although the kinetics are slower than those of typical GPCRs, it remains possible that the calcium increase is due to the activation of G proteins by Celsr2 and Celsr3 (Shima et al 2007). While adhesion GPCR coupling to G proteins remains a possibility, it is also possible that adhesion GPCRs might mediate transmembrane signal transduction by interacting with other intracellular proteins. Notably, several adhesion GPCR proteins, namely, GPR124, GPR125, the brain-specific angiogenesis-inhibitory receptor (BAI) 1-3, Gpr133, VLGR1, possess a C-terminal PDZBM which mediates interaction with various PDZ domain containing proteins (Bjarnadottir et al 2007). For instance, BAI1 has been shown to interact with BAI1-associated protein 1(BAP1), a novel member of the membrane-associated guanylate kinase homologue family via its PDZ motif, and similarly, GPR124 and GPR125 can interact with the human homologue of the *Drosophila* disc large tumor suppressor, a PDZ domain containing protein

(Shiratsuchi et al 1998; Yamamoto et al 2004). Moreover, the PDZBM of VLGR1 is responsible for its interaction with Usher proteins to form ankle-link complexes in inner ear hair cells (Ebermann et al 2010; Michalski et al 2007; Reiners et al 2005; Sun et al 2012; van Wijk et al 2006).

To gain insights into the potential functions of adhesion GPCRs during vertebrate development, I characterized the expression of adhesion GPCRs during zebrafish embryogenesis. I found 30 annotated or partially annotated adhesion GPCRs in the sequenced zebrafish genome. They represent members from all seven groups of adhesion GPCRs found in humans. By RT-PCR, I determined that the transcripts of seven adhesion GPCR genes are expressed during zebrafish gastrulation stages and eight adhesion GPCR genes are maternally deposited. In addition, study of Gpr125 fusion protein revealed no evidence of GPS-mediated cleavage. Furthermore, interfering with the function of Gpr124 resulted in defects in multiple tissues in the caudal region of zebrafish embryos, including the notochord and vasculature. These studies add more information on the post-translation processing of adhesion GPCRs and facilitate our understanding of their functions during vertebrate development.

Results

30 annotated or partially annotated adhesion GPCR genes are present in the zebrafish genome

A previous study reported 22 adhesion GPCR genes in the zebrafish genome (Fredriksson & Schioth 2005). However, this study did not provide

adequate EST sequences to verify the annotated coding sequence for each adhesion GPCR gene. In addition, the whole annotation process of the zebrafish genome was incomplete when this study was carried out (Fredriksson & Schioth 2005). Hence, it is likely that a considerable portion of genes were missed in this initial study. Therefore, I applied bioinformatics methods to search for and to verify the adhesion GPCRs encoded in the zebrafish genome. By conducting BLAST searches of the zebrafish genomic databases with the peptide sequences of human adhesion GPCRs and searching for GPS motif-containing proteins encoded in the zebrafish genome, I found 30 annotated or partially annotated adhesion GPCRs in the sequenced zebrafish genome (Table 1). The GPCRs included representatives of all seven groups of adhesion GPCRs found in humans. Based on sequence alignment, each of the 30 receptors is likely the homologue of a unique human adhesion GPCR.

The accuracy of the annotation was verified by comparing them to available zebrafish ESTs and full-length sequences of cDNAs cloned from various tissues. The extent of EST coverage varies widely from one adhesion GPCR to another. For instance, in Group III, annotated coding sequences of *cirl* genes are well covered by ESTs, while those of *emr* genes are poorly covered by ESTs. This difference likely reflects the expression levels of difference adhesion GPCRs in the sampled tissues at the stages when the ESTs were cloned.

Table 1. Bioinformatics data of zebrafish adhesion GPCRs.

Number	Gene ID	Gene Name	Genome Location	Identities to human proteins
*1	ENSDARG00000061121	LOC560631	Chromosome 1: 19.61m	72% to lec1(latrophilin2)
2	ENSDARG00000030417	LOC557415	Chromosome 1: 50.79m	39% to polycystic kidney disease protein
3	ENSDARG00000069356	LOC569242	Chromosome 2: 3.74m	74% to LEC2
4	ENSDARG00000041399	LOC100004737	Chromosome 2: 33.85m	37% to EMR3
5	ENSDARG00000026313	-novel-	Chromosome 3: 7.19m	33% to CD97
6	ENSDARG00000018436	LOC562531	Chromosome 3: 44.96m	69% to LEC1
7	ENSDARG00000041404	-novel-	Chromosome 3: 51.86m	30% to EMR1.
8	ENSDARG00000029391	celsr1a	Chromosome 4: 24.02m	CELSR1
9	ENSDARG00000069185	celsr1a	Chromosome 4: 24.16m	CELSR1
10	ENSDARG00000021137	gpr98	Chromosome 5: 47.61m	GPR98 (VLGR)
11	ENSDARG00000027222	wu:fc49b10	Chromosome 7: 34.91m	33% to GPR56
12	ENSDARG00000055825	celsr3	Chromosome 8: 24.54m	CELSR3
13	ENSDARG00000040194	LOC100005340	Chromosome 8: 30.99m	38% to GPR116
*14	ENSDARG00000053344	zgc:103546 IMAGE:7241100	Chromosome 8: 40.60m	74% to GPR133
*15	ENSDARG00000013653	zgc:63629 IMAGE:5603872	Chromosome 11: 7.08m	50% to ELT1
16	ENSDARG00000033029	-novel-	Chromosome 12: 42.61m	channel protein
17	ENSDARG00000071427	-novel-	Chromosome 14: 43.33m	96% to zebrafish Gpr114
18	ENSDARG00000058809	LOC564860	Chromosome 17: 5.46m	33% to GPR113
19	ENSDARG00000025667	si:ch211-149a22.1	Chromosome 19: 35.73m	60% to BAI2
*20	ENSDARG00000054137	gpr126	Chromosome 20: 29.79m	50% to GPR126
*21	ENSDARG00000056168	-novel-	Chromosome 20: 31.53m	35% to GPR116.
*22	ENSDARG00000006278	si:dkey-30j22.2	Chromosome 20: 31.69m	group 7.
23	ENSDARG00000025036	si:dkey-30j22.4	Chromosome 20: 31.71m	group 7.
24	ENSDARG00000070063	-novel-	Chromosome 20: 31.74m	group7.
25	ENSDARG00000042802	si:dkey-30j22.5	Chromosome 20: 31.76m	group7.
26	ENSDARG00000041413	si:ch211-119b12.8	Chromosome 20: 46.68m	GPR97?
27	ENSDARG00000056062	-novel-	Chromosome 21: 19.01m	No description
28	ENSDARG00000019726	celsr2	Chromosome 22: 248	similar to EMR2
*29	ENSDARG00000071088	-novel-	Chromosome 22: 28.94m	34% to GPR128
*30	ENSDARG00000071085	si:ch73-162i18.2	Chromosome 22: 28.96m	41% to GPR128
31	ENSDARG00000058259	celsr1b	Chromosome 25: 10.52m	CELSR1
32	ENSDARG00000034234(PTMA)	zgc:158634	Scaffold Zv7_NA1113: 22.98k	prothymosin-alpha gene
33	ENSDARG00000062746	-novel-	Scaffold Zv7_NA58: 60.00k	39% to GPR116
34	ENSDARG00000052853			
35	ENSDARG00000060911			
36	ENSDARG00000069006(groucho 1)			
37	ENSDARG00000009866			
38	LOC560700 (NCBI)	predicted zebrafish gpr124	chromosome="23"	
39	LOC100003592 (NCBI)	predicted zebrafish gpr125	chromosome 17	
40	LOC560847 (NCBI)	predicted gpr123		

not identified in homologue search

meaning: unlikely to be adhesion GPCR

meaning: not found in GPS search

Seven zebrafish adhesion GPCRs are expressed during gastrulation

The tissue-specific expression of adhesion GPCR genes has been examined systematically in adult mice and rats (Haitina et al 2008). However, the expression profiles of most adhesion GPCRs during embryogenesis have not been reported. To characterize the expression of adhesion GPCR genes during zebrafish embryogenesis, I made cDNA libraries from 16-cell, 70%~90%-epiboly, 3-somite and 1 dpf embryos. These libraries were used to analyze gene expression during the cleavage, the gastrula, the segmentation and the pharyngula periods of zebrafish embryogenesis (Kimmel et al 1995a). Gene-specific primers were designed based on the annotated sequences to detect the expression of 12 adhesion GPCRs, selected from Group I, Group II, Group III, Group IV and Group VII. The transcripts of seven of the 12 adhesion GPCR genes examined were detected in gastrula stage embryos. At least one member from each of the aforementioned five groups was expressed during zebrafish gastrulation. In addition, nine of the 12 genes were expressed in 24 hpf embryos and the transcripts of eight adhesion GPCR genes were maternally deposited (Figure 7 and Table 2).

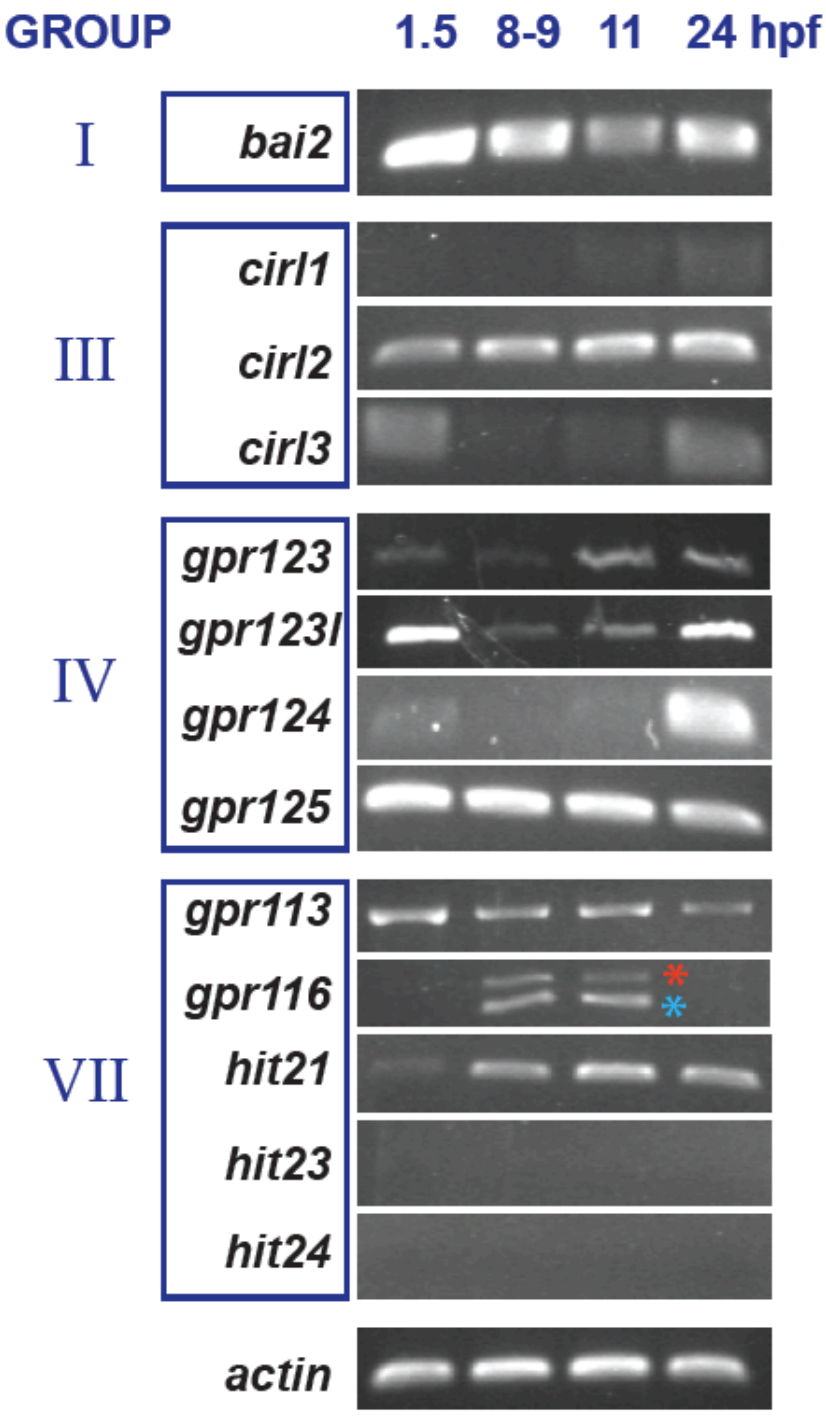

Figure 7. Examining adhesion GPCR gene expression with RT-PCR. Most PCRs yielded products of predicted sizes, except for the ones marked by stars. Blue stars mark products with predicted sizes and red stars mark products of unexpected sizes.

Table 2. Temporal expression profiles of candidate adhesion GPCRs. ● indicates the expression is detected via RT-PCR; ⭘ indicates a minimum amount of expression is detected via RT-PCR; ○ indicates the expression is not detected via RT-PCR.

Stage **Gene**	16- cell	70%-90% epiboly	3- somite	1 dpf
bai2	●	●	●	●
gpr126	●	⭘	●	●
cirl1	○	○	⭘	⭘
cirl2	●	●	●	●
cirl3	⭘	○	⭘	⭘
gpr124	●	●	●	●
gpr125	●	●	●	●
gpr116	●	●	●	●
hit21	⭘	●	●	●
hit23	○	○	○	○
hit24	○	○	○	○

As all four members of the Group IV subfamily were expressed during the first day of development and their expression within this time seemed to be dynamic and distinct, we performed additional RT-PCR analyses on Group IV members with higher temporal resolution during the first five days of developments. Indeed, these analyses revealed that prior to 2 dpf, the temporal expression of these four genes was distinctly regulated (Figure 8). *gpr125*

transcripts were maternally provided and remained present throughout the first five days of development. While maternal transcripts for both *gpr123* and *gpr124* were detected, their expression levels were low during gastrulation and increased significantly at 24 and 14 hpf respectively. *gpr123like* expression was barely detectable until 18 to 24 hpf.

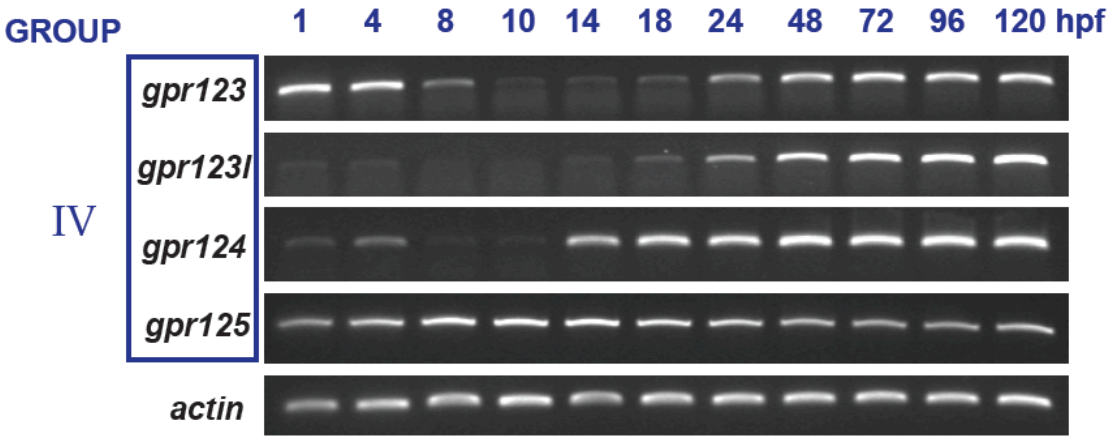

Figure 8. RT-PCR analysis of Group IV adhesion GPCR gene expression during the first 5 days of zebrafish development.

Group IV adhesion GPCRs exhibit distinct spatiotemporal expression patterns

Subsequently, I analyzed the temporal and spatial expression patterns of the Group IV adhesion GPCRs using whole-mount in situ hybridization. Consistent with the RT-PCR results, *gpr123 gpr123like* and *gpr124* had very lowexpression by the end of gastrulation (Figure 9, 10 and 11). In contrast, *gpr125* was expressed ubiquitously at a high level from the maternal through gastrulation to early segmentation stages (Figure 12).

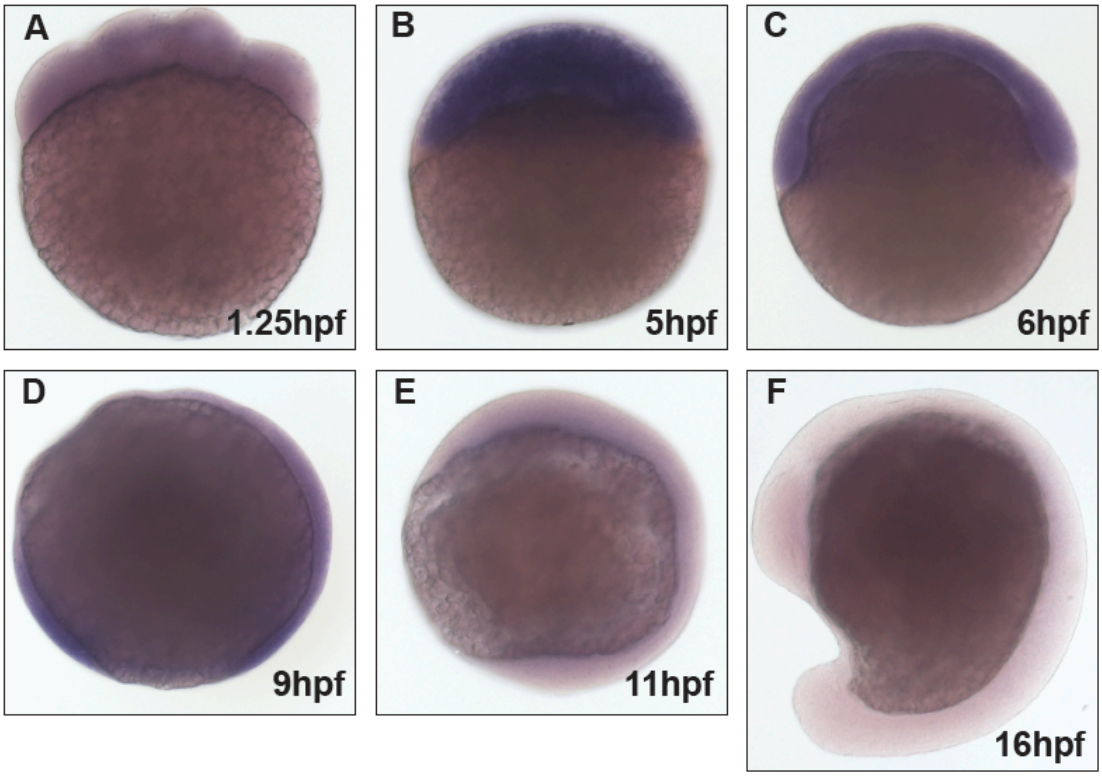

Figure 9. Whole-mount *in situ* hybridization analysis of *gpr123* expression. Lateral views, animal pole up, dorsal right in (C-F).

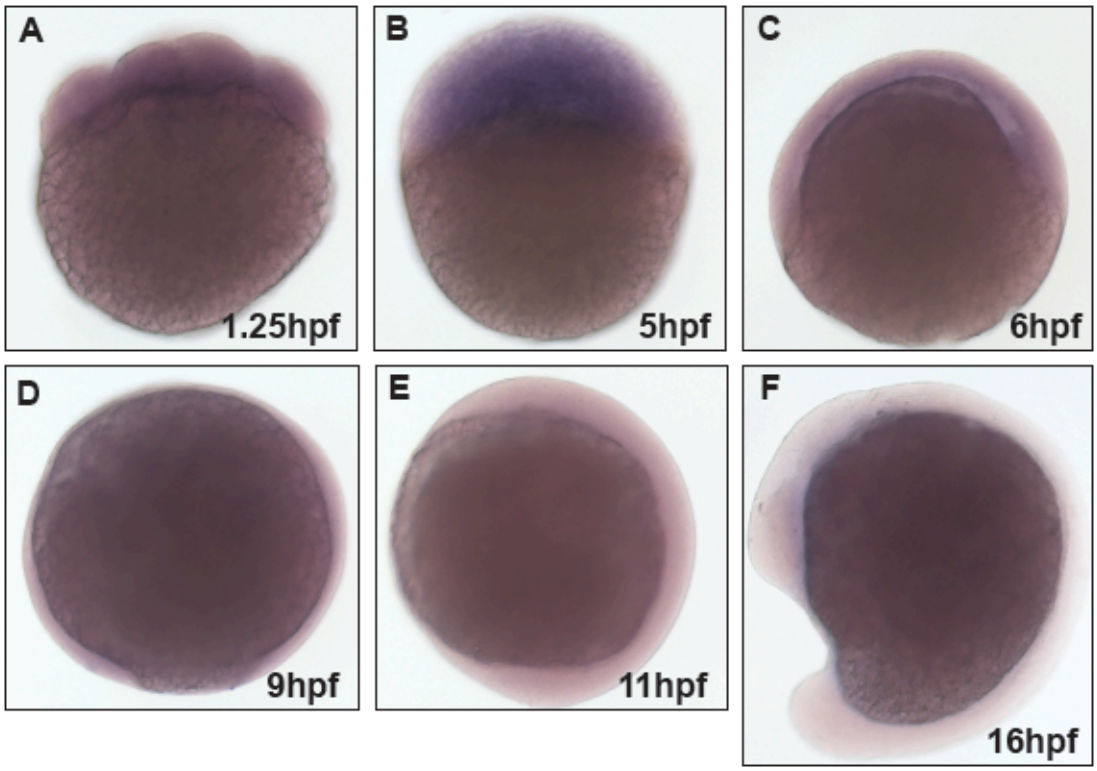

Figure 10. Whole-mount *in situ* hybridization analysis of *gpr123like* expression. Lateral views, animal pole up, dorsal right in (C-F).

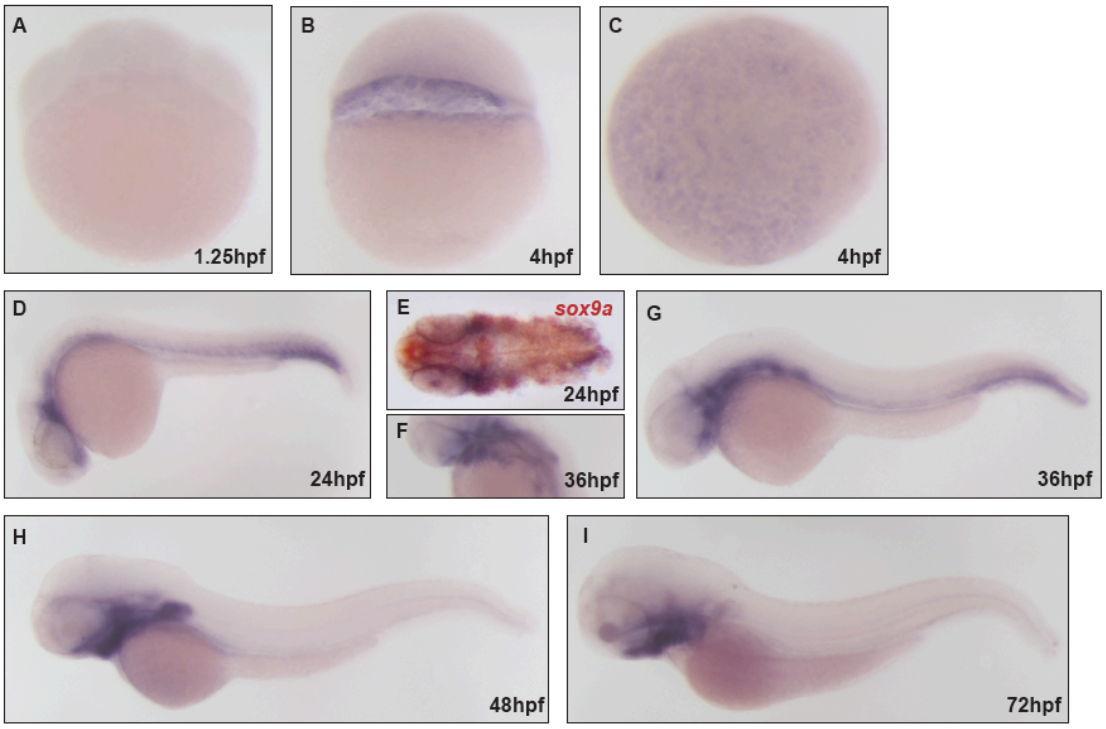

Figure 11. Whole-mount *in situ* hybridization analysis of *gpr124* expression. Lateral views, animal pole up in (A and B). Animal pole view in (C). Lateral views, anterior left, dorsal up in (D, F, G-I). Dorsal view, anterior left in (E).

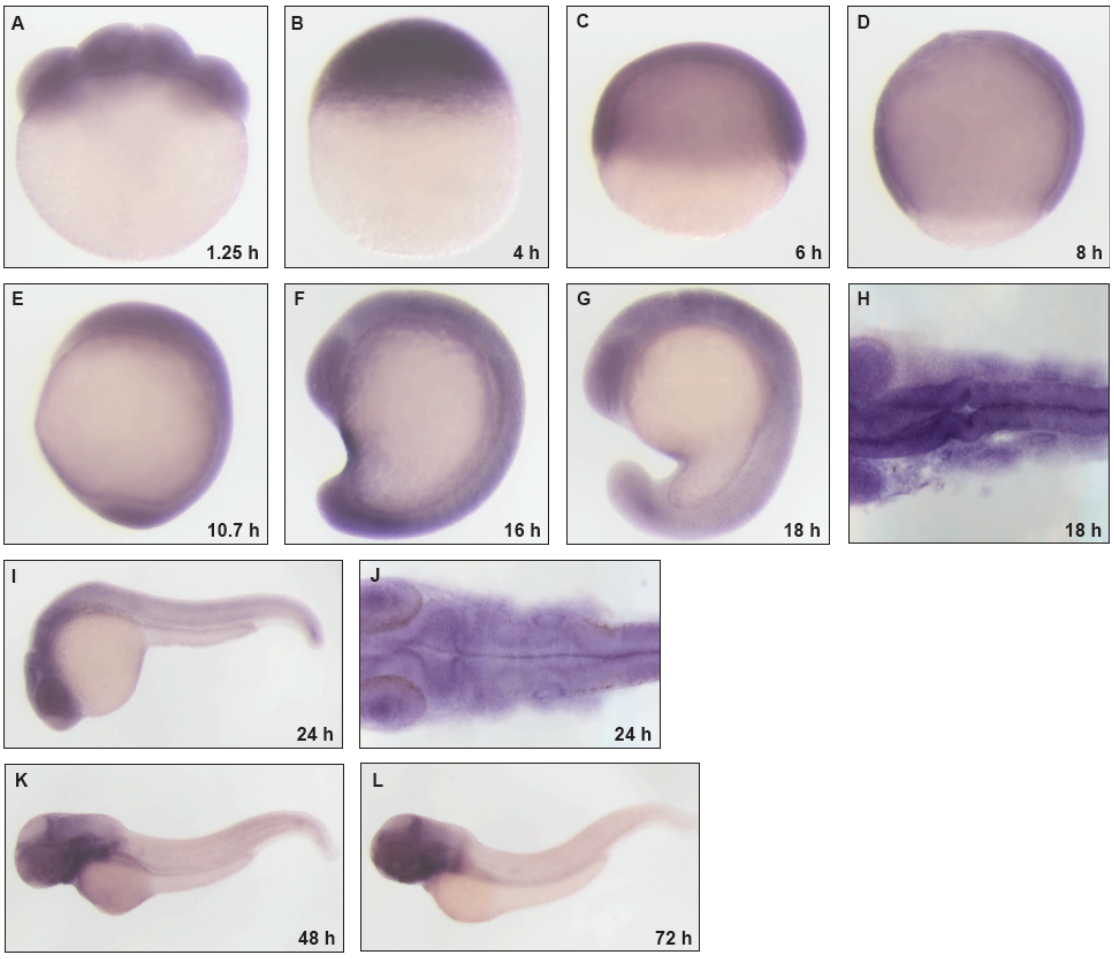

Figure 12. Whole-mount *in situ* hybridization analysis of *gpr125* expression. Lateral views, animal pole up in (A and B). Lateral views, anterior up, dorsal left in (C-G). Dorsal views, anterior left in (H and J). Lateral views, anterior left, dorsal up in (I, K and L).

At 24 hpf, *gpr124* expression was enriched in the head and tail region (Figure 11D). Co-localization between *gpr124* and *sox9a*, a chondrogenic factor expressed in pharyngeal arches (Chiang et al 2001; Yan et al 2002; Yan et al 2005), suggested that *gpr124* was expressed in the pharyngeal arch primordial (Figure 11E), and at later stages, the pharyngeal arches were positive for *gpr124* (Figure 11F-I). The specific expression of *gpr124* in the pharyngeal arches warrants future investigation of its potential function in chondrogenesis of the pharyngeal arches.

On the other hand, *gpr125* transcripts showed a different localization at later stages (Figure 12). Specifically, at 25 hpf, *gpr125* expression became enriched in the rostral region, including the hindbrain at the level of the otic vesicles, where tangential migration of FBMN occurs (Figure 12H and J) (Wada et al 2005; Wada & Okamoto 2009). By 48 hpf, *gpr125* expression was more prominent in the midbrain-hindbrain boundary, the pharyngeal arches and the pectoral fin buds (Figure 12K and L).

Gpr124 and Gpr125 share high similarities in protein domain composition

To further characterize *gpr124* and *gpr125*, I cloned the full-length coding regions of these two genes. Gpr124 and Gpr125 share a high degree of identity in protein sequence between their extracellular and transmembrane regions and remarkably their extracellular regions are composed of almost identical functional domains and motives (Figure 13). Therefore, Gpr124 and Gpr125 might act

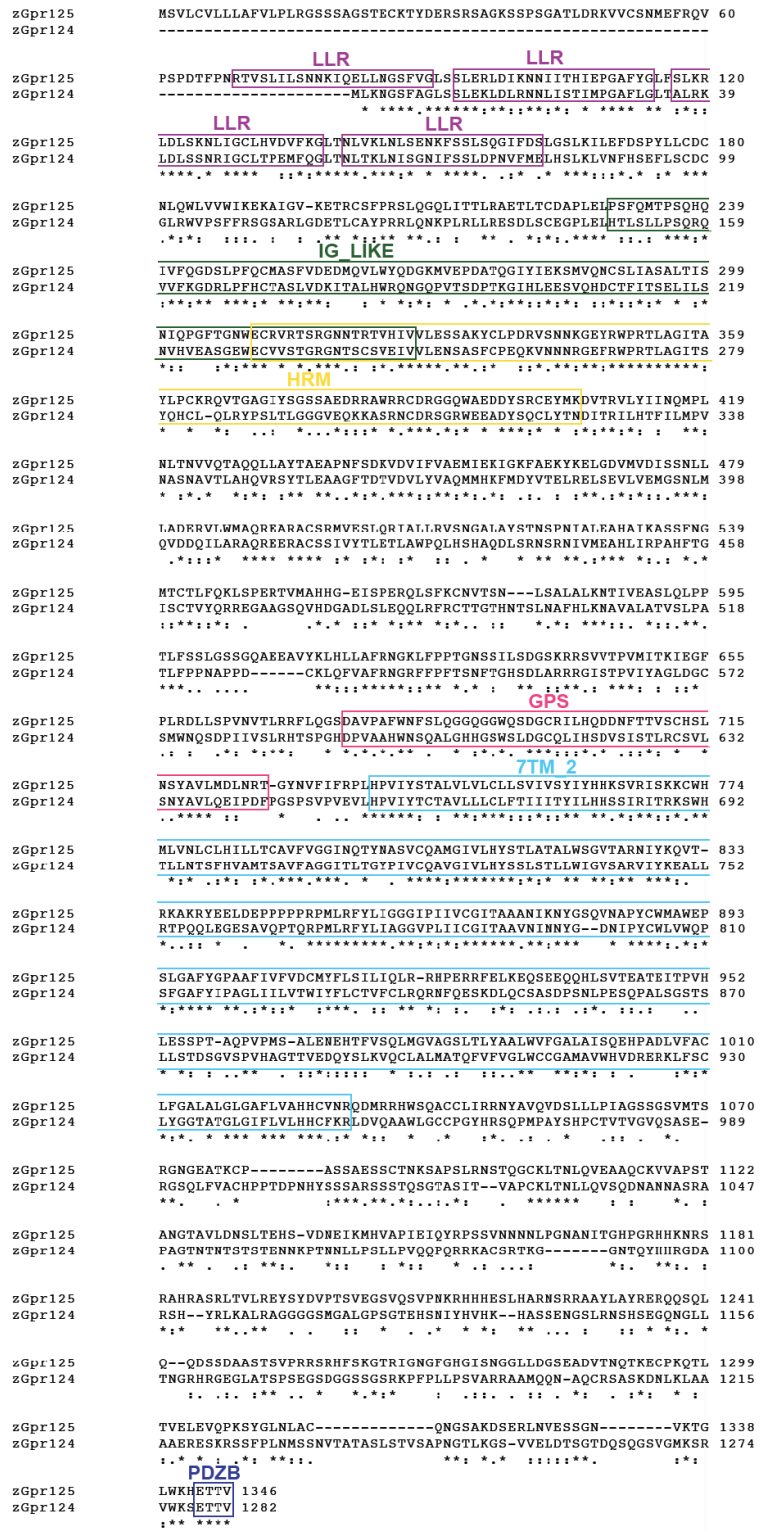

Figure 13. Protein sequence alignment between Gpr125 and Gpr124. LRR, leucine-rich repeat; IG_like, immunoglobulin_like; HRM, hormone receptor domain; GPS, GPCR proteolytic site; 7TM_2, seven-pass transmembrane type 2; PDZB, PDZ domain binding motif.

redundantly in tissues where they both are expressed at the same time. However, their intracellular regions are largely different except for the last 12 amino acids, which include a PDZBM (Figure 13). In addition, the distinct spatiotemporal expression patterns of *gpr124* and *gpr125* could allow them to contribute uniquely to development. In support of this notion, *Gpr125* knock-in null mice are morphologically normal and fertile, whereas deletion of *Gpr124* results in embryonic lethality from CNS-specific angiogenesis arrest in forebrain and neural tube in mice (Kuhnert et al ; Seandel et al 2007). Compound *Gpr125;Gpr124* mutants have not been reported.

To assess whether GPS motif mediated cleavage occurs in Gpr125, we made a construct encoding Gpr125 with a C-terminal Cherry fusion protein and expressed it in zebrafish embryos. Embryonic tissues were collected for SDS-PAGE gel electrophoresis and western blot analysis with anti-Cherry antibody to determine the size of the Cherry fusion peptide. As shown in Figure 14, the Gpr125-Cherry fusion protein exists as an uncleaved full-length peptide. Previously, it has been reported that the (-2)H(-1)L(+1)T/S cleavage consensus sequence is not present in human GPR124 and GPR125 (Promel et al 2012). Further review of the sequences of the zebrafish *gpr124* and *gpr125* homologues revealed the absence of the consensus cleavage sequence within their GPS motif. Therefore, the endogenous Gpr124 and Gpr125 proteins likely exist in their uncleaved forms. Lack of GPS cleavage activity has also been shown for several adhesion GPCRs, including CELSR/Fmi, and LAT-1/Latrophilin (Promel et al 2012; Usui et al 1999). Moreover, the GPS motif mediated cleavage per se has

been shown experimentally to be dispensable for the surface expression and function of LAT-1/Latrophilin (Promel et al 2012). Therefore, it is possible that GPS-mediated cleavage is not required for Gpr125 trafficking or activity.

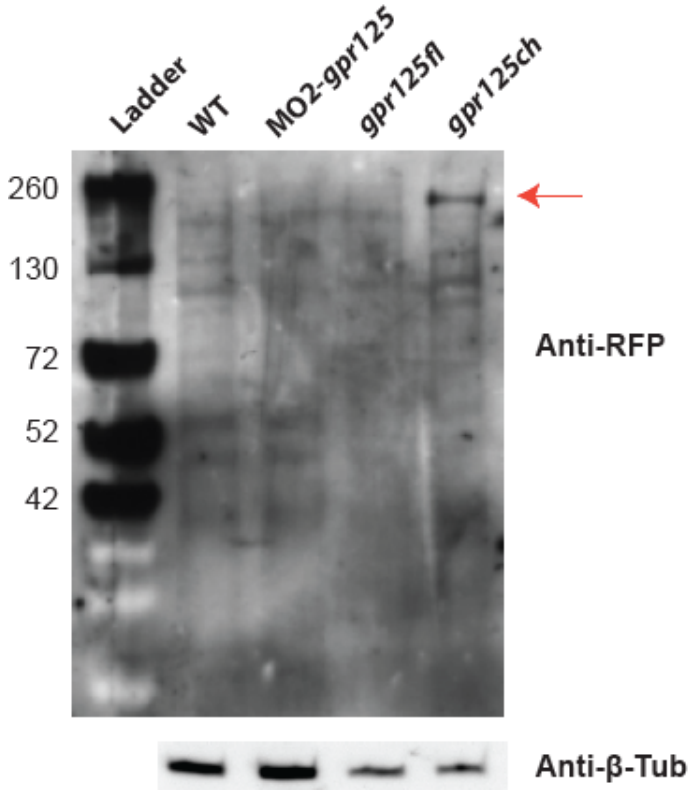

Figure 14. Western blotting analysis of Gpr125-Cherry fusion protein at 9 hpf. Red arrow marks a band matching the size of full-length Gpr125-Cherry fusion protein (174kD) present only in the sample from *gpr125-cherry* RNA injected embryos.

Gpr124 may contribute to multiple developmental processes

To assess if *gpr124* and *gpr125* are essential for early development, we designed antisense morpholino oligonucleotides (MO) to disrupt their function. Here, I describe the phenotypes of *gpr124* morphants (MO injected embryos). Studies of *gpr125* function will be presented in Chapter III.

As *gpr124* maternal transcripts are present at a low level, I decided to design MO to disrupt splicing of zygotic *gpr124* transcripts. The MO was designed to block the acceptor site of exon 6 and therefore was predicted to cause deletion of exon 6. Successful blocking of splicing will generate an immediate premature stop codon. To test the effectiveness of the MO, a pair of primers flanking exon 5 and 10 was designed. As shown in Figure 15, preventing splicing of exon 6 resulted in a smaller PCR product. When examined at 24 hpf, MO-*gpr124* specifically blocked *gpr124* transcript splicing in a dose-dependent manner, achieving nearly 100% reduction of the normal transcript at 5ng and above 70% interference at 3ng.

Interestingly, *gpr124* morphants exhibited several defects related to chondrogenesis. At 24 hpf, *gpr124* morphants showed dysmorphogenesis of the posterior trunk region. Assessment of notochord integrity by *collogen 9a (col9a) in situ* hybridization, revealed a disruption of the continuous staining in the notochord. Abnormal accumulation of cells expressing *col9a* was accompanied by the lack of staining in the adjacent region in the notochord. Occasionally, cells expressing *col9a* were spotted in ectopic positions outside of the notochord

(Figure 16E and F; 67%, n=21). At later stages, *gpr124* morphants exhibited abnormal jaw morphology and those injected with higher doses of MO-*gpr124* had more severe phenotypes (Figure 16H and I). Both the defects in the posterior trunk region and the jaw defects are consistent with the expression of *gpr124* in the posterior body and the pharyngeal arches.

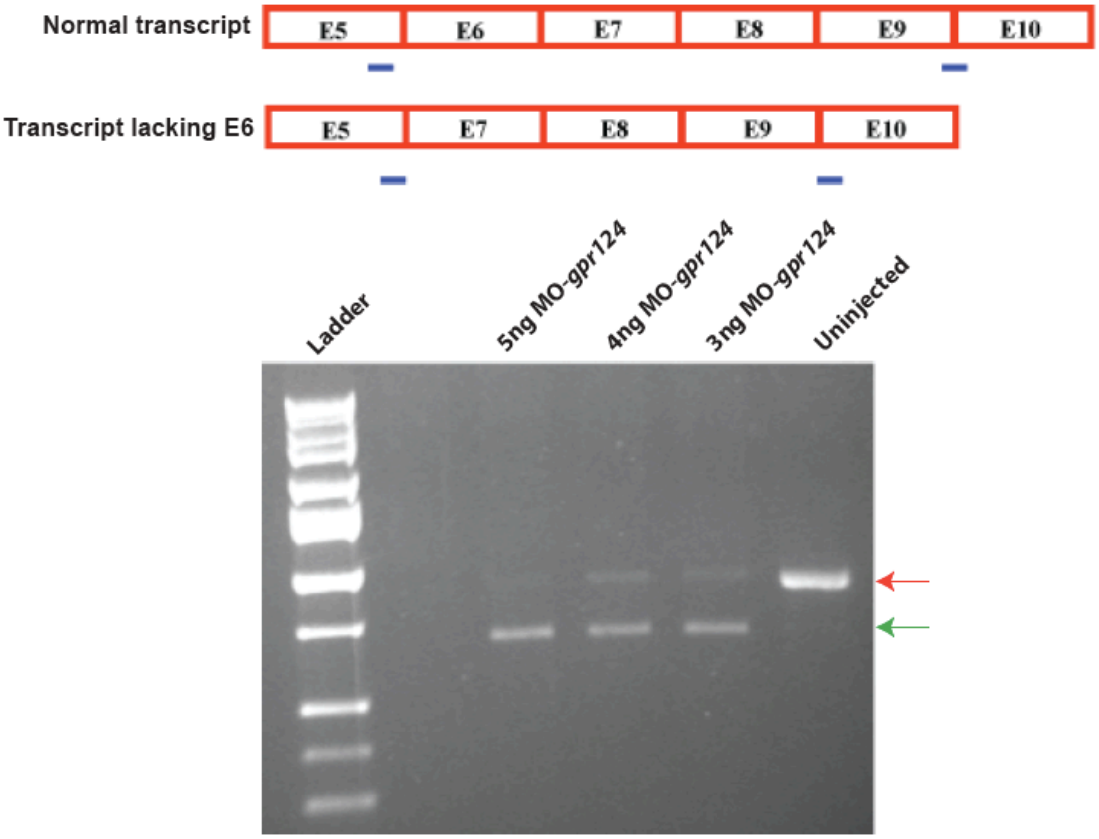

Figure 15. The effectiveness of *gpr124* splicing MO in 24 hpf embryos. Blue lines indicate primer-annealing locations. Red arrow marks PCR product from normal transcript (892bp) and green arrow marks PCR product from transcript lacking exon 6 (678bp).

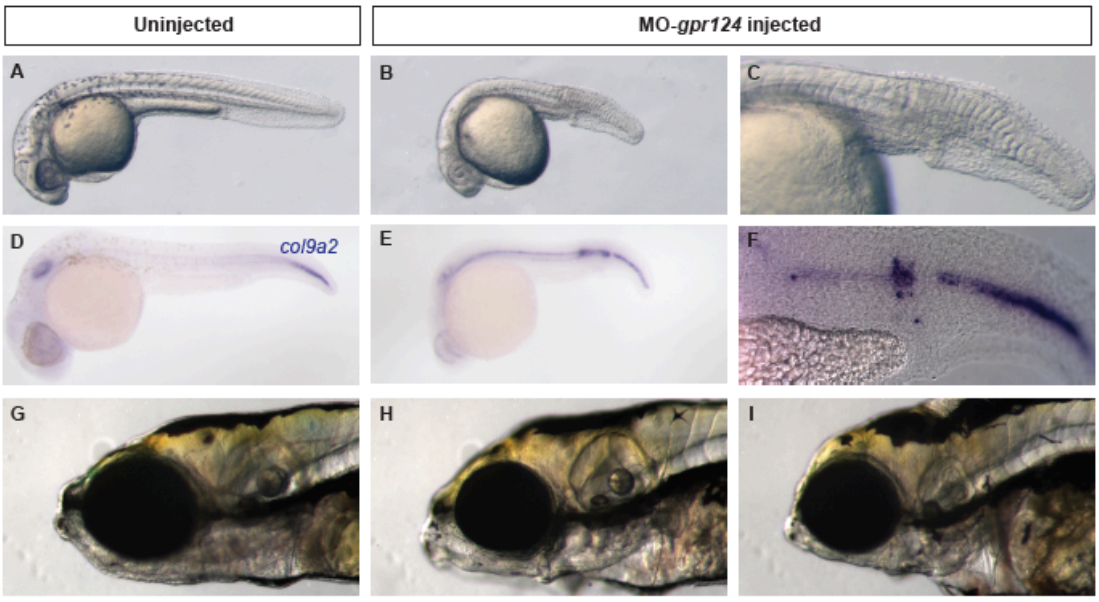

Figure 16. Phenotypes of *gpr124* morphants. (A-C) Lateral views of uninjected (A) and 3ng MO-*gpr124* injected embryos (B) at 1dpf. Anterior left, dorsal up. (C) is the enlarged view of the posterior region of an embryo similar to that in (B). (D-F) Lateral views of uninjected (D) and 3ng MO-*gpr124* injected embryos (E) after *collage 9a in situ* hybridization at 1dpf. Anterior left, dorsal up. (F) is the enlarged view of the posterior region of an embryo similar to that in (E). (G-I) Lateral views of uninjected (G), 3ng (H) and 4ng MO-*gpr124* injected embryos (I) at 7dpf. Anterior left, dorsal up.

Discussion

In summary, owing to their unique structure, adhesion GPCRs have been proposed to have vital dual roles in cellular adhesion and signaling (Yona et al 2008). This notion is corroborated by the involvement of several GPCRs in distinct developmental diseases. In this study, I have found 30 zebrafish adhesion GPCR homologues, each corresponding to a unique human adhesion GPCR. Utilizing an RT-PCR approach, I have identified seven adhesion GPCR expressed during gastrulation. Four of the seven adhesion GPCRs expressed during gastrulation belong to the Group IV subfamily. RT-PCR revealed dynamic temporal expression profiles of these four genes during the first five days of development. Each exhibited unique spatial expression patterns in the first three days of development.

Through *in silico* protein structure analyses based on the full-length coding sequences of the genes cloned in this study, I confirmed that, like their human counterparts, zebrafish Gpr124 and Gpr125 share high sequence identity and possess the same protein domains and motives in their extracellular domains. Analysis of a Gpr125-Cherry fusion protein revealed that the protein was present predominantly as an uncleaved form, providing experimental evidence to support the previously reported lack of a cleavage consensus sequence in the Gpr125 GPS motif (Promel et al 2012).

Loss-of-function experiments using *gpr124* MO revealed morphogenetic defects, which are specific to the tissues where *gpr124* is expressed. Based on our experimental data presented in this and the following chapters, we propose

that Group IV adhesion GPCRs play important roles during early zebrafish embryogenesis.

Experimental procedures

Computer-based identification of zebrafish adhesion GPCR genes

Ensembl search tool, BLASTP (http://www.ensembl.org/Multi/blastview), was used to search for potential zebrafish homologues of human adhesion GPCRs. For a given human peptide sequence, BLASTP was used to generate a list of zebrafish protein hits. Meanwhile, GPS domain (accession number, IPR000203) searches generated a list of zebrafish GPS motif-containing proteins. For all GPS motif-containing proteins and BLASTP hits sharing 30% or greater identity with human adhesion GPCRs, their domain compositions were examined. If the protein had a predicted TM7 domain and extracellular domains similar to those of a human adhesion GPCR, it was recorded as a potential zebrafish adhesion GPCR. The accuracy of the annotated coding sequences corresponding to these genes was evaluated by examining their expressed sequence tag (EST) coverage and when available their cDNA clones.

RT-PCR

Total RNA was extracted with TRI_{ZOL} LS reagent (Invitrogen) from 16-cell, 70%~90%-epiboly, 3-somite and 1 dpf wild-type (WT) embryos. cDNA was produced with the SuperScript III first-strand synthesis system (Invitrogen). Specific primers for each candidate adhesion GPCR were designed to amplify

Table 3. Nucleotide sequences of primers and antisense morpholino oligonucleotides used in chapter II.

Primer name	**Sequences**
β-actin	5'- ATGGATGAGGAAATCGCTGCCCTGGTC -3'
	5'- CCTGATGTCTGGGTCGTCCAACAATGG -3'
bai2-q	5'- GTTACGGCACGCCAAGTTAT -3'
	5'- CTGGAGATCACCCCACACTT -3'
cirl1-q	5'- CCTTTGTGGCTACTGCTTTC -3'
	5'- CGGATCATCTTGTGAAGAGT -3'
cirl2-q	5'- CTATTACGCATCAGGCTACC -3'
	5'- GAGTCGGGTTTCATAGACAT -3'
cirl3-q	5'- TCTCACAGGATATGGAGTGC -3'
	5'- GAATGGCTGTATGGTGAAAC -3'
gpr124-q	5'- CCTGTCAAACGTCCATGTTG -3'
	5'- GGAGGTGATGCCAGCTAGAG -3'
gpr125-q	5'- GGAAACTCCAGCATCCTCAG -3'
	5'- ACACGGTGGTGAAGTTGTCA -3'
gpr123-q	5'- GGGAATCGTGCTGCATTACT -3'
	5'- GCCGTAGTTGTCGATGTTGA -3'
gpr123-like-q	5'- ATGCTGCTCTGCCTGCTAAT -3'
	5'- GCCAACCACTTGACAGATCA -3'
gpr56-q	5'- ATCGAATGTGCTGGATGACA -3'
	5'- CAAAATCGAGGAAACCCAGA -3'
gpr126-q	5'- TCCTCAAGTTTTGCATCGTG -3'
	5'- GCCGTTACGTCCACAGATTT -3'
gpr116-q	5'- CAAACCTACATCCGACACCA -3'
	5'- AGGCCTCAGATTGCTTTTCA -3'
gpr113-q	5'- AAAGGACGTAGCCAAGAGCA -3'
	5'- CTCTCCAACGCAGTTTGTCA -3'
No.21-q	5'- TTTGTCGTTGTCCGATGTGT -3'
	5'- GCAGTTTTCCTCGTAATGCC -3'
No.23-q	5'- GCCTGTTTGTTCATGTGGTG -3'
	5'- TGACACTGGAGACCTGGGTT -3'
No.24-q	5'- GGTGGCACTATTTGGGGTTA -3'
	5'- TCCTCATGATGCTGTGCTGT -3'
emr1-q	5'- AGTCCTGGAGTGAATAATGTGG -3'
	5'- ACACAGATGAAGAGCAACACAG -3'
emr2-q	5'- AGTCCTGGAGTGAATAATGTGG -3'
	5'- CTGGGAGAGGTTCTTTACACAG -3'
emr3-q	5'- AGTCCTGGAGTCAATAATGTGG -3'
	5'- GGAGCTGATCTGTGATAGGTTC -3'
cirl2-probe	5'- CGGACAAATCCAGGACTTCA -3'
	5'- TCAAAATGCAGCATCGTCCA -3'
No.21-probe	5'- TTGGAGATCAGTGACATCAGCCAGAGG -3'
	5'- GTCCCCTTTGTCCAGCTGAAGATGATG -3'
gpr123-probe	5'- TCGCCTCCATCATCACCTACATAGTGC -3'
	5'- AATGTGAAATGAAAGTTCCCGCTCTCG -3'
gpr123-like-probe	5'- GGACCAACTGCCTTCTTGGTCTTGGTA -3'
	5'- CATGTTGACTACTGTTCCGGCTCAGTG -3'
gpr124-probe 1	5'- GGAGGAACAGCTACCGGTTTAGGCATC -3'
	5'- TTATACAGTCGTCTCGCTCTTCCATACCCT -3'
gpr124-probe 2	5'- CAACTAAGATTTCGCTGCACCACAGGA -3'
	5'- TCAGGCAGAAAACAGTGCACAGGAAGT -3'
gpr125-probe 1	5'- GAGCTCAAAGAACAATCCGAGGAGCA -3'
	5'- TACTCGCGCAAAACTGTGAGCCTGCTA -3'
gpr125-probe 2	5'- TAGGAGTGAAGGAAACTCGCTGCTCGT -3'
	5'- GCTTGACAAACGCTCGCATTGTATGTC -3'
gpr124fl	5'- ATGCTGAAAAATGGCTCCTTC -3'
	5'- TTATACAGTCGTCTCGCTCTTCCA -3'
gpr125fl	5'- ATGTCGGTGCTTTGCGTC -3'
	5'- CTACACAGTAGTTTCATGCTTCCAC -3'
gpr124splc	5'- CTTCCATTCTGAGTTCCTGTCGT -3'
	5'- CAGCTCACGCAGTTCTGTAACAT -3'
MO name	
MO-*gpr124spl*	5'- TACTCCAGCCGTCGTTGATATGTTC -3'

products ~200bp in length (Table 3). In order to avoid genomic DNA contamination and to verify annotations, primers were designed to amplify fragments composed of multiple widely separated exons. For adhesion GPCRs expressed during or shortly after gastrulation, ~1kb fragments of their coding sequences were cloned to serve as templates to generate labeled anti-sense RNA probes for whole-mount *in situ* hybridization (WISH). Primer sequences for template amplification were listed in Table 3.

The full-length *gpr124* and *gpr125* coding sequences were amplified using *gpr124fl* and *gpr125fl* primers (Table 3) with Easy-A high-fidelity PCR cloning enzyme (Agilent Technologies) and subcloned into pCR8 vector (Invitrogen). A construct containing sequence encoding Gpr125 with a Cherry protein fused to its C-terminus was made by recombining Gpr125 coding sequence from pCR8 and Cherry coding sequence from p3E-Cherry into the recombination-compatible pCS-Dest2 vector (Villefranc et al 2007) with Gateway® LR clonase® II plus enzyme (Invitrogen)

Whole-mount *in situ* hybridization (WISH)

To assess the maternal mRNA deposition of adhesion GPCR genes, embryos at cleavage stage (before the onset of zygotic transcription), were fixed in 4% paraformaldehyde (Sigma) overnight at 4°C for WISH analyses. To examine their spatial and temporal expression during gastrulation, early, late gastrulation stages and early segmentation stages embryos were fixed similarly for WISH analyses. To complete their expression profile, tissue-specific expression during the pharyngula and the hatching period was analyzed with

WISH. Antisense probes were synthesized with RNA labeling kits (Roche). WISH analyses were performed as described previously (Marlow et al 1998).

Western blot analysis

Embryos overexpressing Gpr125-Cherry protein were collected at 9 hpf and deyolked according to (Link et al 2006). The samples were dissolved in 2 μl 2X Laemmli SDS-sample buffer per embryo and incubated at 65 °C for 30 min to denature 7TM-contaning proteins without rendering them insoluble. After full speed centrifugation for 2 min at room temperature, samples were loaded on a SDS-PAGE gel (Fisher Bioreagents). Electrophoresis and transfer were performed according to manufactures manual using Bio-Rad equipment and PVDF membranes from Millipore. Membranes were blocked in 4% BSA in TBST at room temperature for 1h prior to incubation with antibodies. Antibodies were diluted in TBST with 4% BSA. Primary antibodies used were: rat monoclonal anti-RFP antibody (1:1000, Chromotek, clone 5F8) and mouse monoclonal anti-β-Tubulin antibody (1:1000, Sigma DM1A) and secondary antibody was goat polyclonal anti-mouse HRP conjugate (1:10000, Millipore, 12-349). Amersham™ ECL plus western blotting detection system (GE Healthcare) was used and signals were detected with Amersham Hyperfilm™ ECL (GE Healthcare) or Fujifilm LAS-3000.

CHAPTER III

THE ADHESION GPCR GPR125 MODULATES DISHEVELLED DISTRIBUTION AND PLANAR CELL POLARITY SIGNALING

Running title: Gpr125 modulates PCP signaling

This paper has been published under the same tile in *Development*, 2013
Xin Li[1,2], Isabelle Roszko[3], Diane S. Sepich[3], Mingwei Ni[4], Heidi E. Hamm[1,5], Florence L. Marlow[2*] & Lilianna Solnica-Krezel[1,3,6*]
[1]Neuroscience Graduate Program, Vanderbilt University School of Medicine, Nashville, TN 37232, USA; [2]Department of Developmental and Molecular Biology, Albert Einstein College of Medicine, Bronx, NY 10461, USA; [3]Department of Developmental Biology, Washington University School of Medicine, St. Louis, MO 63110, USA; [4]Department of Surgery, New York Hospital Medical Center of Queens, Flushing, NY 11355, USA; [5]Department of Pharmacology, Vanderbilt University School of Medicine, Nashville, TN 37232, USA; [6]Department of Biological Sciences, Vanderbilt University, Nashville, TN 37232, USA
*Corresponding author emails: Email: solnical@wustl.edu and florence.marlow@einstein.yu.edu

Introduction

During embryogenesis, gastrulation establishes the three germ layers and the animal body plan. Vertebrate gastrulation relies on polarized cell behaviors to drive convergence and extension (C&E) movements that narrow embryonic tissues mediolaterally and elongate them anterio-posteriorly (Gray et al 2011; Keller et al 2000b; Solnica-Krezel 2005; Yin et al 2009). In dorsal regions of *Xenopus* and zebrafish gastrulae, cells become elongated and align along the mediolateral embryonic axis, allowing preferential intercalation between their anterior and posterior neighbors to drive C&E (Jessen et al 2002; Keller et al

2000b; Lin et al 2005; Marlow et al 2002; Topczewski et al 2001). Modulation of cell adhesion and intercellular signaling have been proposed to instruct such complex cell behaviors (Yin et al 2009). However, the molecules implementing these actions are not fully identified.

Currently, the Wnt/PCP signaling system, equivalent to the PCP pathway coordinating wing hair and ommatidia orientation in *Drosophila* (Goodrich & Strutt 2011; Simons & Mlodzik 2008), is the best-studied pathway regulating C&E movements in vertebrates (Gray et al 2011; Tada & Kai 2009; Yin et al 2009). Polarized cell behaviors underlying C&E, including directed cell migration and polarized planar and radial intercalations, are exquisitely sensitive to PCP signaling levels, as excess or insufficient Wnt/PCP pathway component function impairs C&E movements (Carreira-Barbosa et al 2003; Jessen et al 2002; Marlow et al 2002; Wallingford et al 2000). In addition to regulating C&E, a subset of Wnt/PCP components also regulate the caudal tangential migration of facial branchiomotor neurons (FBMN) in zebrafish and mouse (Carreira-Barbosa et al 2003; Jessen et al 2002; Wada et al 2005; Wada & Okamoto 2009; Wada et al 2006).

PCP pathway components are known to localize asymmetrically in multiple tissues manifesting planar polarity. In the fly wing epithelia, the receptor Frizzled and cytoplasmic proteins Dishevelled (Dsh/Dvl in vertebrates) and Diego localize to the distal side of the cell, where the wing hair will eventually emerge, the transmembrane protein Van gogh/Strabismus and cytoplasmic protein Prickle (Pk) localize proximally, and the seven transmembrane protocadherin

Flamingo/Starry night is present at both cell edges (Axelrod 2001; Bastock et al 2003; Feiguin et al 2001; Strutt et al 2002; Tree et al 2002). This stereotyped asymmetric localization of Pk and Dvl on opposing anterior and posterior membranes has been observed in the neural plate and dorsal mesodermal cells undergoing C&E in zebrafish (Ciruna et al 2006; Yin et al 2008). Such molecular asymmetries are considered either a consequence of cell polarization or an essential step in the process of Wnt/PCP-mediated cell polarization (Goodrich & Strutt 2011; Gray et al 2011; McNeill 2010; Simons & Mlodzik 2008).

Asymmetric localization of PCP components in polarized epithelia and protein interaction studies supports a model whereby PCP components interact in asymmetric membrane complexes spanning the juxtaposed cells to generate planar polarization (Goodrich & Strutt 2011; McNeill 2010). Recently, Dsh was shown to cluster PCP complexes into membrane subdomains in cells of *Drosophila* pupal wings (Strutt et al 2011), raising the possibility that clustering of asymmetric PCP complexes into membrane subdomains might provide a local self-enhancement mechanism that establishes and/or maintains planar polarity (Strutt et al 2011). Interestingly, membrane clustering of PCP components occurs between *Xenopus* Van gogh-like 2 (Vangl2, vertebrate homolog of Van gogh/Strabismus) and *Drosophila* Pk expressed in *Xenopus* animal cap explants, and among zebrafish Frizzled7 (Fzd7), Wnt11 and *Xenopus* Dvl expressed in zebrafish blastula (Jenny et al 2003b; Witzel et al 2006). In the latter case, subdomain formation correlates with increased persistence of membrane contacts partially dependent on vertebrate Flamingo homologues, Cadherin EGF

LAG seven-pass G-type receptors (Celsrs) (Witzel et al 2006).

Celsrs belong to the family of adhesion G protein-coupled receptors (GPCRs), which are chimeras of adhesion molecules and transmembrane signal transducer GPCRs (Fredriksson et al 2003). Owing to their unique structure, adhesion GPCRs are postulated to play dual roles in cell adhesion and signal transduction (Yona et al 2008). Recent studies of GPR56, GPR124 and Gpr126 implicate adhesion GPCRs in diverse developmental processes, including brain development, blood vessel formation and myelination in zebrafish and mammals (Kuhnert et al ; Monk et al 2009; Monk et al 2011; Piao et al 2004). As components of the PCP pathway, Celsr adhesion GPCRs have been reported to regulate zebrafish gastrulation and FBMN migration (Carreira-Barbosa et al 2009; Formstone & Mason 2005; Wada et al 2006).

To better understand the molecular mechanisms underlying gastrulation movements and uncover the functions of uncharacterized adhesion GPCRs, we surveyed adhesion GPCRs to identify candidate regulators of zebrafish gastrulation. Here, we identified Gpr125 adhesion GPCR as a modulator of C&E gastrulation movements and FBMN migration. We provide evidence that Gpr125 functionally interacts with multiple Wnt/PCP components and directly interacts via its intracellular domain with Dvl. Mutual redistribution of Gpr125 and Dvl fusion proteins into discrete membrane subdomains and their ability to selectively recruit additional PCP components into these domains suggest that Gpr125 might act as a component of the PCP membrane complexes and modulator of Wnt/PCP signaling in vertebrates.

Results

Excess Gpr125 disrupts C&E movements and underlying cell polarity

Like other adhesion GPCRs, Gpr125 has a long extracellular subunit with protein-protein interacting domains and a GPCR subunit (Figure 17A). The last four amino acids (ETTV) of Gpr125 constitute a PDZ-binding motif (Figure 17A), which is also found in transmembrane PCP pathway components, Fzd and Vangl2 (Hering & Sheng 2002; Jessen et al 2002). Using semi-quantitative RT-PCR and whole-mount *in situ* hybridization (WISH) analyses, we determined that *gpr125* transcripts were maternally provided and uniformly distributed at blastula and gastrula stages (Figure 17B-D). Notably, at 25 hpf, *gpr125* expression became enriched in the rostral region, including the hindbrain at the level of the otic vesicles, where tangential migration of FBMN occurs (Figure 17E) (Wada et al 2005; Wada & Okamoto 2009).

Since gastrulation movements are sensitive to both elevated and reduced levels of their regulators (Carreira-Barbosa et al 2003; Jessen et al 2002; Lin et al 2009; Marlow et al 2002; Wallingford et al 2000; Zeng et al 2007), we investigated Gpr125 function through both gain- and loss-of-function (GOF and LOF) approaches. Microinjection of synthetic *gpr125* RNA into wild-type (WT) zygotes caused dose-dependent shortening of the anterio-posterior (AP) axis and synophthalmia or cyclopia (Figure 18A-K), phenotypes suggestive of C&E defects (Carreira-Barbosa et al 2003; Formstone & Mason 2005; Heisenberg et al 2000; Jessen et al 2002; Marlow et al 2002; Marlow et al 1998; Topczewski et al 2001). To determine if such dysmorphologies were due to an earlier C&E

gastrulation defect, we compared expression of tissue-specific markers in *gpr125* RNA injected and control embryos at late gastrulation (2-somite stage) (Figure 18L-O). The expression of *distal-less homeobox 3* (*dlx3)* in the border of the neural ectoderm, and *paraxial protocadherin* (*papc*) in the adaxial and paraxial mesoderm revealed mediolaterally broader but anterio-posteriorly shorter neural ectoderm, notochord, and somites (89%, n= 37; Figure 18M,O). In addition, the prechordal mesoderm, marked by *hatching gland 1* (*hgg1*), failed to migrate beyond the anterior edge of the neural ectoderm and was abnormally elongated in 35% of *gpr125*-injected embryos (n= 37; Figure 18M). Compromised anterior movement of the prechordal mesoderm relative to the overlying neural ectoderm has been proposed to cause synophthalmia or cyclopia in embryos with deficient or excess PCP pathway components (Heisenberg et al 2000; Marlow et al 2002; Marlow et al 1998). At high doses of *gpr125* RNA (*i.e.* 400 pg), a small fraction of embryos exhibited dorsoventral axis patterning defects, including expansion of dorsal markers at 5 hpf (XL, FLM and LSK unpublished data) and tail truncation at 24 hpf (Figure 18E). Therefore, Gpr125 GOF phenocopies C&E defects reported for GOF/LOF of PCP pathway components (Carreira-Barbosa et al 2009; Formstone & Mason 2005; Jessen et al 2002; Marlow et al 2002; Topczewski et al 2001) and disrupts patterning only when expressed in great excess. At the cellular level, Gpr125-Cherry overexpressing embryos had extra columns of cells in the notochord as compared to controls, indicating a deficiency

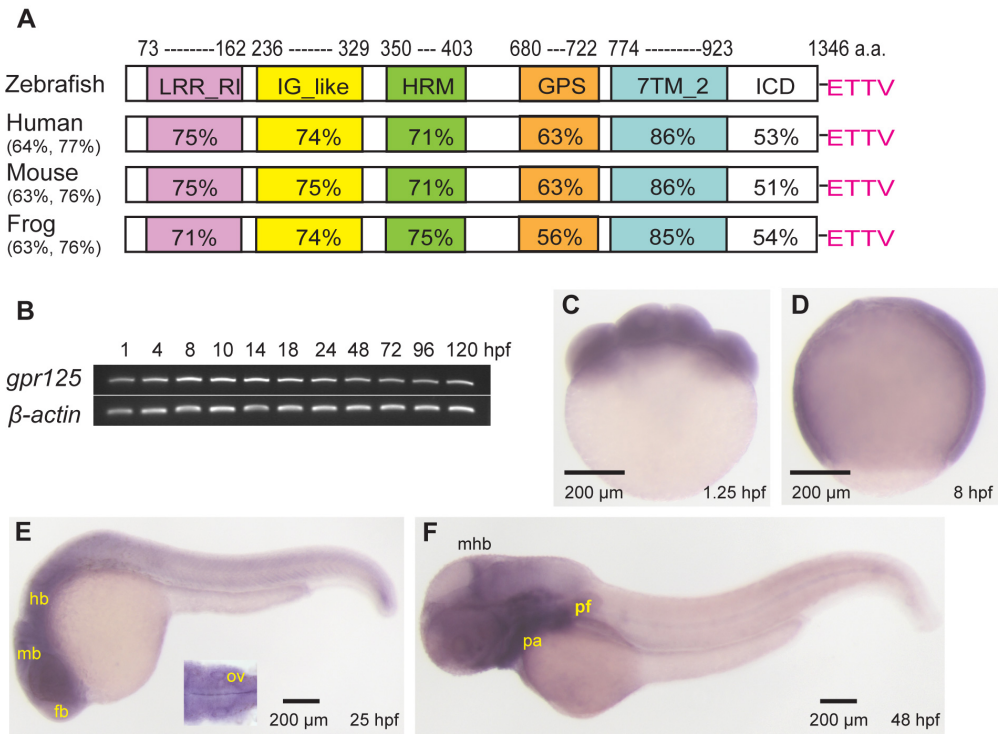

Figure 17. Predicted protein domains and spatiotemporal expression profile of *gpr125* during early zebrafish development. (A) Schematics of predicted zebrafish Gpr125 protein domains. The percentage of amino acid identities or similarities between Gpr125 peptide sequences in vertebrates for the whole protein are included in parentheses, and for individual domains on the schema. LRR_RI, leucine-rich repeat_ribonuclease inhibitor type; IG_like, immunoglobulin_like; HRM, hormone receptor domain; GPS, GPCR proteolytic site; 7TM_2, seven-pass transmembrane type 2; and ICD, intracellular domain. The PDZBM (ETTV) at the C-terminus are labeled in pink. (B) RT-PCR of *gpr125* transcripts from 1 to 120 hpf. *β-actin* was used as a loading control. (C-F) WISH profile of *gpr125* expression. Lateral views, anterior up in (C; D) and left in (E; F). fb, forebrain; hb, hindbrain; mb, midbrain; mhb, midbrain-hindbrain boundary; ov, otic vesicle; pa, pharyngeal arches; and pf, pectoral fin.

Figure 18. Excess Gpr125 leads to C&E movement defects. (A-E) Lateral views of uninjected or *gpr125* RNA injected embryos at 1 dpf. Anterior left. (B-E) AP axis length phenotypic categories. Blue: greater than 95%; green: 80%-95%; yellow: 40%-79%; and red: smaller than 40% of control embryos' average AP axis length. Arrowheads in D and E indicate the cyclopic eyes and change of head position. (F-J) Ventral views of uninjected or *gpr125* RNA injected embryos at 3 dpf. Anterior left. Eye fusion defects were categorized into five groups (*I*-*V*) according to (Marlow et al 1998). (K) Quantification of AP axis shortening and eye fusion phenotypes. The colored bars correspond to the AP axis length phenotypic categories shown in (B-E). Eye fusion phenotypes were quantified by cyclopia index (CI) according to (Marlow et al 1998). CI values are above the bars and numbers of embryos analyzed inside the bars. (L-O) WISH analyses of marker gene expression in uninjected or 200 pg *gpr125* RNA injected embryos at the 2-somite stage. (L; M) Animal pole views, ventral up. (N; O) Dorsal views, anterior up. n, notochord; ne, neural ectoderm border; pm, prechordal mesoderm; and s, somites. Red line indicates the width of the notochord at the first somites. (P-Q) Membrane EGFP (mEGFP) labeled notochord (n) of control or 200 pg *gpr125-Cherry* RNA injected embryos at the 1-somite stage. Anterior up. All measured notochord cells are outlined and the notochord boundary of the *gpr125*-injected embryo is marked with dashed lines. (R-U) Analyses of LWR and ML alignment in the ectoderm or notochord of control (n=3 embryos, 158 and 131 cells respectively) or 200 pg *gpr125-Cherry* RNA injected embryos (n=6 embryos, 266 and 220 cells respectively) at the 1-somite stage. Rose diagrams depict cell orientation relative to the AP axis (vertical dashed line). Corresponding LWRs are expressed as mean±SEM in the lower right corners. (V and W) Punctate and cytosolic distribution of Pk-GFP in control or *gpr125* RNA injected embryos. (X) Classes of Pk-GFP distribution in control or *gpr125* RNA injected embryos (155 or 183 cells, respectively). (Y and Z) ML alignment and LWR of ectodermal cells analyzed for Pk-GFP localization in control or *gpr125* RNA injected gastrulae.

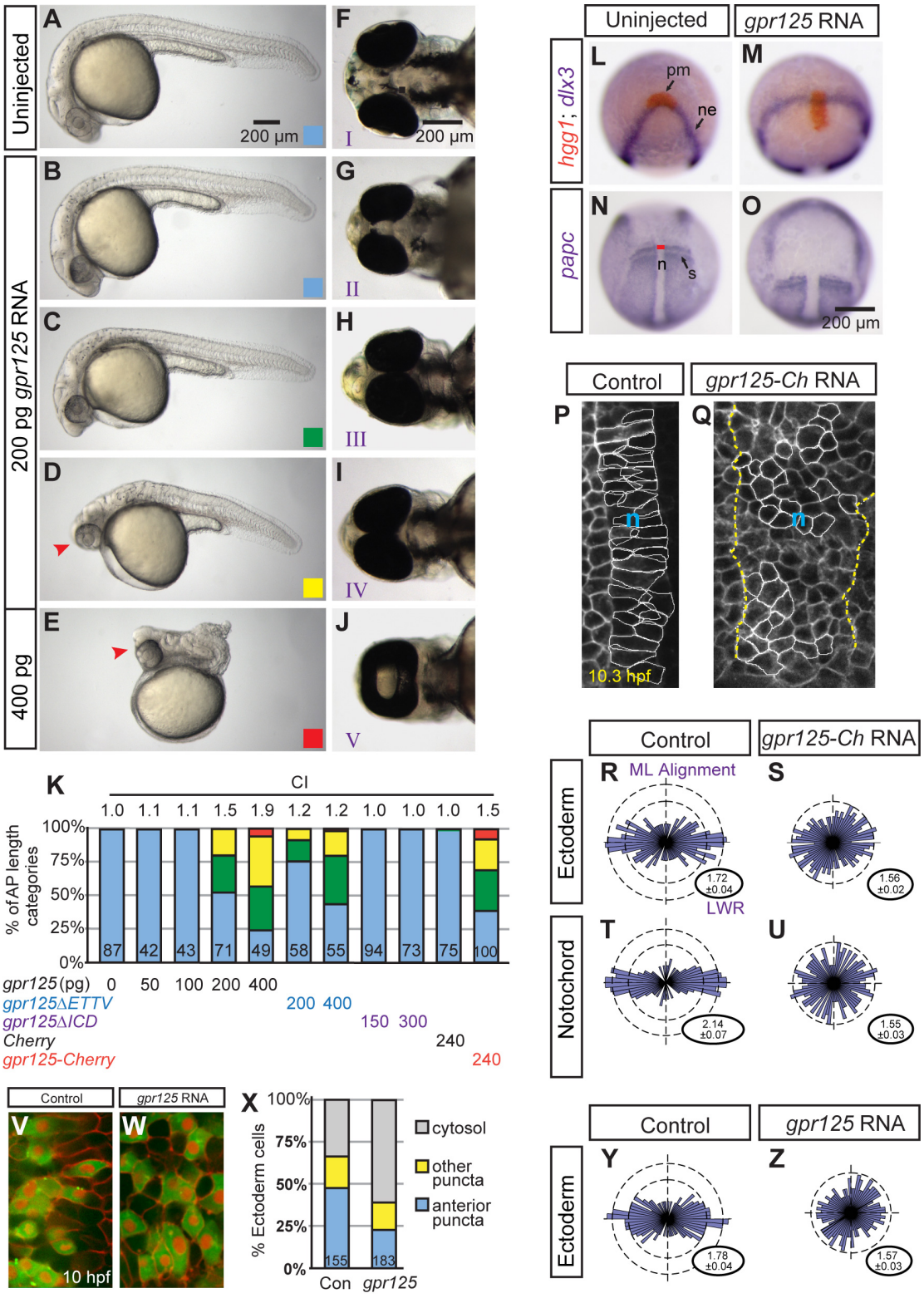
Uninjected
200 pg gpr125 RNA
400 pg
A
B
C
D
E
F
G
H
I
J
200 µm
I
II
III
IV
V
Uninjected
gpr125 RNA
hgg1; dlx3
papc
L
M
N
O
pm
ne
n
s
200 µm
Control
gpr125-Ch RNA
P
Q
n
10.3 hpf
K
CI
1.0 1.1 1.1 1.5 1.9 1.2 1.2 1.0 1.0 1.0 1.5
% of AP length categories
100%
75%
50%
25%
0%
87 42 43 71 49 58 55 94 73 75 100
gpr125 (pg) 0 50 100 200 400
gpr125ΔETTV 200 400
gpr125ΔICD 150 300
Cherry 240
gpr125-Cherry 240
Control
gpr125-Ch RNA
Ectoderm
Notochord
R
ML Alignment
S
1.72 ±0.04
LWR
1.56 ±0.02
T
U
2.14 ±0.07
1.55 ±0.03
Control
gpr125 RNA
V
W
10 hpf
X
% Ectoderm cells
100%
75%
50%
25%
0%
155
183
Con
gpr125
cytosol
other puncta
anterior puncta
Control
gpr125 RNA
Ectoderm
Y
Z
1.78 ±0.04
1.57 ±0.03

in mediolateral intercalation (Figure 18Q). Indeed, morphometric analysis revealed defects in mediolateral cell elongation and alignment, two PCP-dependent polarized cell behaviors essential for mediolateral intercalation (Gray et al 2011; Keller et al 2000b). In 1-somite stage control embryos, 55% of dorsal ectodermal cells oriented their long axes within a 20° arc perpendicular to the notochord and exhibited an average length-to-width ratio (LWR) of 1.72±0.04 (n= 158; Figure 18R). Moreover, 76% of notochord cells oriented mediolaterally with an average LWR of 2.14±0.07 (n= 131; Figure 18T), consistent with previous reports (Jessen et al 2002; Marlow et al 2002; Topczewski et al 2001). In contrast, in *gpr125-Cherry* RNA-injected embryos, only 32% of ectodermal cells and 30% of notochord cells exhibited normal mediolateral alignment (Figure 18S and U) and showed reduced LWRs of 1.56±0.02 (n= 266; $p<0.001$) and 1.55±0.03 (n= 220; $p<0.001$), respectively. In addition, we analyzed *Drosophila* Pk-GFP localization in Gpr125 overexpressing ectodermal cells (Figure 18V-Z). Consistent with previous reports, Pk-GFP puncta preferentially localized at the anterior edge of ectodermal cells in control gastrulae (Figure 18V and X) (Ciruna et al 2006; Yin et al 2008). However, in embryos overexpressing Gpr125, the percentage of cells with anterior Pk-GFP puncta decreased concomitant with an increase in cells with cytoplasmic Pk-GPF (Figure 18W and X). These results indicate that *gpr125* GOF impaired both molecular and morphological planar cell polarities during C&E movements.

Reduced Gpr125 enhances C&E defects of PCP mutants

To determine if *gpr125* is essential for C&E movements, we used two antisense morpholino oligonucleotides (MOs) to disrupt its translation. Both MOs blocked translation of synthetic RNA encoding GFP fused to *gpr125* MO target sequences (Figure 19A-I). However, given that MO1-*gpr125* caused non-specific cell death, which was suppressed by concurrent loss of *p53* function (Figure 19J-K) (Robu et al 2007), MO2-*gpr125* was mainly used in this study. Although *gpr125* MOs did not cause specific morphological defects in WT embryos (Figure L-W), they enhanced the phenotypes of PCP mutants (Figure 20-22). PCP homozygous mutants, such as maternal-zygotic (MZ) *scribble1 (scrb1)/landlocked (llk)* (Wada et al 2005) and *vangl2/trilobtie (tri)* (Jessen et al 2002; Marlow et al 1998), exhibit shortened AP axis and variable degrees of cyclopia. Intriguingly, injection of MO2-*gpr125*, but not a control MO, further shortened the AP axis and significantly increased the penetrance and expressivity of cyclopia in these mutants (Figure 20A-F and Table 4). Similar enhancement of cyclopia was observed with MO1-*gpr125* and MO2-*gpr125* in MZ*wnt11/silberblick (slb)* homozygous mutants (Figure 20G and Table 5) (Heisenberg et al 2000). Notably, MO2-*gpr125* injection caused significant shortening of the AP axis relative to uninjected or control MO-injected *scrb1/llk* and *vangl2/tri* heterozygous embryos, which do not manifest morphologic C&E defects (Figure 20H-J) (Solnica-Krezel et al 1996; Wada et al 2005). Supporting the specificity of MO2-*gpr125*, synthetic *gpr125* RNA lacking the MO2-*gpr125* binding site, but not water or RNA encoding membrane EGFP (mEGFP),

Figure 19. Effective *gpr125* MOs cause no noticeable morphological defects in WT embryos. (A-D) Live images of uninjected (A), 100 pg *5'-gpr125-T1-GFP* RNA (GFP reporter for MO1-*gpr125*) injected (B), or 100 pg *5'-gpr125-T1-GFP* RNA and MO1- *gpr125* co-injected embryos (C-D) at the 70%-epiboly stage. (E-H) Live images of uninjected (E), 100 pg *5'-gpr125-T2-GFP* RNA (GFP reporter for MO2-*gpr125*) injected (F), or 100 pg *5'-gpr125-T2-GFP* RNA and MO2-*gpr125* co-injected embryos (G-H) at the 75%-epiboly stage. (I) Western blot quantification of GFP reporter protein levels in MO1-*gpr125* injected embryos. The density of the GFP bands was normalized to that of the Actin bands and the signal intensity relative to uninjected embryos is shown. Error bars, ± SEM. **p < 0.01, ***p < 0.001. (J-K) Lateral views of 5.4 ng MO1-*gpr125* injected WT (J) or $p53^{M214K/M214K}$ embryos (K) at 1 dpf. Anterior left. Arrows in (J) indicate regions of significant cell death. (L-O) WISH analyses of marker gene expression in uninjected (L and N) and 2.7 ng MO1-*gpr125* injected embryos (M and O) at the 2-somite stage. (L; M) Animal pole views, ventral up. (N; O) Dorsal views, anterior up. n, notochord; ne, neural ectoderm border; pm, prechordal mesoderm; and s, somites. Red line in (N) indicates the width of the notochord at the first somites. (P-W) Uninjected embryos or embryos injected with increasing doses of MO2-*gpr125* at 1 dpf or 3 dpf.

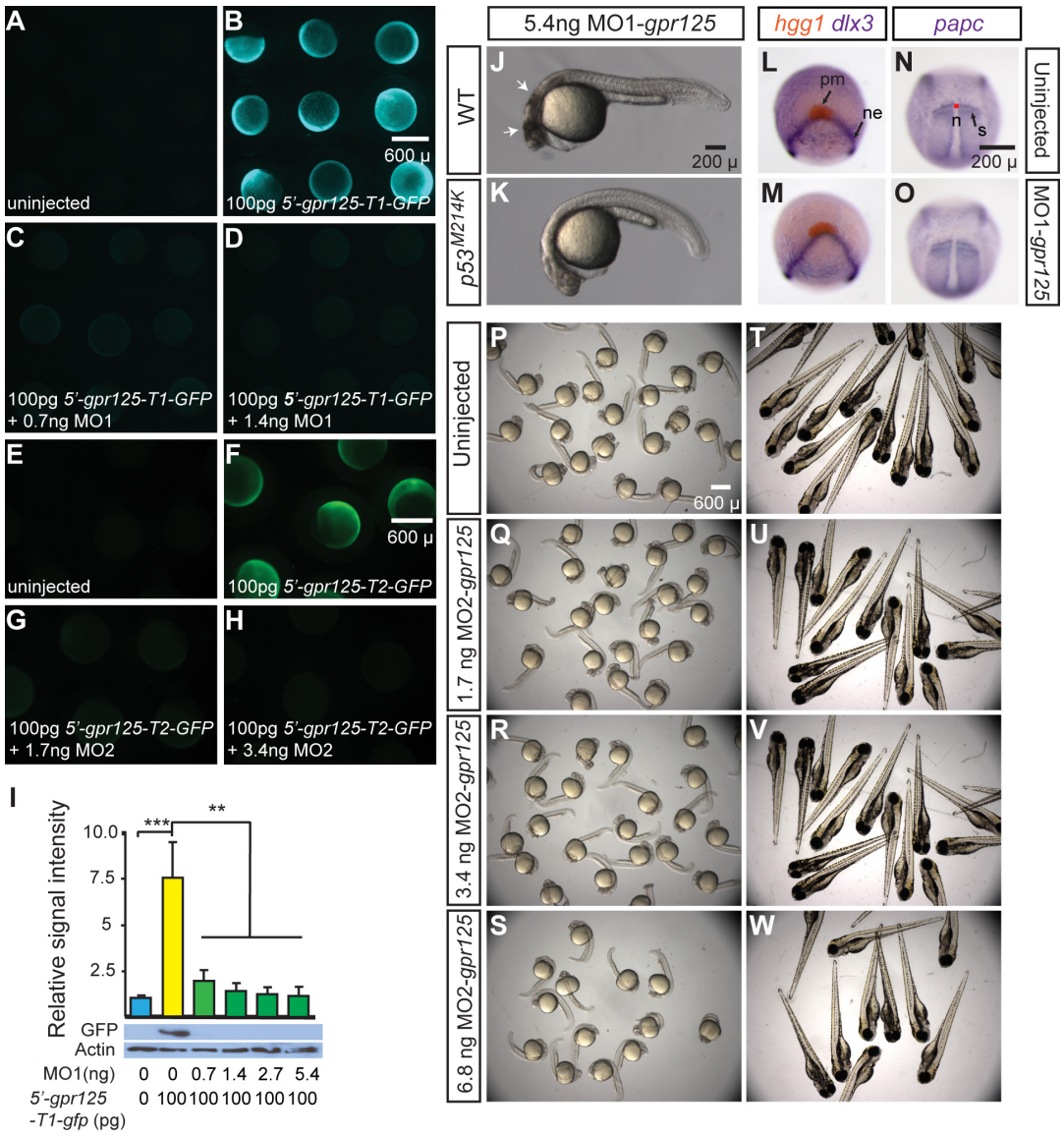
A
uninjected
B
600 µ
100pg 5'-gpr125-T1-GFP
C
100pg 5'-gpr125-T1-GFP
+ 0.7ng MO1
D
100pg 5'-gpr125-T1-GFP
+ 1.4ng MO1
E
uninjected
F
600 µ
100pg 5'-gpr125-T2-GFP
G
100pg 5'-gpr125-T2-GFP
+ 1.7ng MO2
H
100pg 5'-gpr125-T2-GFP
+ 3.4ng MO2
I
Relative signal intensity
10.0
7.5
5
2.5
***
**
GFP
Actin
MO1(ng) 0 0 0.7 1.4 2.7 5.4
5'-gpr125 -T1-gfp (pg) 0 100 100 100 100 100
5.4ng MO1-gpr125
hgg1 dlx3
papc
WT
p53M214K
J
200 µ
K
L
pm
ne
M
N
n
s
200 µ
O
Uninjected
MO1-gpr125
Uninjected
1.7 ng MO2-gpr125
3.4 ng MO2-gpr125
6.8 ng MO2-gpr125
P
600 µ
Q
R
S
T
U
V
W

Figure 20. Knockdown of *gpr125* enhances defects of *scrbl1/llk* and *vangl2/tri* mutants. (A-B'') Lateral views of uninjected, control MO or MO2-*gpr125* injected MZ*scrb1/llk*$^{rw468/rw468}$ or *vangl2/tri*$^{vu67/vu67}$ homozygotes at 1 dpf. Anterior left. The bracket in (A) marks posterior body. Arrowheads in (A'') and (B'') indicate the cyclopic eyes and change of head position. Fractions of affected embryos are indicated. (C-D') Ventral views of uninjected or 3.4 ng MO2-*gpr125* injected MZ*scrb1/llk*$^{rw468/rw468}$ or *vangl2/tri*$^{vu67/vu67}$ embryos at 3 dpf. Anterior left. (E-G) Quantification of CI of MZ*scrb1/llk*$^{rw468/rw468}$, *vangl2/tri*$^{vu67/vu67}$, and MZ*wnt11/slb*$^{tz216/tz216}$ embryos at 3 dpf injected with *gpr125* MOs and/or RNA or water. The numbers of analyzed embryos are inside the bars. Brown colored bars represent results from three independent experiments with error bars of ± SEM. Yellow and blue colored bars are results from single experiments with results of additional repetitions shown in Table 4 and 5. *p < 0.05, **p < 0.01, ***p < 0.001. (H-I'') Lateral views of uninjected, 3.4 ng control MO injected or 3.4 ng MO2-*gpr125* injected MZ*scrb1/llk*$^{rw468/+}$ or *vangl2/tri*$^{vu67/+}$ heterozygotes at 1 dpf. Anterior left. Fractions of affected embryos are indicated, except for (I; I') where more than 50 embryos were analyzed. (J) Quantification of AP axis length in *scrb1/llk*$^{rw468/+}$ and *vangl2/tri*$^{vu67/+}$ embryos at 1 dpf. The numbers of analyzed embryos are inside the bars. Error bars, ± SEM. ***p < 0.001. (K-L'') Lateral views of uninjected, 3.4 ng MO2-*gpr125*, or 3.4 ng MO2-*gpr125* and 11.5 pg *gpr125* RNA co-injected *vangl2/tri*$^{vu67/vu67}$ or *vangl2/tri*$^{vu67/+}$ embryos at 1 dpf. Anterior left. (M) Quantification of the impacts of *gpr125* MO and RNA on the AP axis defects of *vangl2/tri*$^{vu67/vu67}$ *vangl2/tri*$^{vu67/+}$ embryos at 1 dpf. The numbers of analyzed embryos are inside the bars. Error bars, ± SEM. *p < 0.05, **p < 0.01, ***p < 0.001.

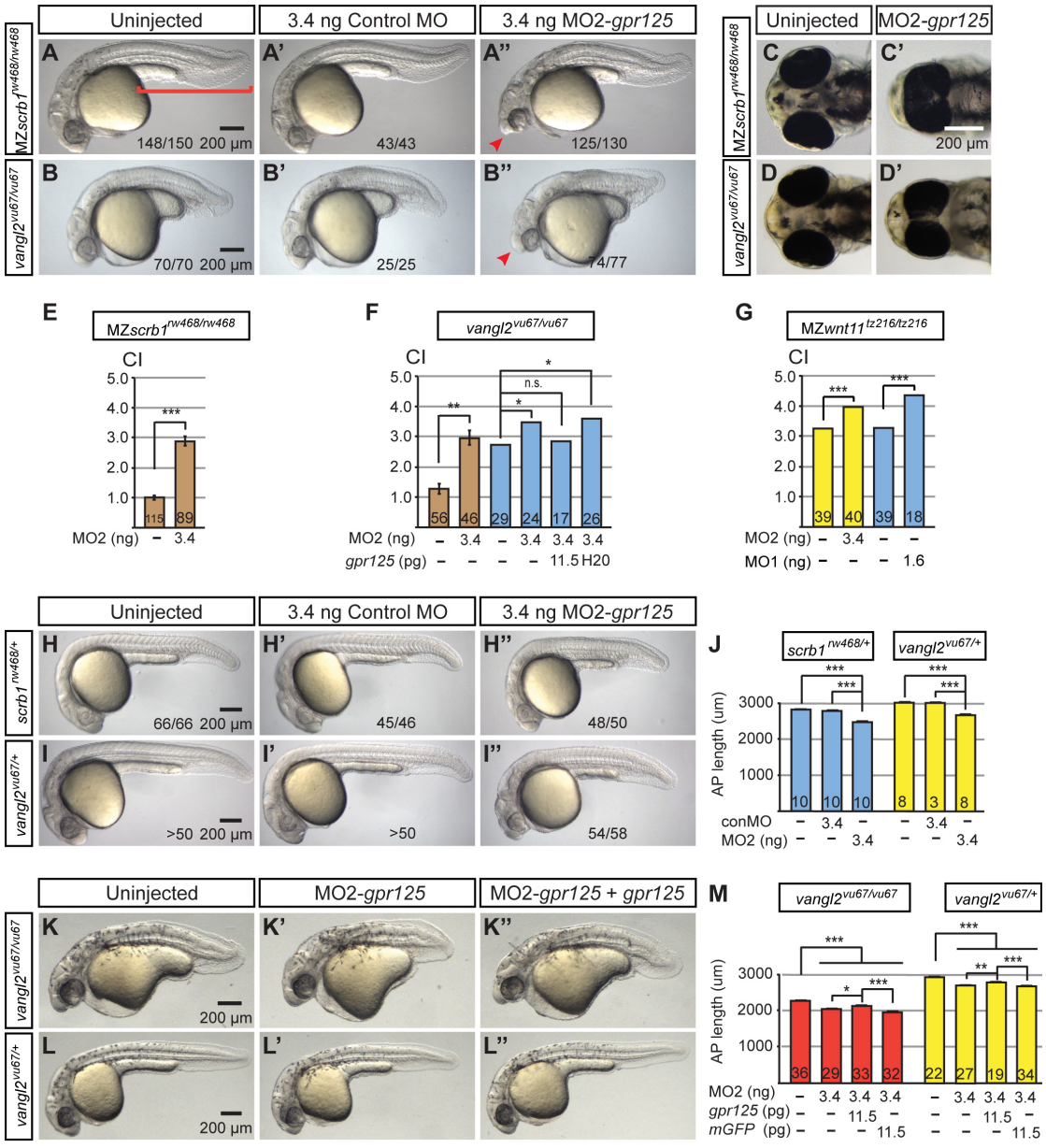
Uninjected
3.4 ng Control MO
3.4 ng MO2-gpr125
MO2-gpr125
MO2-gpr125 + gpr125
MZscrb1rw468/rw468
vangl2vu67/vu67
scrb1rw468/+
vangl2vu67/+
MZwnt11tz216/tz216
A
A'
A''
B
B'
B''
C
C'
D
D'
148/150 200 µm
43/43
125/130
70/70 200 µm
25/25
74/77
200 µm
E
F
G
CI
MO2 (ng)
gpr125 (pg)
MO1 (ng)
H
H'
H''
I
I'
I''
66/66 200 µm
45/46
48/50
>50 200 µm
>50
54/58
J
AP length (um)
conMO
K
K'
K''
L
L'
L''
M
mGFP (pg)

Table 4. Cyclopia indices of MO2-*gpr125* and/or *gpr125* RNA injected *vangl2/tri*$^{vu67/vu67}$ embryos. G# denotes individual clutches of embryos.

Injection group	**Cyclopia index**	**Number of embryos**
(G1) Uninjected	2.10	63
(G1) 3.4ng MO2-*gpr125*	3.33	15
(G1) 3.4ng MO2-*gpr125* +11.5pg *gpr125*	2.83	24
(G1) 11.5pg *gpr125*	2.35	20
(G2) Uninjected	3.44	18
(G2) 3.4ng MO2-*gpr125*	4.21	19
(G2) 3.4ng MO2-*gpr125* +11.5pg *gpr125*	3.44	27
(G3) Uninjected	2.57	23
(G3) 3.4ng MO2-*gpr125*	4.00	15
(G3) 3.4ng MO2-*gpr125* +11.5pg *gpr125*	3.93	14
(G4) Uninjected	2.76	29
(G4) 3.4ng MO2-*gpr125*	3.5	24
(G4) 3.4ng MO2-*gpr125* +11.5pg *gpr125*	2.88	17
(G4) 3.4ng MO2-*gpr125* +H2O	3.62	26
(G5) Uninjected	1.59	29
(G5) 3.4ng MO2-*gpr125*	3.45	20
(G5) 3.4ng MO2-*gpr125* +25pg *gpr125*	3.28	18
(G6) Uninjected	2.39	18
(G6) 3.4ng MO2-*gpr125*	3.65	20
(G6) 3.4ng MO2-*gpr125* +25pg *gpr125*	3.35	17
(G7) Uninjected	1.75	4
(G7) 3.4ng MO2-*gpr125*	3.25	4
(G7) 3.4ng MO2-*gpr125* +11.5pg *gpr125*	2.4	5
(G7) 3.4ng MO2-*gpr125* +H2O	3.5	4
(G8) Uninjected	2.86	14
(G8) 3.4ng MO2-gpr125	3.29	7
(G8) 3.4ng MO2-gpr125 +H2O	3.75	12

Table 5. Cyclopia indices of MO2-*gpr125* injected *wnt11/slb*$^{tz216/tz216}$ embryos. G# denotes individual clutches of embryos.

Injection group	Cyclopia index	Number of embryos	T-test value
(G1) H2O	3.32	25	1.58E-04
(G1) 3.4ng MO2-*gpr125*	4.10	31	
(G2) H2O	4.10	42	4.51E-05
(G2) 3.4ng MO2-*gpr125*	4.50	40	
(G3) H2O	3.26	39	4.46E-11
(G3) 3.4ng MO2-*gpr125*	3.98	40	

significantly suppressed MO2-*gpr125* enhancement of AP axis shortening of both *vangl2/tri* homozygotes and heterozygotes (Figure 20K-M) and cyclopia defects of *vangl2/tri* homozygotes (Figure 20F and Table 4). Consistent with the enhanced axis shortening at 1dpf, MO2-*gpr125* injection caused wider and shorter neural ectoderm and axial and paraxial mesoderm in *scrb1/llk* and *vangl2/tri* homozygotes and heterozygotes at 2-somite stage (Figure 21 A-J). At the cellular level, reduced Gpr125 function caused significant reduction of LWR and mediolateral alignment of cells in the notochord compared

to control *vangl2/tri* heterozygotes and homozygotes (Figure 21K-R). In summary, these results indicate that when PCP signaling is reduced, the function of Gpr125 function becomes critical for polarized cell behaviors underlying C&E movements.

Figure 21. Knockdown of *gpr125* enhances defects of *scrbl1/llk* and *vangl2/tri* mutant phenotypes at 2-somite stage. WISH analyses of uninjected (A and A') or 3.4 ng control MO-injected (C, C', E, E', G, and G') or 3.4 ng MO2-*gpr125* injected (B, B', D, D', F, F', H and H') *scrb1/llk*$^{rw468/+}$, *scrb1/llk*$^{rw468/rw468}$, *vangl2/tri*$^{vu67/+}$ or *vangl2/tri*$^{vu67/vu67}$ embryos at the 2-somite stage. (A-H) Animal pole views, ventral up. (A'-H') Dorsal views, anterior up; n, notochord; ne, neural ectoderm border; pm, prechordal mesoderm; and s, somites. Red line in (A') indicates the width of the notochord at the first somites. Arrowhead in (H) indicates impaired prechordal mesoderm migration. (I-J) Quantification of first somite length or notochord width at the same AP level in control (Con) or MO2-*gpr125* (MO2) injected *scrb1/llk*$^{rw468/+}$, *scrb1/llk*$^{rw468/rw468}$, *vangl2/tri*$^{vu67/+}$, or *vangl2/tri*$^{vu67/vu67}$ embryos at the 2-somite stage. The numbers of analyzed embryos are inside the bars. Error bars, ± SEM. *p < 0.05, **p < 0.01, ***p < 0.001. (K-N) Membrane Cherry (mCherry) labeled notochord of control or MO2-*gpr125* injected *vangl2/tri*$^{vu67/+}$ or *vangl2/tri*$^{vu67/vu67}$ embryos at the 2-somite stage. (O-R) Analyses of LWR and ML alignment in the notochord of control or MO2-*gpr125* injected *vangl2/tri*$^{vu67/+}$ (300 cells for control and 500 cells for MO2-*gpr125* injected embryos) or *vangl2/tri*$^{vu67/vu67}$ (110 cells for control and 199 cells for MO2-*gpr125* injected embryos) embryos at the 2-somite stage. Rose diagrams depict cell orientation relative to the AP axis (vertical dashed line). P<0.0001 for *vangl2/tri*$^{vu67/+}$ samples and p=0.0003 for *vangl2/tri*$^{vu67/vu67}$ samples. Corresponding LWRs are expressed as mean±SEM in the lower right corners. P<0.0001 for both groups.

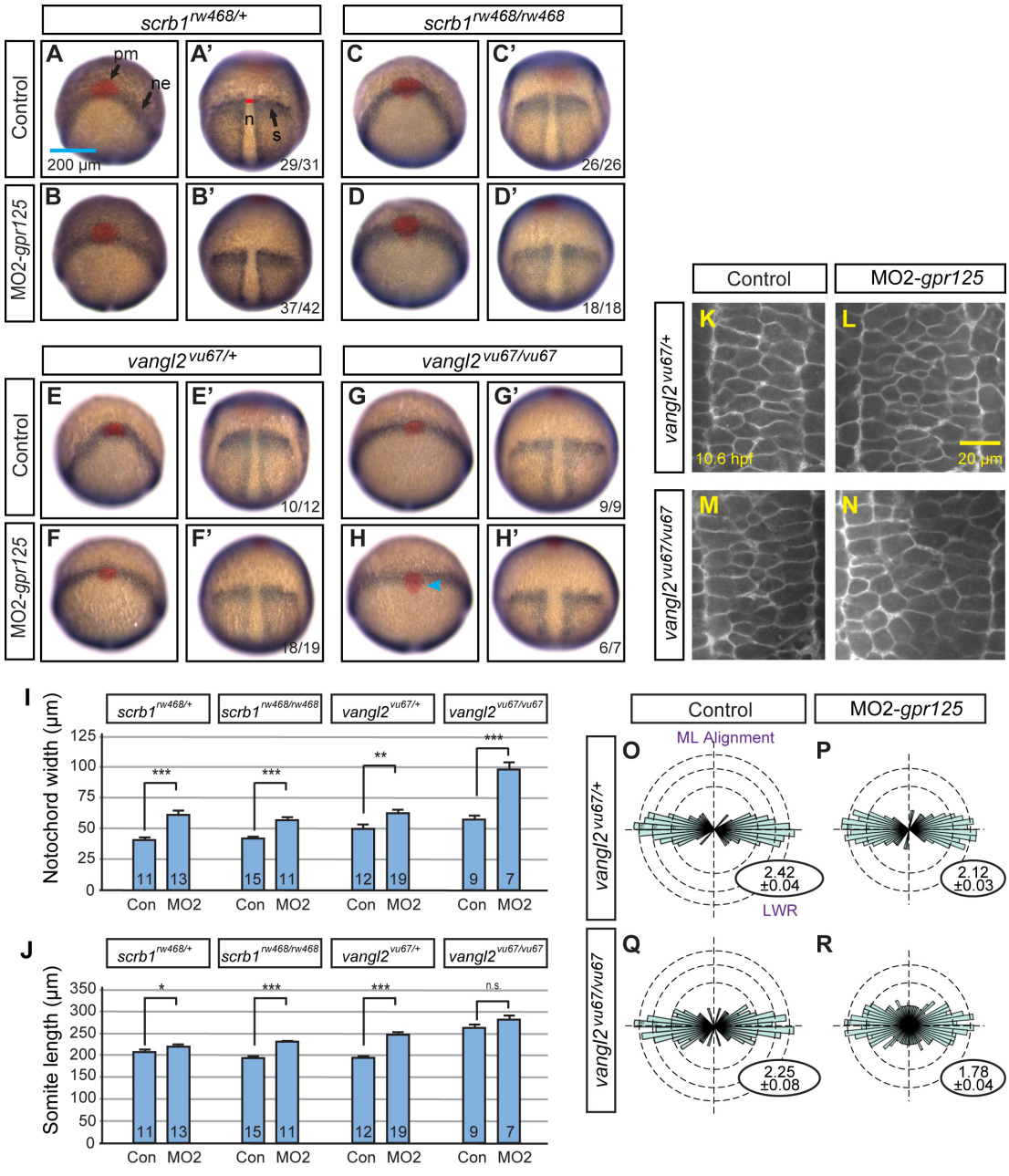
scrb1rw468/+
scrb1rw468/rw468
Control
MO2-gpr125
A
A'
B
B'
C
C'
D
D'
pm
ne
n
s
200 µm
29/31
26/26
37/42
18/18
vangl2vu67/+
vangl2vu67/vu67
E
E'
F
F'
G
G'
H
H'
10/12
9/9
18/19
6/7
Control
MO2-gpr125
vangl2vu67/+
vangl2vu67/vu67
K
L
M
N
10.6 hpf
20 µm
I
Notochord width (µm)
scrb1rw468/+
scrb1rw468/rw468
vangl2vu67/+
vangl2vu67/vu67
125
100
75
50
25
0
***
***
**
***
11
13
15
11
12
19
9
7
Con
MO2
J
Somite length (µm)
350
300
250
200
150
100
50
0
*
***
***
n.s.
O
P
Q
R
ML Alignment
LWR
2.42 ±0.04
2.12 ±0.03
2.25 ±0.08
1.78 ±0.04

Reduced Gpr125 enhances neuronal migration defects of *scrb1/llk* and *vangl2/tri* heterozygotes

As *scrb1/llk* and *vangl2/tri* also regulate tangential migration of FBMNs in zebrafish and mouse (Carreira-Barbosa et al 2003; Jessen et al 2002; Wada et al 2005; Wada & Okamoto 2009; Wada et al 2006), we asked whether *gpr125* interacts with these genes in the context of FBMN migration. Although injection of MO2-*gpr125* rarely impaired FBMN migration in WT embryos (Figure 22A-D), it strongly enhanced FBMN migration defects in PCP compromised genetic backgrounds (Figure 22E-O). At 48 hpf, FBMNs migrated into rhombomere 6 (r6) and r7 in 92% of *scrb1/llk* heterozygous embryos and migrated partially into r5 and r6 in only 8% of such embryos (Figure 22E and I). Gpr125 depletion significantly increased the number of embryos exhibiting partial FBMN migration (57%, n=65; Figure 22G and I) and strikingly, in 35% of these injected embryos, FBMNs failed to leave r4 (Figure 22H and I). FBMN migration defect were similarly enhanced in *vangl2/tri* heterozygous embryos (Figure 22J-O). By contrast, injection of control MOs at equivalent doses had no effect on FBMN migration in either genetic background (Figure 22, I, L, M and O). Therefore, *gpr125* interacts with PCP genes to promote FBMN migration.

Gpr125 recruits Dvl-GFP to membrane subdomains via direct interaction

Functional interactions between Gpr125 and PCP components and planar polarity defects of Gpr125 overexpressing gastrulae are consistent with a role of Gpr125 in modulating Wnt/PCP signaling. As Dvl membrane translocation is a

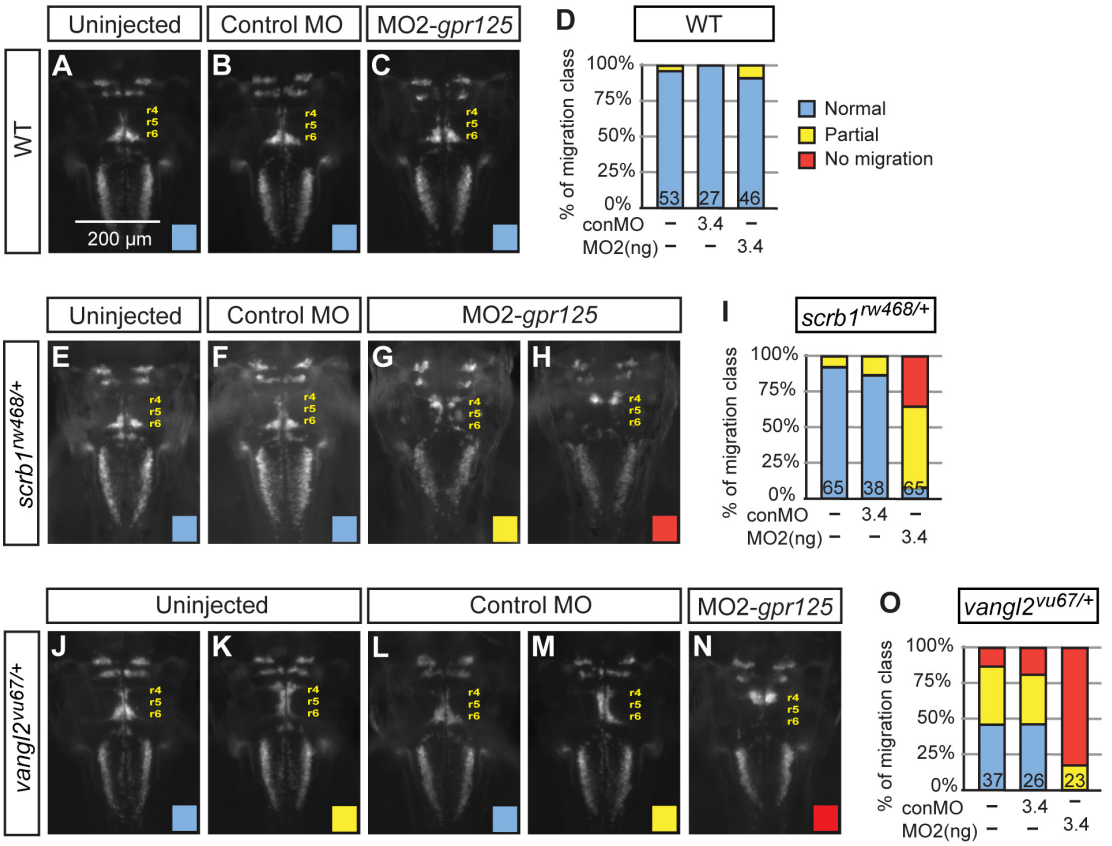

Figure 22. *gpr125* interacts with *scrb1/llk* and *vangl2/tri* in FBMN migration. Dorsal views of *islet1*(*isl1):GFP* expressing neurons in uninjected, 3.4 ng control MO, or 3.4 ng MO2-*gpr125* injected WT siblings of *scrb1/llk* or *vangl2/tri* heterozygous embryos at 48 hpf. Anterior up. r4 (rhombomere 4), r5 and r6 positions are labeled. (D) Frequency of FBMN migration phenotypic classes observed in WT embryos. Blue, normal; yellow, partial; and red, no migration. (E-H) Dorsal views of *isl1:GFP* expressing neurons in uninjected, 3.4 ng control MO or 3.4 ng MO2-*gpr125* injected *scrb1/llk*$^{rw468/+}$ embryos at 48 hpf. (I) Frequency of the FBMN migration phenotypic classes observed in *scrb1/llk*$^{rw468/+}$ embryos. (J-N) Dorsal views of *isl1:GFP* expressing neurons in uninjected, 3.4 ng control MO or 3.4 ng MO2-*gpr125* injected *vangl2/tri*$^{vu67/+}$ embryos at 48hpf. (O) Frequency of FBMN migration phenotypic classes observed in *vangl2/tri*$^{vu67/+}$ heterozygotes.

prerequisite for vertebrate Wnt/PCP signaling (Park et al 2005) and Gpr125 contains a PDZBM (PDZBM) (Figure 17), we tested whether Gpr125 influenced Dvl subcellular localization using previously described membrane recruitment assays (Carreira-Barbosa et al 2003; Witzel et al 2006). Synthetic RNA encoding *Xenopus* Dvl-GFP and zebrafish Gpr125 were injected at the 1-cell stage and Dvl-GFP distribution was assayed at the late blastula stage (4-5 hpf), prior to PCP signaling-dependent mediolateral cell polarization (Jessen et al 2002; Marlow et al 2002; Tada & Kai 2009; Topczewski et al 2001; Yin et al 2009). Consistent with previous reports (Carreira-Barbosa et al 2003; Wallingford et al 2000; Witzel et al 2006), Dvl-GFP mainly formed cytoplasmic puncta when expressed alone (n=20/20; Figure 23A-A''). In contrast, when co-expressed with Gpr125, Dvl-GFP occupied patch-like subdomains at cell membranes (n=36/36; Figure 23B-B''). Gpr125 mutant protein lacking the C-terminal ETTV peptide (*gpr125ΔETTV*), resulted in less prominent Dvl-GFP patches (n=13/13; Figure 23C-C''). As quantified in Figure 23E and F, ΔETTV recruited less Dvl-GFP to the membrane compared to the full-length receptor, and the Dvl-GFP subdomain size shifted towards smaller categories. Consistent with its reduced activity in Dvl membrane recruitment assays, Gpr125ΔETTV overexpression induced C&E defects with lower penetrance and severity than full-length Gpr125 (Figure 18K). When the entire intracellular domain of Gpr125 was deleted (Gpr125ΔICD), no Dvl-GFP recruitment was observed in co-expression experiments (n=18/18; Figure 23D-D''). Consistently, Gpr125ΔICD did not disrupt C&E at doses

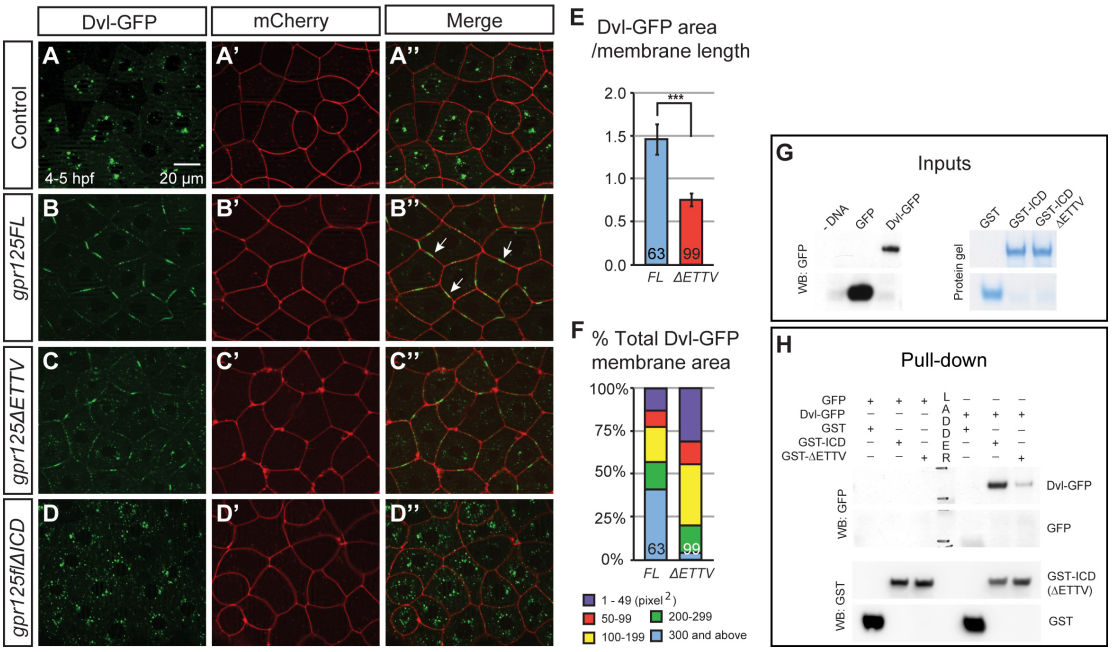

Figure 23. Gpr125 promotes Dvl-GFP localization in discrete membrane subdomains via direct interaction. (A-D") Animal pole views of live embryos at 4-5 hpf co-injected with 150 pg *dvl-GFP* and 50 pg *mCherry* RNA in the absence (A-A") and presence of 380 pg *gpr125FL* (B-B"), *gpr125ΔETTV* (C-C") or *gpr125ΔICD* RNA (D-D"). Arrows in (B") point to Dvl-GFP membrane subdomains. (E) Ratio of Dvl-GFP membrane area to the length of the membrane measured on embryos expressing full length or Δ ETTV Gpr125. Numbers of membranes analyzed are inside bars. (F) Size distribution of Dvl-GFP membrane subdomains in embryos expressing full length or Δ ETTV Gpr125. (G and H) Pull-down assay with GST- and GFP- fusion proteins. 10% of GFP-fusion protein inputs were blotted with anti-GFP antibody and 100% GST fusion protein inputs were stained with Denville Blue™ Protein Stain (G). Pull-down results were analyzed by western blotting using anti-GFP and anti-GST antibodies (H).

equivalent to the effective doses of RNA encoding full-length Gpr125 (Figure 18K).

To test for direct binding between Dvl and Gpr125 intracellular domain (Gpr125ICD), we performed pull-down experiments with purified glutathione S-transferase (GST)-Gpr125ICD, GST-Gpr125ICDΔETTV fusion proteins and *in vitro* translated *Xenopus* Dvl-GFP (Figure 23G and H). We found that GST-Gpr125ICD pulled down Dvl-GFP, indicative of a direct interaction. The ΔETTV form pulled down less Dvl-GFP (Figure 23H), suggesting that ETTV promotes Gpr125ICD binding to Dvl. Taken together, our results suggest that Gpr125 modulates PCP signaling by interacting with Dvl and promoting its accumulation in membrane subdomains.

Dvl clusters Gpr125 and select PCP components into membrane subdomains

Cytoplasmic core PCP components, including Dvl, cluster PCP complexes in cell membranes of *Drosophila* pupal wings (Strutt et al 2011). Given that Dvl-GFP localized to membrane subdomains when co-expressed with Gpr125, we asked whether Gpr125 colocalized with Dvl in these membrane subdomains using a Gpr125 C-terminal Cherry fusion protein (Gpr125-Cherry), which when overexpressed impaired C&E movements and underlying cell polarity comparable to the WT protein (Figure 18K, Q, S and U). In zebrafish blastulae, Gpr125-Cherry expressed alone displayed uniform membrane distribution (n=17/17; Figure 24A-A''), but it colocalized with Dvl-GFP in prominent membrane subdomains in co-expression experiments (n=12/12; Figure 24B-B''

and Mov. S1). Similarly, when co-expressed, Dvl-GFP clustered Gpc4/Kny-GFP into membrane subdomains in late blastulae (n=10/12, Figure 24D-D'' and Mov. S2). Interestingly, these Dvl-mediated PCP membrane subdomains preferentially localized at the central regions of cell contacts between neighboring blastomeres (Figure 24E). In addition, Dvl-GFP promoted uniform membrane localization of endogenous Vangl2/Tri in late blastulae (n=4/5; Figure 24G''), when endogenous Tri/Vangl2 was mainly cytoplasmic in uninjected embryos (Figure 24F).

Next, we investigated whether Gpr125 influenced the distribution of other PCP components, including Fzd7-CFP, Gpc4/Kny-GFP and endogenous Vangl2 in blastulae expressing Gpr125-Cherry, but no change of their distribution was observed (Figure 25). In contrast, when co-expressed with Dvl-YFP, Gpr125-Cherry, Fzd7-CFP and Dvl-YFP co-localized in membrane subdomains (n=17/22; Figure 26A-A''). Moreover, mosaic expression of Gpr125 enhanced Gpc4/Kny-GFP clustering when Dvl was overexpressed (n=6/10; Figure 26B-B''). In contrast to Fzd7 and Gpc4, neither endogenous nor overexpressed zebrafish Vangl2 was enriched in Gpr125-Cherry and Dvl-GFP-containing subdomains (C-F; n=15/15 for endogenous Vangl2; n=5/5 for overexpressed Vangl2). These results suggest that analogous to *Drosophila*, distinct PCP complexes can form in vertebrates, and Fzd7 and Gpc4/Kny may be components of large Dvl-containing protein complexes, formation of which is promoted by Gpr125.

Figure 24. Dvl clusters Gpr125 and Gpc4/Kny into membrane subdomains and promotes uniform Vangl2/Tri membrane localization in late blastulae (4-5 hpf). (A-B") Animal pole views of live blastulae co-injected with 267 pg *gpr125-Cherry* RNA and either 150 pg *mGFP* RNA (A-A") or 150 pg *dvl-GFP* RNA (B-B"). Arrows in (B") point to Gpr125-Cherry:Dvl-GFP membrane subdomains. (C-D") Animal pole views of live blastulae co-injected with 60 pg *gpc4/kny-GFP* RNA, 50 pg *mCherry* RNA (C-C") and 150 pg untagged *dvl* RNA (D-D"). Arrows in (D") point to Gpr4/Kny-GFP membrane subdomains. (E) Graphic representation of the relative distribution of Dvl-GFP:Gpr125-Cherry and Gpc4/Kny-GFP:Dvl subdomains along cell membranes. Membrane length was normalized as one. (F-F') Animal pole views of a whole-mount immunostained WT blastula with Vangl2 antibody and β-catenin antibodies. (G-G'') Animal pole views of a 50 pg *mCherry* and 150 pg *dvl-GFP* RNA-injected bastula immunostained for GFP, RFP and Vangl2.

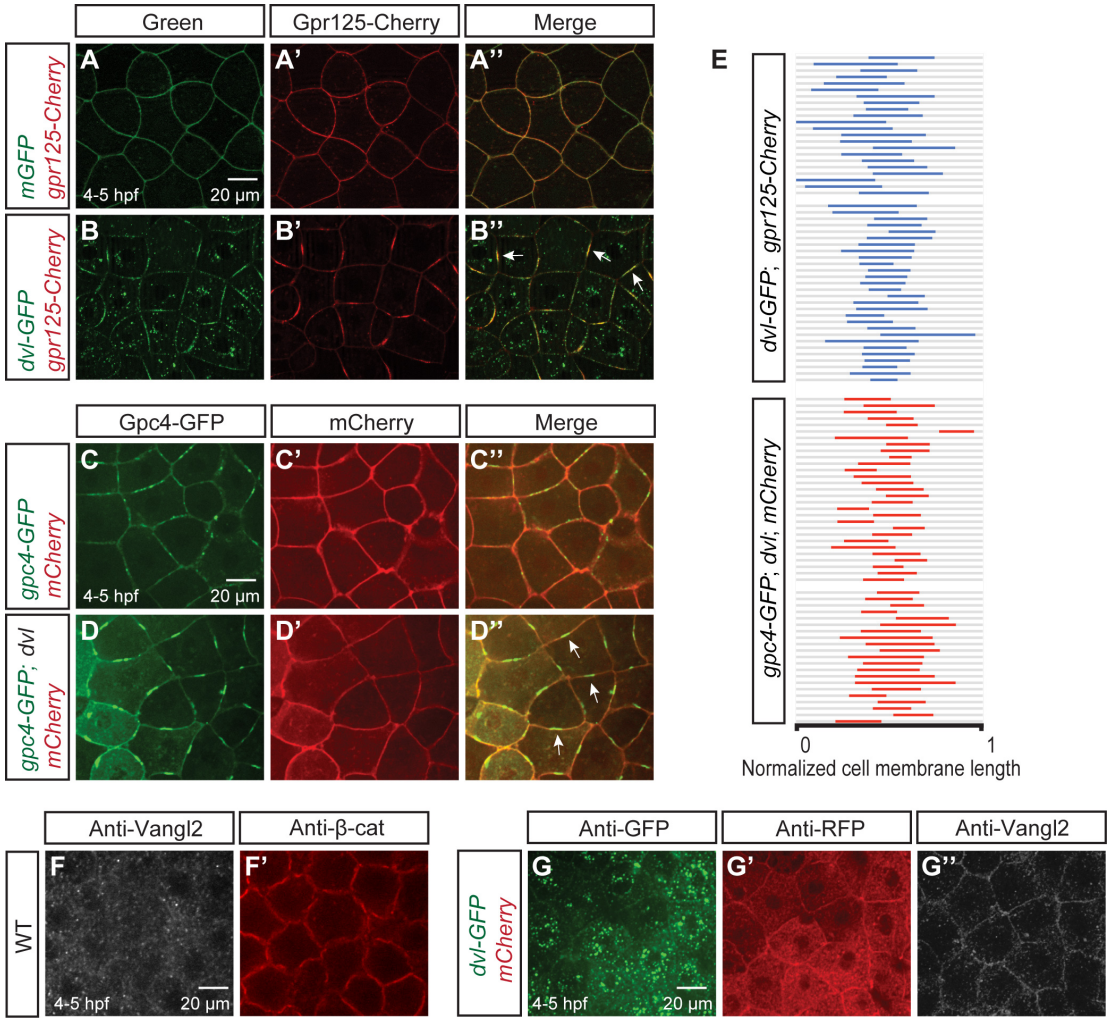
Green
Gpr125-Cherry
Merge
mGFP gpr125-Cherry
dvl-GFP gpr125-Cherry
A
A'
A''
B
B'
B''
4-5 hpf
20 μm
Gpc4-GFP
mCherry
Merge
gpc4-GFP mCherry
gpc4-GFP; dvl mCherry
C
C'
C''
D
D'
D''
E
dvl-GFP; gpr125-Cherry
gpc4-GFP; dvl; mCherry
0
1
Normalized cell membrane length
Anti-Vangl2
Anti-β-cat
WT
F
F'
Anti-GFP
Anti-RFP
Anti-Vangl2
dvl-GFP mCherry
G
G'
G''

To assess the interaction between Gpr125, Dvl and Vangl2 during C&E movements, we examined the relative distribution of Gpr125-Cherry, Dvl-GFP and endogenous Vangl2 at 10 hpf. Gpr125-Cherry localized to cell membranes and formed puncta both on the membrane and in the cytosol (Figure 27A'-A''). Endogenous Vangl2 localized mainly to the cell membranes (Figure 27B) and membrane staining was not observed in MZ*vang/tri*$^{vu67/vu67}$ mutants (Figure 27C). Intriguingly, when co-expressed during gastrulation, Gpr125-Cherry and Dvl-GFP colocalized in large membrane patches, but endogenous Vangl2 was not enriched in Gpr125-Cherry:Dvl-GFP patches (Figure 27D-F''). Therefore, Gpr125 might primarily interact with Dvl containing protein complexes during C&E movements.

To assess the interaction between Gpr125, Dvl and Vangl2 during C&E movements, we examined the relative distribution of Gpr125-Cherry, Dvl-GFP and endogenous Vangl2 at 10 hpf. Gpr125-Cherry localized to cell membranes and formed puncta both on the membrane and in the cytosol (Figure 27A'-A''). Endogenous Vangl2 localized mainly to the cell membranes (Figure 27B) and membrane staining was not observed in MZ*vang/tri*$^{vu67/vu67}$ mutants (Figure 27C). Intriguingly, when co-expressed during gastrulation, Gpr125-Cherry and Dvl-GFP colocalized in large membrane patches (Figure 27F-F'). By contrast, endogenous Vangl2 was not enriched in Gpr125-Cherry:Dvl-GFP patches (Figure 27A; D-F''). Therefore, Gpr125 might primarily interact with Dvl containing protein complexes during C&E gastrulation movements.

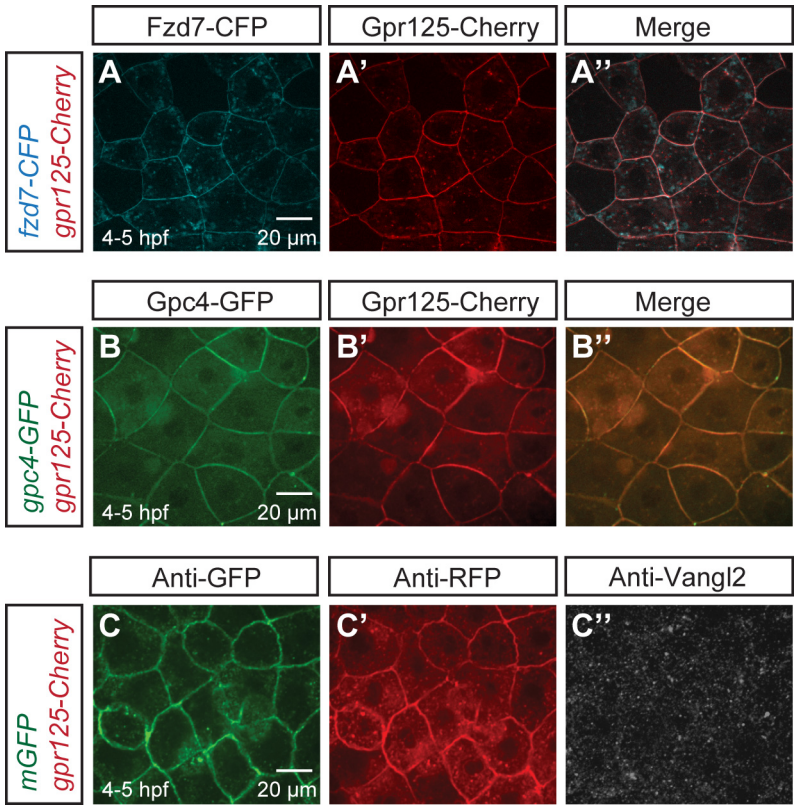

Figure 25. Gpr125-Cherry alone did not affect PCP components localization in late blastulae (4-5 hpf). (A-A'') Animal pole views of a blastula co-injected with 110 pg *fzd7-CFP* and 300 pg *gpr125-Cherry* RNA. (B-B") Animal pole views of a blastula co-injected with 60 pg *gpc4/kny-GFP* and 300 pg *gpr125-Cherry* RNA. (C-C'') Animal pole views of a 300 pg *gpr125-Cherry* and 150 pg *mGFP* RNA- injected blastula immunostained for GFP, RFP and Vangl2.

Figure 26. Gpr125 promotes localization of select PCP components in Dvl-containing membrane subdomains in late blastulae (4-5 hpf). (A-A'') Live blastula co-injected with 110 pg *fzd7-CFP*, 150 pg *dvl-YFP* and 300 pg *gpr125-Cherry* RNA. (B-B'') Live blastula co-injected with 60 pg *gpc4/kny-GFP*, 150pg *dvl* at the one-cell stage, and 4 pg *H2B-RFP* and 20 pg *gpr125FL* RNAs in one blastomere at the 16~32-cell stage. The star in (B") marks an H2B-RFP positive nucleus and arrows point to membrane subdomains. (C-D") Blastula injected with 300 pg *gpr125-Cherry*, 150 pg *dvl-GFP* (C-C'') and 50 pg zebrafish *vangl2/tri* (D-D'') RNA-injected blastulae immunostained for GFP, RFP and Vangl2. Animal pole views in (A-D) (E-F) Quantification of fluorescent intensity ratios inside/outside domain for Vangl2, Gpr125-Cherry and Dvl-GFP in embryos injected with 300 pg *gpr125-Cherry,* 150 pg *dvl-GFP (*E) and 50 pg zebrafish *vangl2* RNAs (F).

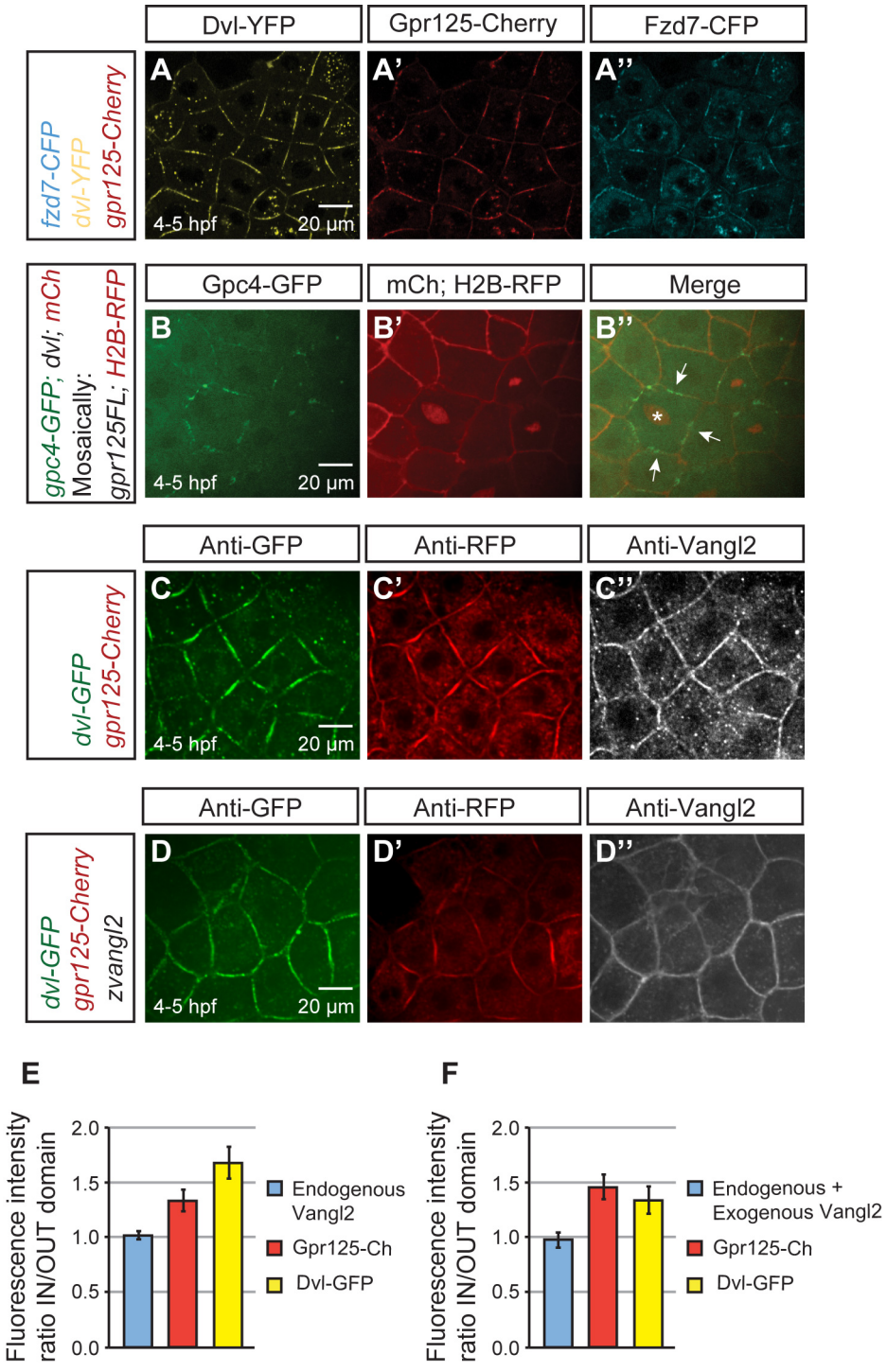
Dvl-YFP
Gpr125-Cherry
Fzd7-CFP
fzd7-CFP
dvl-YFP
gpr125-Cherry
A
A'
A''
4-5 hpf
20 μm
Gpc4-GFP
mCh; H2B-RFP
Merge
gpc4-GFP; dvl; mCh
Mosaically:
gpr125FL; H2B-RFP
B
B'
B''
4-5 hpf
20 μm
Anti-GFP
Anti-RFP
Anti-Vangl2
dvl-GFP
gpr125-Cherry
C
C'
C''
4-5 hpf
20 μm
Anti-GFP
Anti-RFP
Anti-Vangl2
dvl-GFP
gpr125-Cherry
zvangl2
D
D'
D''
4-5 hpf
20 μm
E
Fluorescence intensity
ratio IN/OUT domain
2.0
1.5
1.0
0.5
0.0
Endogenous
Vangl2
Gpr125-Ch
Dvl-GFP
F
Fluorescence intensity
ratio IN/OUT domain
2.0
1.5
1.0
0.5
0.0
Endogenous +
Exogenous Vangl2
Gpr125-Ch
Dvl-GFP

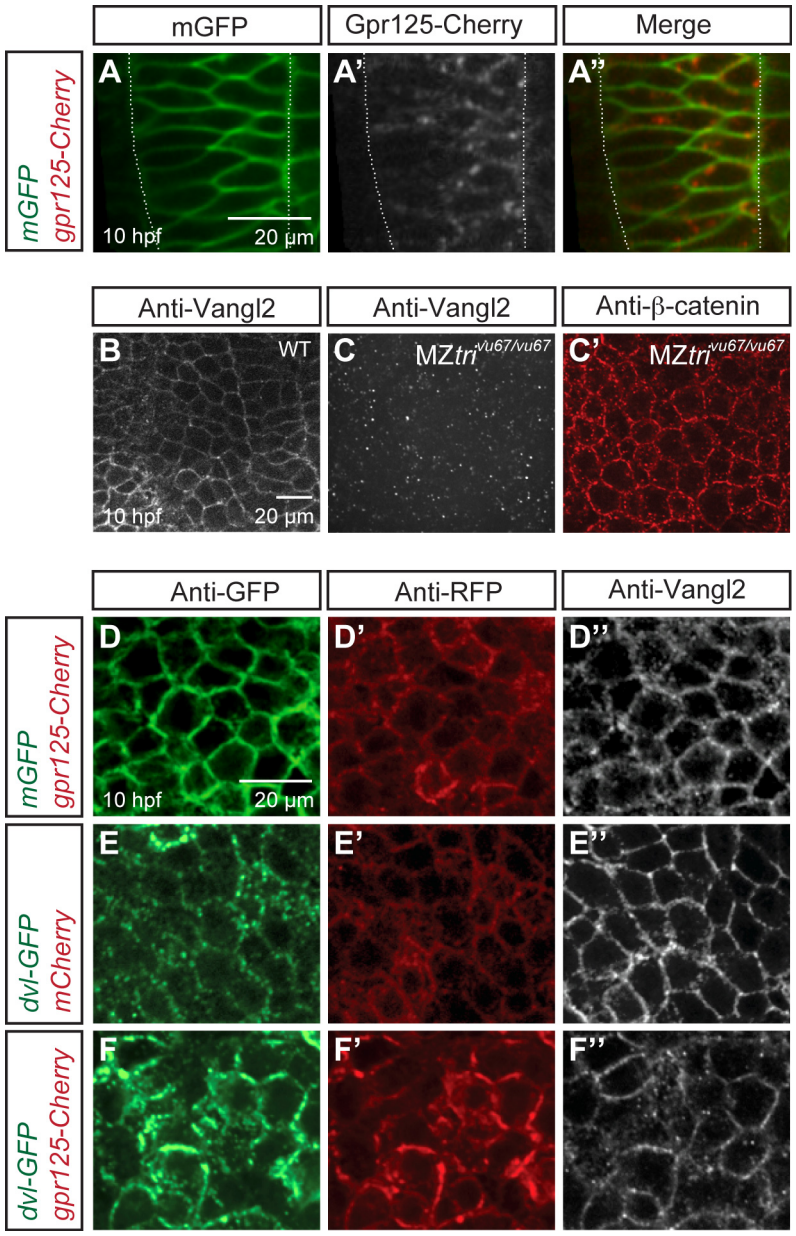

Figure 27. Gpr125-Cherry and Dvl-GFP colocalize during gastrulation (10 hpf). (A-A'') Dorsal views of a gastrula injected with 50 pg *gpr125-Cherry* and 150pg *mGFP* RNA. White dash lines outline the notochord. (B-C') Whole-mount immunostaining for endogenous Vangl2 and β-catenin in WT (B) or MZ*vang/tri*$^{vu67/vu67}$ gastrulae (C-C'). (D-F'') Dorsal mesoderm of gastrulae co-injected with 150 pg *mGFP* and 300 pg *gpr125-Cherry* RNAs (D-D''), 150 pg *dvl-GFP* and 50 pg *mCherry* RNAs (E-E'') or 150 pg *dvl-GFP* RNA and 300 pg *gpr125-Cherry* RNAs (F-F") and immunostained for GFP, RFP and Vangl2.

Discussion

Previously, the expression of *Gpr125* was reported in various tissues of mouse embryos and adults, including the pluripotent spermatogonial progenitor cells (Homma et al 2008; Pickering et al 2008; Seandel et al 2007); however, its function was not known. Here, we identified zebrafish Gpr125 as a novel modulator of C&E gastrulation movements and tangential FBMN migration, two processes evolutionarily conserved among vertebrates that require PCP signaling (Gray et al 2011; Wada & Okamoto 2009). Towards elucidating the genetic and cellular mechanisms by which Gpr125 regulates these processes, we showed that excess Gpr125 impaired Wnt/PCP-dependent cellular polarities underlying normal C&E gastrulation movements. Moreover, reduction of *gpr125* expression exacerbated C&E and neuronal migration defects of several Wnt/PCP component mutants. At the molecular level, we showed that Gpr125 interacted with and recruited Dvl into membrane subdomains, and promoted accumulation of select PCP components in such membrane subdomains.

We created a *gpr125* LOF condition with two antisense MOs, which were very effective at blocking translation of GFP reporters bearing *gpr125* MO target sequences. However, the effectiveness of the MOs in blocking translation of endogenous Gpr125 protein could not be evaluated due to lack of a Gpr125 antibody. Nevertheless the MOs likely created at least a partial LOF condition, as they enhanced the C&E gastrulation and FBMN migration defects of homozygous and heterozygous PCP mutants, whereas a control MO failed to do so (Figure 20-22). Similar to the interaction between *gpr125* and PCP pathway

genes reported here, exacerbation of C&E defects has been reported for compound PCP pathway mutants compared to single mutants (Carreira-Barbosa et al 2003; Kilian et al 2003; Marlow et al 1998). More importantly, co-injecting a form of *gpr125* RNA lacking the MO targeting sequence partially suppressed the exacerbation of C&E defects in *gpr125* MO injected PCP mutants. The lack of morphological defects in *gpr125* morphants (MO injected embryos) is consistent with the report that *Gpr125* knock-in null mice are grossly normal and fertile (Seandel et al 2007). Since *gpr125* RNA is maternally deposited and we were not able to determine the abundance of maternal protein, the lack of early developmental defects in *gpr125* morphants could be due to maternal protein contribution. Alternatively, as observed for *celsr/flamingo* genes, redundancy with other adhesion GPCRs or PCP pathway components might mask the loss of Gpr125 function (Carreira-Barbosa et al 2009).

We showed that the Gpr125 intracellular domain interacted directly with Dvl in pull-down experiments (Figure 23) and was required for Dvl recruitment into membrane subdomains upon Gpr125 overexpression in zebrafish blastula (Figure 23). Given that Dvl membrane translocation is a prerequisite for vertebrate Wnt/PCP signaling (Park et al 2005) and C&E movements are altered by increased activity of PCP components (Carreira-Barbosa et al 2003; Formstone & Mason 2005; Jessen et al 2002; Marlow et al 2002; Topczewski et al 2001; Wallingford et al 2000), this interaction likely in part accounts for C&E defects caused by Gpr125 GOF and possibly the exacerbated C&E defects caused by Gpr125 LOF in PCP mutants. Interestingly, we did not detect

significant differences in mediolateral elongation or cell orientation among cells with distinct Pk distribution patterns in either control gastrulae or those overexpressing Gpr125 (data not shown). Moreover, we observed little change in Pk-GFP distribution due to Gpr125 depletion in both WT and tri het (data not shown). Therefore, it is plausible that Pk is not a direct interacting protein of Gpr125 and it is important in the future to examine whether Gpr125 LOF would influence Dvl distribution. Since Dvl is not required for FBMN migration (Jessen et al 2002; Wada & Okamoto 2009), Gpr125 and the relevant PCP components likely regulate FBMN migration and C&E via distinct mechanisms.

We found that the PDZBM of Gpr125 was partially responsible for Dvl binding and recruitment (Figure 23). The requirement of the PDZBM for Dvl binding varies among different proteins. It is dispensable for binding of Fzd or Vangl2/Tri to Dvl (Park & Moon 2002; Umbhauer et al 2000; Wong et al 2003). However, the PDZBM mediates direct binding between *Xenopus* Dvl and its cytoplasmic interacting protein Dapper/Dact (Cheyette et al 2002; Gloy et al 2002; Teran et al 2009; Wong et al 2003). As in Gpr125, the Dapper PDZBM, is –TTV and the Threonine at the -2 position has been reported to be within hydrogen bonding distance of a highly conserved Arginine 325 residue present in Dvl proteins and essential for Dvl interaction with Dapper (Cheyette et al 2002). Additional Gpr125 motif(s) mediating Dvl binding remain to be defined.

Previous reports show that Fzd7 recruits Dvl uniformly to the cell membrane when overexpressed in the zebrafish blastula and promotes Dvl accumulation into discrete membrane subdomains when co-expressed with

Wnt11 (Witzel et al 2006). We observed that Dvl clustered Gpr125 into membrane subdomains and vice versa, even without co-expression of Wnt11 (Figure 23 and Figure 24). Notably, Gpr125 promoted accumulation of Fzd7 and Gpc4/Kny in the subdomains (Figure 26). These observations are consistent with a recently discovered role for endogenous Dsh in clustering PCP complexes into membrane subdomains in *Drosophila* wing epithelia (Strutt et al 2011). Moreover, our study raises the possibility that other proteins such as Gpr125 cooperate with Dvl to promote formation of such membrane subdomains. Interestingly, *Drosophila* Pk forms membrane clusters when co-expressed with *Xenopus* Vangl2 in cells of *Xenopus* animal cap explants (Jenny et al 2003b), but in zebrafish blastula, Pk co-expression inhibits Fzd7-mediated recruitment of Dvl to the cell membrane possibly by destabilizing Dvl (Carreira-Barbosa et al 2003). Although it remains to be tested, based on additional evidence that Pk and Dvl fusion proteins localize to opposing cell edges in zebrafish gastrula (Ciruna et al 2006; Yin et al 2008), it is tempting to speculate that distinct clusters of endogenous PCP complexes might exist during C&E movements in vertebrates. Moreover, because the membrane subdomains containing Gpr125 and Dvl were enriched in Fzd and Gpc4/Kny but not of Vangl2/Tri, it is also intriguing that Gpr125 could be involved in formation of asymmetric PCP complexes. As proposed for *Drosophila* PCP signaling, clustering of PCP complexes could afford a self-enhancement mechanism contributing to the establishment and/or maintenance of planar polarity (Strutt et al 2011). Particularly during C&E, as mesenchymal cells are moving and changing their contacts rather frequently,

local organization of PCP proteins into subdomains could facilitate efficient establishment of planar polarity in the context of dynamic cell rearrangements.

It is unclear how clustering of PCP complexes might contribute to polarized cell behaviors driving C&E movements. Nevertheless, formation of Wnt11: Fzd7: Dvl subdomains has been correlated with increased persistence of membrane contacts. In addition, Celsrs have been demonstrated to contribute substantially to this effect, likely owing to their ability to mediate adhesion (Shima et al 2004; Usui et al 1999; Witzel et al 2006). Like Celsrs, Gpr125 is an adhesion GPCR and its extracellular domain contains protein modules known to mediate protein-ligand interactions suitable for regulating intercellular communication and cell adhesion (de Wit et al 2011; Pal et al 2012). Therefore, it is worth testing in the future whether Gpr125 might function in PCP subdomains to regulate cell adhesion.

In summary, we identified zebrafish Gpr125 as a novel modulator of C&E gastrulation movements and tangential FBMN migration. Gpr125 influences the Wnt/PCP pathway activity in part via interacting with and modulating the distribution of Dvl. Our discovery that Gpr125 contributes to C&E during gastrulation, a processes where all known PCP components act, and later during FBMN migration, where only a subset of PCP genes are required, opens up exciting avenues for further studies of Gpr125 function, in particular towards understanding how Wnt/PCP signaling regulates cell and tissue polarity in distinct contexts and other developmental processes, such as stem cell maintenance (Sugimura et al 2012).

Experimental Procedures

Zebrafish lines

AB, ABWIK, *llk*^{RW468}, *tri*^{vu67} (Chunyue Yin, Jason R Jessen, Isabelle Roszko, and LSK unpublished nonsense allele), *slb*^{tz216}, *tp53*^{M214K}, and Tg(*isl1-GFP*) were used in this study (Berghmans et al 2005; Heisenberg et al 2000; Jessen et al 2002; Wada et al 2005). Embryos obtained from natural spawnings were staged according to morphological criteria (Kimmel et al 1995b).

RT-PCR and cloning of zebrafish *gpr125*

Total RNA was extracted with TRI_{ZOL} LS reagent (Invitrogen) from WT embryos at the indicated stages. cDNA was produced with SuperScript III first-strand synthesis system (Invitrogen). To detect *gpr125* transcripts, PCR was performed using *gpr125*-q primers (Table 6) with GoTaq Flexi DNA polymerase (Promega). The full-length *gpr125* coding sequence was amplified using *gpr125*-fl primers (Table 6) with Easy-A high-fidelity PCR cloning enzyme (Agilent Technologies) and subcloned into pCR8 vector (Invitrogen), from which various deletion forms of Gpr125 were amplified with the primers listed in Table 6 and subcloned into pCR8 and subsequently into pCS-based vectors (Villefranc et al 2007) or *E. coli* expression vector pDEST^{TM}15 (Invitrogen) with Gateway® LR clonase® II enzyme mix or LR clonase® II plus enzyme (Invitrogen)

RNA and MO injection

Capped RNA was synthesized using mMessage mMachine Kit (Ambion). Two non-overlapping MOs (MO1-*gpr125* and MO2-*gpr125*) targeting the 5'UTR region were used. The effectiveness of each MO in blocking the translation of RNA encoding GFP fused to the MO target sequence (GFP reporter) was

determined. The non-specific toxicity of MO1-*gpr125* was confirmed by complete suppression of cell death in *p53*$^{M214K/M214K}$ null mutants (Figure 19J and K). Sequences of all MOs used are listed in Table 6.

Table 6. Nucleotide sequences of the primers and antisense morpholino oligonucleotides used in Chapter III.

Primer name	**Sequences**
β-actin	5'- ATGGATGAGGAAATCGCTGCCCTGGTC -3' 5'- CCTGATGTCTGGGTCGTCCAACAATGG -3'
gpr125-q	5'- GGAAACTCCAGCATCCTCAG -3' 5'- ACACGGTGGTGAAGTTGTCA -3'
gpr125-probe	5'- GAGCTCAAAGAACAATCCGAGGAGCA -3' 5'- TACTCGCGCAAAACTGTGAGCCTGCTA -3'
gpr125-probe-2	5'- TAGGAGTGAAGGAAACTCGCTGCTCGT -3' 5'- GCTTGACAAACGCTCGCATTGTATGTC -3'
Cla1-5'-*gpr125*-T1-SpeI	5'- AGAGAGATCGATTGCTAATCTGACCCCCTTCT -3' 5'- AGAGAGACTAGTTACTCCAGCCGTCGTTGATA -3'
Cla1-5'-*gpr125*-T2-SpeI	5'- AGAGAGATCGATGCTCTATGGCTTTGGACGAA -3' 5'- AGAGAGACTAGTTACTCCAGCCGTCGTTGATA -3'
gpr125FL	5'- ATGTCGGTGCTTTGCGTC -3' 5'- CTACACAGTAGTTTCATGCTTCCAC -3'
gpr125ΔETTV	5'- GCTTGACAAACGCTCGCATTGTATGTC -3' 5'- CTAGCTCTTCCATACCCTGCT -3'
gpr125ΔICD	5'- ATGTCGGTGCTTTGCGTC -3' 5'- TCATTGTCGGTTTACGCAATGG -3'
gpr125ΔStop codon	5'- ATGTCGGTGCTTTGCGTC -3' 5'- CACAGTAGTTTCATGCTTCCACA -3'
MO name	
MO1-*gpr125*	5'- TACTCCAGCCGTCGTTGATATGTTC -3'
MO2-*gpr125*	5'- TAGCATATAAATAGCCTTTCCGTGC -3'
Control MO	5'- CCTCTTACCTCAGTTACAATTTATA -3'

AP axis, notochord and somite measurements

Embryos were imaged using Olympus SZ61 or Zeiss Discovery dissecting microscopes and Olympus or Zeiss AxioCam MRM cameras in PictureFrame or Axiovision Rel 4.6 (Zeiss). For AP axis length, embryos were traced from the forebrain to the tip of the tail fin. For notochord width, straight lines were drawn perpendicular to the AP axis between the lateral borders of the notochord at level of first somites. For somite length, the first somites were traced. The distance was measured with ImageJ software (NIH) (Marlow et al 1998).

Whole-mount *in situ* hybridization (WISH)

Antisense probes were synthesized with RNA labeling kits (Roche). DNA fragments amplified with *gpr125*-probe1 primers and *gpr125*-probe2 primers (Table S1) were used as templates for *gpr125* probe synthesis. WISH analyses were performed as described previously (Marlow et al 1998).

Whole-mount immunostaining

Embryos were fixed in 100% Prefer fixative (Anatech) for 40 minutes at room temperature. Immunostaining was performed with a standard protocol. Antibodies were diluted in blocking buffer containing 0.5% BSA, 10% serum, 0,1% Triton X-100 and 2% DMSO in PBS. Primary antibodies used were: anti-zebrafish Tri/Vangl2 (rabbit, 1:500, made by the Vanderbilt University Antibody Core), anti-GFP (mouse, 1:500, Clontech, #632375) and rat anti-RFP (1:1000, Chromotek, clone 5F8). Secondary antibodies were: Alexa Fluor 568 goat anti-rat, Alexa Fluor 647 goat anti-rabbit, Alexa Fluor 488 goat anti-mouse (1:500, Invitrogen).

Cell polarity analyses

Measurements and analyses of LWR and mediolateral alignment were performed according to (Myers et al 2002a). WT embryos were injected with 200 pg *gpr125-Cherry* + 100 pg *mEGFP* (membrane-targeting EGFP), or 300 pg of *mEGFP* synthetic RNA. 150pg *mCherry* (membrane-targeting Cherry) RNA was injected into *vangl2/tri* embryos for membrane labeling. Embryos were fixed overnight in 4% PFA and confocal stacks were collected. Image analysis was performed in ImageJ (NIH) and Fiji (Schindelin et al 2012), where cells were outlined by hand. LWR and angles of the long axis were measured with Fit Ellipse. Statistical tests were performed in Vector Rose (SPAZ software). Rose diagrams were drawn using Rose.NET (Todd A. Thompson, http://mypage.iu.edu/~tthomps/programs/home.htm).

In vivo subcellular protein localization analyses

Pk localization experiments: 1-cell embryos were injected with 200 or 300 pg *gpr125* and 100 pg *mCherry* synthetic RNA, or an equivalent amount of *mCherry* RNA. At the 16-cell stage, 1 cell was injected with 16-19 pg of *pk-GFP* RNA (Yin et al 2008). At tailbud to 2-somite stage, Z-stacks were collected using Quorum Spinning disc Confocal/ IX81-Olympus inverted microscope. Image analysis was performed in ImageJ (NIH) and Fiji.

To monitor protein localization in late blastulae, 1-cell stage embryos were injected with specific combinations of RNA at doses specified in the figures. In mosaic expression experiments, *Histone2B-RFP* (*H2B-RFP*) and *gpr125FL* RNA were injected into one blastomere at the 16-32 cell stage. The superficial layer of

live or immunostained blastulae at 4-5 hpf were imaged with a Zeiss Axioobserver microscope equipped with Apotome a 40X oil lens (Zeiss) and MRm digital camera (Zeiss), and Axiovision Rel 4.7 software (Zeiss), Leica TCS SP5 confocal or Quorum Spinning disc Confocal/ IX81-Olympus inverted microscope and Metamorph Acquisition software. For Dvl-GFP subdomain quantification, embryos were imaged using identical settings for the green channel and cells from 5 embryos of each group were randomly selected for measuring membrane length, Dvl-GFP particle size and number in ImageJ (NIH). The average threshold of three membranes expressing Dvl-GFP alone was used to set the background threshold for subdomain analysis. To monitor protein localization in the gastrulae, RNA were injected at the specified doses at the one-cell stage and embryos were fixed at 10 hpf for immunostaining. Images were acquired with a Quorum Spinning disc Confocal/ IX81-Olympus inverted microscope and Metamorph Acquisition software.

Pull-down and western blot analyses

Control GST protein was produced from pGEX-4T-1 (GE Healthcare) in XL-1Blue *E. coli* and GST-fusion proteins were produced from pDEST^{TM}15-based vectors in BL21-AI™ *E. coli* according to manufacture's protocol (Invitrogen). Pierce glutathione magnetic beads (Thermo Scientific) were used in purification and subsequent pull-down experiments. Dvl-GFP and EGFP proteins were translated *in vitro* in TNT coupled reticulocyte lysate systems (Promega). Pull-down was performed according to *Promega Protocols & Applications Guide* (www.promega.com) with the following modifications: cells were lysed in lysis

buffer (50 mM NaH_2PO_4, 300 mM NaCl, 1 mM EDTA, and 1% TritonX-100, pH 8.0) with freshly added Lysozyme (200 µg/ml), DTT (1mM) and complete Mini, EDTA-free protease inhibitor cocktail tablets and washed in lysis buffer without lysozyme in the presence of 5% glycerol. All pull-down procedures were performed at 4°C. Denville Blue™ Protein Stain (Denville Scientific) was used to detect GST-fusion proteins in SDS-PAGE gels (Fisher Bioreagents). Western blot analysis was conducted with primary antibodies, mouse monoclonal anti-GFP antibody (1:2000, Roche, clones 7.1 and 13.1) and mouse monoclonal anti-GST antibody HRP conjugate (1:8000, Santa Cruz, sc-138HRP), and secondary antibody, Goat polyclonal anti-mouse HRP conjugate (1:10000, Millipore, 12-349). Amersham™ ECL plus western blotting detection system (GE Healthcare) was used and signals were detected with Amersham Hyperfilm™ ECL (GE Healthcare) or Fujifilm LAS-3000.

Statistical analyses

Data analyses were performed in GraphPad Prism (GraphPad Software) and Excel (Microsoft). All results were expressed as means ± SEMs. Differences between two groups were analyzed by two-tailed student's T-test. Differences among three groups were analyzed by one way ANOVA, followed by Bonferroni's post hoc test. Statistical significance was set at $p < 0.05$.

Acknowledgements

We thank Drs. Andreas Jenny, Carl-Philipp Heisenberg, Fang Lin, Hitoshi Okamoto, John Wallingford, Lei Feng and Avik Choudhuri for their generosity in

sharing reagents and fish lines, Drs. Andreas Jenny, Adrian Santos-Ledo, Kelly Monk and Ryan S. Gray for comments on the manuscript, Linda Lobos for editing, and Analytical Imaging Facility at Albert Einstein College of Medicine, Dr. Y.G. Yeung, FLM and LSK lab members for helpful discussions and technical support. We acknowledge the research assistants in our fish facilities for fish care. This work was supported in part by NIH grants R01GM089979 to FLM and R01GM77770 and GM55101 to LSK.

Chapter IV

OVERVIEW AND FUTURE DIRECTIONS

In this thesis, I describe work toward defining the potential biological functions of adhesion GPCRs during vertebrate development, with particular focus on the role of Gpr125 in C&E gastrulation movements. Through computer-based data mining, RT-PCR analysis and molecular cloning, I determined that the human adhesion GPCR family is well conserved in the zebrafish genome. I also discovered that out of 12 adhesion GPCRs with no previously reported expression or functional data during development, nine are expressed in zebrafish embryos before 24hpf and seven are expressed during gastrulation. These results constitute the first systematic expression survey of adhesion GPCRs during early vertebrate development. The large fraction of adhesion GPCRs expressed during early embryogenesis motivates further functional studies of the potentially significant contribution of this GPCR family to vertebrate development.

To advance our knowledge of the molecular processing of adhesion GPCRs, I also investigated the potential cleavage event mediated by the GPS motif of Gpr125. Proteolytic cleavage at the GPS motif has been identified as an intrinsic post-translational modification process of many adhesion-GPCRs (Arac et al 2012; Jin et al 2007; Krasnoperov et al 2002; Lin et al 2004; Lin et al 2010; Luo et al 2012; Moriguchi et al 2004; Okajima et al 2010). Over the last decade,

the conserved cleavage site, molecular mechanism and potential functional implications of the GPS proteolysis have been gradually unveiled (Arac et al 2012; Krasnoperov et al 2002; Lin et al 2004; Lin et al 2010; Luo et al 2012; Okajima et al 2010; Yu et al 2007). Through cloning, expression and western blotting analyses of tagged Gpr125 protein, my work indicates that Gpr125 is likely present as an uncleaved form. This result provides experimental evidence corroborating a recent report that several adhesion GPCRs, including Gpr125, do not have the consensus cleavage sequence in their GPS motif and therefore might not undergo proteolytic cleavage (Promel et al 2012). Our results along with those of others support the notion that GPS domain-mediated cleavage and subsequent dimerization of the resulting subunits may only apply to some but not all adhesion GPCRs. Intriguingly, recent studies of LAT-1/Latrophilin in *Caenorhabditis elegans* indicate the GPS motif might provide important functions independent of proteolytic cleavage (Promel et al 2012).

Previously, the expression of *Gpr125* was reported in various tissues of mouse embryos and adults, including the pluripotent spermatogonial progenitor cells (Homma et al 2008; Pickering et al 2008; Seandel et al 2007); however, its function was not known. In our study, we identified zebrafish Gpr125 as a novel modulator of C&E gastrulation movements and tangential FBMN migration, two processes manifesting planar polarity that are evolutionarily conserved among vertebrates (Solnica-Krezel 2005; Wada & Okamoto 2009) (Figure 28). Towards elucidating the molecular and cellular mechanisms by which Gpr125 regulates these processes, we showed that *gpr125* interacted with PCP genes in

molecular-genetic studies. Whereas downregulation of Gpr125 expression with antisense MOs did not cause any overt phenotypes in wild-type embryos, it exacerbated C&E and FBMN migration movement defects in embryos harboring mutations in the Wnt/PCP pathway components (Figure 28). Reciprocally, and as observed for PCP genes, excess Gpr125 impaired PCP-dependent cellular and molecular polarities required for or associated with normal C&E gastrulation movements (Figure 28). Therefore, this study for the first time revealed a function of Gpr125 during vertebrate development.

To uncover the molecular mechanism of Gpr125 function during C&E movements, we tested the ability of Gpr125 to directly interact with PCP components. As on one hand, Dvl has a PDZ domain and its membrane translocation is important for PCP signaling and on the other hand, Gpr125 has a PDZBM and localizes on the membrane, we tested whether Gpr125 can directly interact with Dvl. Indeed, Gpr125 ICD is able to pull down Dvl and its PDZBM is partially responsible for this interaction. This result suggests that Gpr125 could be a new component of Wnt/PCP pathway.

Next, studies of subcellular distribution between Gpr125 and various PCP components carried out in this thesis work add further mechanistic insights to our understanding of PCP signaling in vertebrates. Our collaborative “blastomere localization assays” showed that when overexpressed in zebrafish late blastulae, Gpr125 promoted localization of Dvl in membrane subdomains in contrast to punctate distribution in the cytosol when Dvl was expressed alone. Furthermore, Dvl was able to cluster Gpr125, Kny-GFP into membrane subdomains while

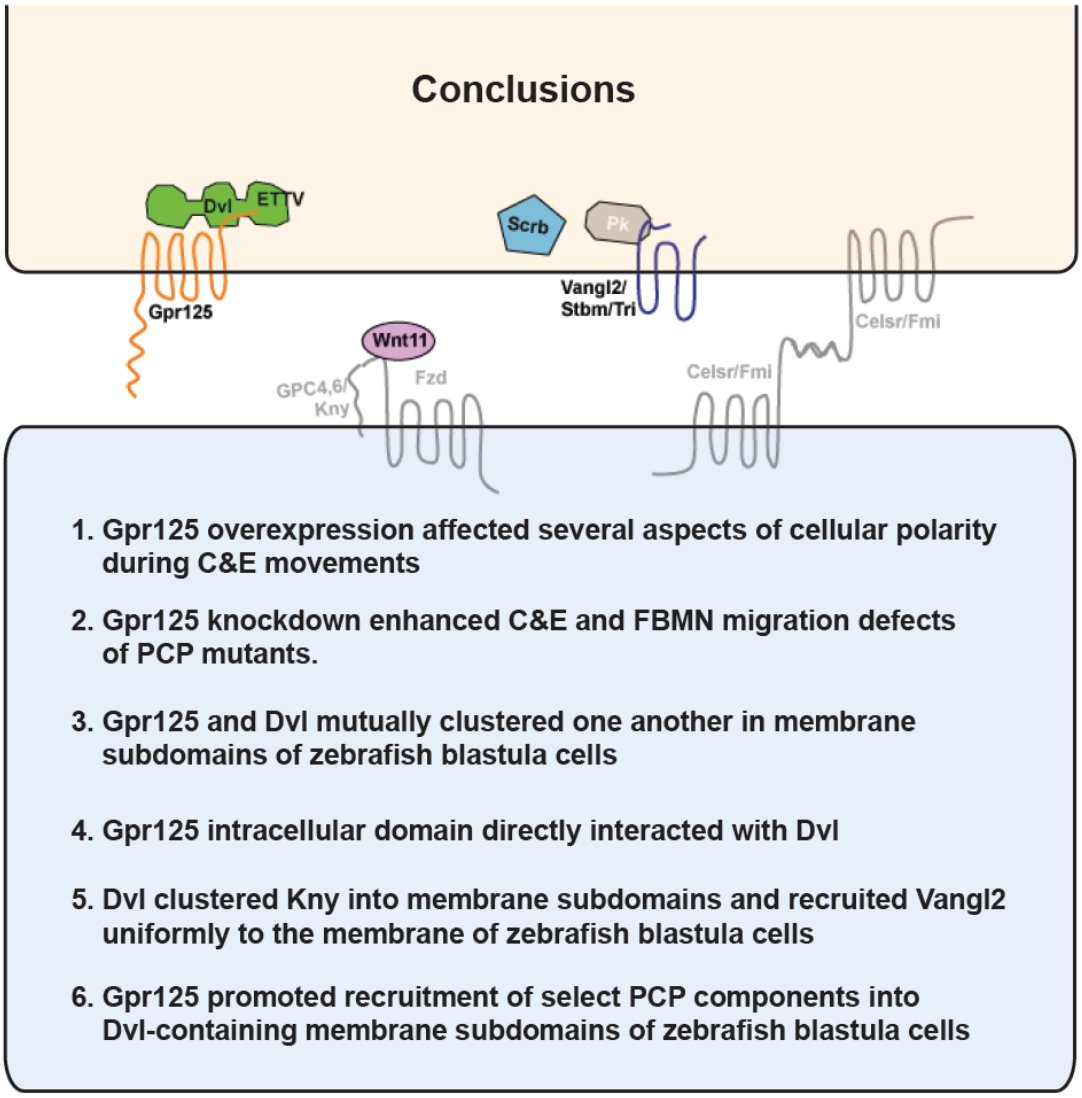

Figure 28. Conclusions supporting the role of Gpr125 as a novel component of the Wnt/PCP signaling system.

promoting uniform membrane localization of endogenous Tri/Vangl2 (Figure 28). These observations along with the previously reported ability of Dvl to form membrane subdomains with Fz7 in the presence of Wnt11 resonate with the report in *Drosophila* proposing essential roles for Dvl in clustering PCP components to form and stabilizing supramolecular complexes (Strutt et al 2011). In addition, we found Dvl-Gpr125 subdomains were also enriched in Fz7 and Kny-GFP but not Vangl2/Tri (Figure 28). These results suggest Fz7 and Kny may be components of large Dvl-containing protein complexes, formation of which is stimulated by Gpr125.

Based on these observations, we propose Gpr125 acts as a novel Wnt/PCP signaling component in zebrafish (Figure 28). We hypothesize that Gpr125 facilitates formation of asymmetric PCP supramolecular complexes, which are thought to mediate PCP signaling between neighboring cells (Jenny et al 2003b; Strutt et al 2011; Witzel et al 2006). Given the data on posterior enrichment of Dvl and anterior of Pk (Ciruna et al 2006; Yin et al 2008) and Trilobite (I. Roszko & LSK unpublished data), we speculate that Gpr125 promotes formation of Dvl, Fz, Knypek complexes that are likely more abundant on the posterior cell membranes. Our discovery of a function for Gpr125 in C&E during gastrulation, a processes where all known PCP components act, and later during FBMN migration, where only a subset of PCP genes are required, opens up exciting avenues for further studies of Gpr125 function, in particular towards understanding how Wnt/PCP signaling operates to regulate cell and tissue polarity in these unique morphogenetic processes.

In this thesis study, several results need to be interpreted with caution and need future verification when additional tools are available. Firstly, we utilized both gain-of-function and loss-of functions approaches to study the function of Gpr125 particularly during C&E movements. We decided to employ a gain-of-function approach, as it is characteristic of C&E and other cell movements that both elevated or reduced function of its regulators impair cell polarity and thus lead to similar morphogenetic defects. However, keeping in mind the potential for overexpression to cause nonspecific protein interactions, we were cautious about our interpretation based on overexpression studies and only did so when the loss-of-function experiments also suggested an involvement of Gpr125 in C&E and FBMN migration.

Secondly, I attempted to generate antibodies against zebrafish Gpr125 in order to determine the localization of its endogenous protein, the form of its mature protein and the efficiency of *gpr125* MOs. However, none of the 16 antibody clones against various Gpr125 peptides generated by Abmart, (Shanghai, China) appeared to recognize Gpr125 in western blotting or immunofluorescence experiments. Therefore, I generated Gpr125 fluorescent fusion proteins and employed them to determine localization in zebrafish embryos and the form of its mature protein present in zebrafish embryo lysate. Although they are useful alternatives, possible pitfalls exist, such as the attenuation of protein activity or new protein interactions caused by the fluorescent moiety and cellular defects caused by overexpression. Encouragingly, my colleague succeeded in detecting endogenous Vangl2 by

immunohistochemistry with an antibody against zebrafish Vangl2; thus, we were able to use it in my thesis to test the impacts of Gpr125 and Dvl on endogenous Vangl2 localization. With ever-increasing efforts to produce antibodies that are specific for zebrafish proteins, it is likely that future studies will define endogenous Gpr125 distribution. Alternative, we can try to knock in a tag to endogenous gpr125 by using a new technique established in the Ekker laborboraty (Bedell et al) .

Lastly, due to the lack of a *gpr125* mutant, we created a *gpr125* loss-of-function condition using antisense MOs-mediated translation interference. Although, the two MOs we employed were very efficient at blocking translation of GFP reporters bearing *gpr125* target sequences, I could not evaluate the effectiveness of the MOs in blocking translation of endogenous Gpr125 protein, due to lack of a Gpr125 specific antibody. Nevertheless, it is likely that the MOs created at least a partial LOF condition, as they were able to enhance the defects of PCP mutants while a control MO failed to do so. More importantly, co-injecting a MO-resistant form of *gpr125* RNA partially suppressed the enhancement of C&E defects in MO2-*gpr125*-injected PCP mutants, supporting the notion that the defects observed in MO2-*gpr125*-injected embryos were specifically due to reduced *gpr125* function. In the future, we plan to test and extend our model in a genetic LOF scenario when a *gpr125* mutant and other reagents, such as antibodies, are available.

Gpr125 overexpression affects several aspects of cellular polarity during C&E movements

Previous work in our laboratory identified domains of distinct C&E movements in the developing gastrula, with no C&E in the ventral mesoderm, increasing C&E in the lateral mesoderm towards dorsal, modest C&E in the medial paraxial mesoderm, and robust extension with moderate convergence in the axial mesoderm (Figure 29) (Myers et al 2002a). Within each of these C&E domains, cells exhibit distinct morphologies and behaviors. Ventral cells are round and they initially spread over the yolk, and then move toward the vegetal pole (Myers et al 2002a). At mid-gastrulation stage, convergence starts in the lateral mesoderm, where cells are modestly elongated, do not align with the embryonic ML axis and exhibit slow dorsal-directed migration. This cell behavior requires function of Stat3 transcription factor and $G\alpha_{12/13}$ but is independent of PCP signaling (Figure 29) (Lin et al 2005; Miyagi et al 2004; Sepich et al 2005). At late gastrulation, mesodermal cells migrating into the dorsal-lateral region become more elongated along their ML axis and undergo fast dorsal-directed migration and therefore lead to rapid convergence (Figure 29). In contrast to the slow dorsal-directed migration, fast dorsal-directed migration requires proper PCP signaling, as compromised Vangl2/Tri and Rok2 function result in reduced C&E, in part due to an impaired ability of cells to migrate along straight paths (Jessen et al 2002; Marlow et al 2002). In the paraxial presomitic mesoderm, cells become highly elongated, align parallel to the ML equator and intercalate preferentially in this direction to lengthen the embryo anterio-posteriorly in a PCP

dependent manner (Figure 29) (Keller et al 2000a; Marlow et al 2002; Wallingford et al 2000). Polarized radial intercalations, whereby cells from one layers intercalates to preferentially separate cells along the AP embryonic axis, also contribute to C&E in this paraxial region (Figure 29) (Yin et al 2008). Previous work in our laboratory also demonstrated that the PCP component Rok2 is required cell autonomously for cell elongation and both cell autonomously and

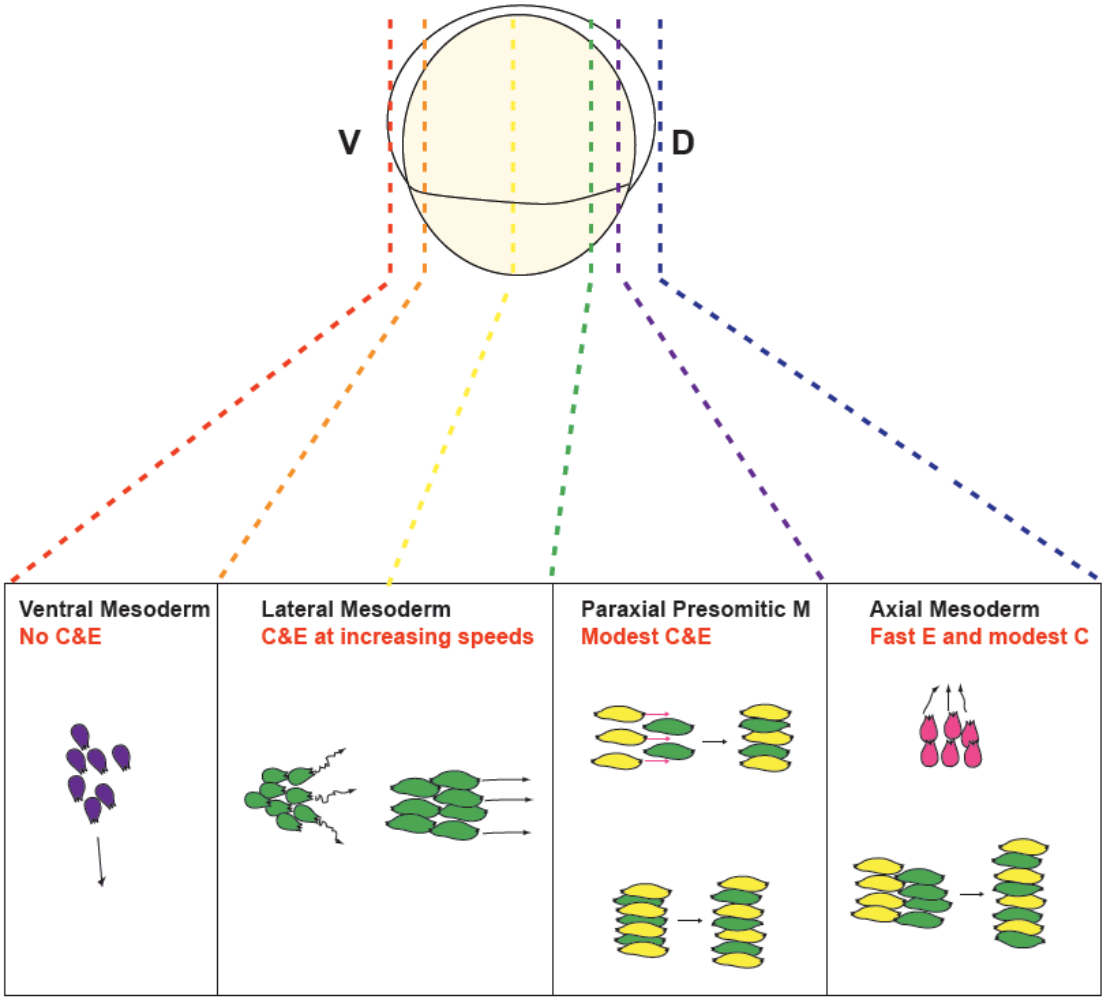

Figure 29. Distinct domains of C&E movements in the mesoderm of zebrafish gastrulae and the underlying cell behaviors.

non-cell autonomously for ML alignment. In addition, a cell can elongate properly regardless of its ML orientation, suggesting that elongation and orientation can be independent properties (Marlow et al 2002). However, some PCP components, like Tri/Vangl2 have cell autonomous and non-autonomous functions in both cell shape and alignment (Jessen et al 2002).

To study the cellular mechanisms underlying C&E defects of *gpr125* overexpressing embryos, we decided to investigate the effect of *gpr125* overexpression on previously studied cell behaviors driving C&E movements. Labeling Gpr125 overexpressing embryos with mGFP revealed extra columns of cells in the notochord at the end of gastrulation, indicating compromised ML intercalation (Figure 18). Morphometric analysis revealed that both mediolateral cell elongation and alignment were impaired in Gpr125 overexpressing gastrulae. Therefore, we concluded that compromised ML cell polarization and consequently ML intercalation contributes to the AP axis reduction in *gpr125* overexpressing embryos. Further studies are needed to address the cell autonomy of Gpr125 function.

It will be also interesting to investigate whether other cell behaviors such as dorsal-directed migration are also affected by Gpr125 overexpression. Based on our results demonstrating that Gpr125 acts at least partially by affecting PCP signaling, we anticipate it would likely have an impact on fast dorsal-directed migration. As slow dorsal-directed migration is independent of PCP signaling, analysis of Gpr125's effect on this cell behavior would provide interesting insight

as to whether Gpr125 acts solely in the processes regulated by PCP signaling or also acts via PCP independent mechanisms.

Besides polarized morphology and behaviors, cells from multiple tissues manifesting planar polarity also exhibit asymmetric distribution of PCP proteins (Goodrich & Strutt 2011; Gray et al 2011; McNeill 2010). These molecular asymmetries are thought to either reflect existing cell polarization or to serve as an essential step for the establishment and/or maintenance of cell polarization by Wnt/PCP signaling (Goodrich & Strutt 2011; Gray et al 2011; McNeill 2010; Simons & Mlodzik 2008). In fly wings, Core PCP proteins become localized to apical junctions early in development and during pupal development these proteins become asymmetrically distributed along the distal-proximal axis in the cell. Fz together with Dsh and Diego localize to the distal membrane, whereas Vang/Stbm and Pk localize to the proximal membrane of cells in the pupal wing disc (Axelrod et al 1998; Bastock et al 2003; Das et al 2004; Jenny et al 2003a; Strutt 2001). As these molecular asymmetries take place before any polarized morphology is recognizable, they are hypothesized to play a pivotal role in the formation of tissue polarity (Goodrich & Strutt 2011; Gray et al 2011; McNeill 2010).

In zebrafish embryos, Pk and Dvl localizing on anterior and posterior membranes respectively has also been observed in neural keel and dorsal mesodermal cells undergoing C&E movements (Ciruna et al 2006; Yin et al 2008). Significantly, these molecular asymmetries are lost in embryos with impaired PCP signaling (Ciruna et al 2006; Yin et al 2008), suggesting that they

reflect cell polarization in the gastrula. Moreover, asymmetric distribution of PCP components along the AP axis could potentially serve as a molecular compass to ensure C&E movements occur in the correct direction. In light of these previous studies (Ciruna et al 2006; Yin et al 2008), we analyzed *Drosophila* Pk-GFP localization in Gpr125 overexpressing ectodermal cells. In embryos overexpressing Gpr125, the percentage of cells with anterior Pk-GFP spots decreased, and this was accompanied by an increase in the fraction of cells with cytoplasmic Pk-GPF. This is reminiscent of the phenotypes previously reported in embryos overexpresssing Xdd1, a dominant negative form of Dvl, and in *trilobite* (*tri*)/*vangl2*; *knypek* (*kny*)/*glypican4* double mutant gastrulae (Yin et al 2008). These results indicate that abnormal cell shape and alignment in *gpr125* GOF embryos is associated with loss of molecular PCP asymmetry.

Another outstanding question regarding protein asymmetry is whether Gpr125 itself is asymmetrically localized. Given that Gpr125 forms clusters with Dvl and Fz, which are at the distal membrane of *Drosophila* wing hair cells and Dvl at the posterior membrane of zebrafish gastrula cells, but not with Vangl2 or Pk, both of which are at the proximal in *Drosophila* and anterior in zebrafish (Axelrod 2001; Bastock et al 2003; Ciruna et al 2006; Feiguin et al 2001; Strutt et al 2002; Tree et al 2002; Yin et al 2008), it is intriguing that Gpr125 could be posteriorly enriched.

How PCP components achieve asymmetric distribution is not well understood. In the fly wing, Fz has been reported to redistribute distally along a polarized microtubule network, which orients along the PD axis with small but

significantly greater proportion of plus end growing distally (Harumoto et al 2010; Shimada et al 2006). Recently, it has been shown that Fmi is rapidly endocytosed from cell membranes, unless it is bound to and stabilized by Fz in the membrane junctions (Strutt et al 2011). Together, these mechanisms have been proposed to drive formation of Fz:Fmi complexes preferentially on distal cell membranes (Strutt et al 2011). During zebrafish gastrulation, PCP pathway has been shown to influence microtubule network and bias the position of MTOC to the cell posterior. In addition, disruption of microtubules prior to ML cell elongation inhibits this ML polarization and anterior Pk-GFP enrichment (Sepich et al 2011). Thus, like in *Drosophila*, microtubules are required for PCP cell polarization during C&E gastrulation movements. In our Gpr125-Cherry overexpression experiments, Gpr125-Cherry was present on the membrane as well as in cytoplasmic puncta, which could conceivably be specific types of vesicles. Therefore, it would be interesting to determine the cytological nature of the Gpr125-Cherry containing puncta and to analyze their dynamics in the future.

Gpr125 and PCP supramolecular complexes

Recently, a model has been proposed for *Drosophila* PCP whereby cytoplasmic PCP components cluster asymmetric PCP membrane complexes into supramolecular complexes (puncta) to modulate establishment and/or maintenance of planar cell polarity (Strutt et al 2011). It has previously been shown that asymmetric Fz-Fmi:Fmi complexes preferentially form between neighboring cells possibly in response to a long-rang cue to serve as the primary

building blocks for the core protein complexes. Subsequent addition of Van gogh/ Sbtm further stabilizes the asymmetric complexes (Strutt & Strutt 2008; Strutt et al 2011). The cytoplasmic components Dsh, Pk and Dgo can then be recruited into the complex. Interestingly, recruitment of these cytoplasmic components clusters the membrane complexes of common polarity into junctional puncta (Strutt et al 2011). The size of PCP supramolecular complexes is thought to reflect or possibly define the cellular asymmetry between neighboring cells, as in *dgo, pk* and *dsh* mutant clones, puncta become progressively smaller with slightly reduced intensity, and correspondingly the tissue polarity defects become more severe (Strutt et al 2011). Although it is still unclear how clustering of asymmetric complexes might lead to the establishment of cellular polarity, an appealing model has been made based on these recent data to at least explain how clustering might result in polarized distribution of asymmetric PCP complexes across a field of cells (Strutt et al 2011). According to this model, the puncta formed by distal or proximal complexes can increase size by recruiting more complexes of the same polarity and/or inhibiting the recruitment of complexes of opposite polarity, leading to local self-enhancement of asymmetric protein distribution. Because intercellular complexes are intrinsically asymmetric, local self-enhancement of distal complexes clustering in one cell leads to a corresponding enhancement of proximal complexes clustering in the neighboring cell. This coupled clustering ensures the asymmetric distribution of distal and proximal complexes within a cell and promotes the propagation of asymmetric distribution of PCP complexes across a field of cells (Strutt et al 2011). However,

it is still enigmatic what signal specifies the global orientation of such puncta relative to the axes of the tissue. Formation of membrane clusters has been observed between *Xenopus* Vangl2 and *Drosophila* Pk in cells within *Xenopus* animal cap explants and among zebrafish Fzd7, Wnt11 and *Xenopus* Dvl in zebrafish blastomeres (Jenny et al 2003b; Witzel et al 2006). Moreover, asymmetric enrichment of exogenous *Drosophila* Pk and *Xenopus* Dvl in highly punctate patterns has been reported in zebrafish cells undergoing C&E and neurulation (Ciruna et al 2006; Yin et al 2008). These observations suggest a similar mechanism involving formation of supramolecular complexes could underlie PCP signaling and PCP-regulated cell polarity during C&E. In this context, as mesenchymal cells are moving and changing their contacts during gastrulation, local organization of PCP proteins into puncta could allow more efficient establishment of planar polarity and allow dynamic rearrangement of polarized interactions between neighboring cells.

Thus far, the mechanisms through which asymmetric membrane complexes are clustered into puncta are not understood (Strutt et al 2011). In my thesis study, we discovered that Gpr125 directly interacted with Dvl, recruited Dvl to cell membranes and promoted clustering of Dvl into discrete membrane subdomains. Reciprocally, Dvl promoted clustering of Gpr125 into membrane subdomains. In addition, we showed that Dvl was able to cluster Kny-GFP into membrane subdomains and to promote uniform membrane localization of endogenous Tri/Vangl2 in late stage blastula. These observations along with previous reports indicate a conserved role for Dvl in clustering PCP components

in vertebrates (Jenny et al 2003b; Witzel et al 2006). Future work is needed to determine whether PCP supramolecular complexes are essential for PCP signaling and the establishment or maintenance of cell polarity during C&E movements. It intriguing that Gpr125 may be a new important positive regulator of formation of PCP supramolecular complexes.

To investigate the role of Gpr125 in PCP supramolecular complexes, we expressed Gpr125 alone (or with Dvl) with various PCP proteins. Interestingly, we found that overexpression of Gpr125 alone did not affect Vangl2 endogenous distribution. Moreover, when co-expressed with Dvl, Gpr125 specifically promoted formation of supramolecular complexes with Fzd7 and Kny but not Vangl2. This finding provides an insight into the molecular basis by which Gpr125 might interact with other PCP components and also suggests the presence of distinct PCP supramolecular complexes in gastrula cells. We showed that Gpr125 can directly interact with Dvl, but it remains to be tested whether it can directly interact with the other PCP components recruited to Gpr125 containing complexes. As Gpr125 and Fmi/Celsr are both adhesion GPCRs, it is tempting to speculate whether Gpr125 has redundant function with Fmi/Celsr, such as the ability to form heterodimer with Fzd. We noticed that when expressed in blastula, Gpr125-Cherry caused deep cells to change their shape from a round morphology to a more hexagonal shape with Gpr125-Cherry localized to membrane contacts. When Fzd7-CFP was co-expressed, its localization pattern was nearly identical to that of Gpr125. In other work, co-expression of Fmi2-YFP with Fzd7-CFP resulted in a similar accumulation of Fdz7-CFP and Fmi2-YFP at

membrane contacts and Fmi proteins contributed partially to cell contact persistence mediated by Wnt11 and Fzd7 (Witzel et al 2006). The similarity in the distribution patterns motivates future studies to address potential Gpr125:Fzd and its functional significance. It also remains a possibility that Gpr125 and Celsr might interact with each other to carry out certain functions.

There are at least three non-exclusive hypothetical models regarding the role of Gpr125 in these complexes (Figure 30). In the simplest model, Gpr125 could play a supportive and nonessential role in the formation of the supramolecular complexes (Figure 30A). Gpr125 embedded in the cell membrane could recruit Dvl to the membrane via its ETTV motif and keep it in proximity to Fzd and therefore increase the propensity for Fzd to interact with Dvl. If, similarly to *Drosophila*, the size of the subdomains reflects or possibly determines cellular polarity (Strutt et al 2011), the ability of both Gpr125 and Fzd to bind to Dvl would largely promote the increase of the size of Dvl-containing supramolecular complexes and the establishment of cellular polarity.

In the second model, I hypothesize that Gpr125 could contribute to the adhesive properties utilized by PCP supramolecular complexes to confer cellular polarity. (Figure 30B). When the extracellular domain of Gpr125 was overexpressed, embryos had delayed epiboly and *in situ* hybridization with a mesodermal marker, *papc,* revealed “salt and pepper” staining pattern, which could either suggest dispersion of cells or change of cell fates in *papc* staining negative area. Although further investigation is required, these results hint at a potential role of the extracellular domain in modulating adhesion, consistent with

the known functions of its protein modules (Carreira-Barbosa et al 2009; de Wit et al 2011; Homma et al 2008). It has been shown that overexpressed Celsr2 is enriched in subdomains formed by exogenous Wnt11, Fzd7, and Dvl in late blastula stage embryos and both overexpressed and endogenous Celsr proteins partially contribute to increased contact persistence between these subdomain-containing membranes (Witzel et al 2006). Intriguingly, Gpr125 also localized to membrane subdomains containing Fzd7 and Dvl in a similar experiment. Therefore, I propose that Gpr125 acts analogously to modulate adhesion between membranes in regions occupied by PCP component subdomains. Notably, neither Celsr proteins nor Gpr125 has been shown to form asymmetric puncta similar to Pk and Dvl during gastrulation. Although it is possible that the endogenous proteins might exhibit such asymmetry, overexpression experiments thus far have not revealed enrichment of Celsr or Gpr125 on particular membranes. The activity of adhesion molecules is known to be influenced by their local environment; thus, it is possible that any adhesion activity of Gpr125 is differentially regulated when it is present in the PCP supramolecular complexes versus in regions outside the membrane subdomains. If this is the case, one might predict that Gpr125 would be regulated by PCP components to contribute to the increase of adhesion in PCP subdomains.

In the context of FBMN migration, the potential role of Gpr125 modulating adhesion in conjunction with PCP components becomes even more appealing. FBMNs in zebrafish and mouse embryonic hindbrain undergo a characteristic tangential migration from rhombomere (r) 4, where they are born, to r6/7.

Cohesion among neuroepithelial cells regulated by PCP components, Fzd3a and Celsr2, has been proposed to prevent FBMNs positioned in the basal neuroepithelium from migrating apically towards the midline of the neuroepithelium (Wada et al 2006). In addition, Stockinger et al. has used a combination of biophysical cell adhesion measurements and high-resolution time-lapse microscopy to determine the role of neuroepithelial cohesion in FBMN migration and has shown that reducing neuroepithelial cohesion by interfering with Cadherin 2 activity causes FBMNs positioned at the basal side of the neuroepithelium to move apically towards the neural tube midline instead of tangentially towards r6/7 (Stockinger et al 2011). Similar approaches can be used in the future to test the potential role of PCP components as well as Gpr125 in maintaining neuroepithelial cohesion. Notably, some previous studies have argued that Dvl function is not required for FBMN migration (Jessen et al 2002; Wada & Okamoto 2009). Therefore the function of Gpr125 during FBMN might involve a mechanism distinct from that used in C&E movements. Addressing the potential interactions between Fzd3a, Celsr2 and Gpr125 might provide some mechanistic insights.

Besides modulating adhesion, PCP signaling has been shown to regulate actin cytoskeleton rearrangement both in *Drosophila* and vertebrates via the activation of small GTPases (Nishimura et al 2012; Strutt 2003). Interestingly, Gpr124, which shares high domain and sequence similarities with Gpr125, has been shown to regulate endothelial cell migration and sprouting in a Cdc42 dependent manner in the mouse central nervous system (Kuhnert et al).

Analogously, Gpr125 might function in PCP supramolecular complexes to regulate cell adhesion and/or cytoskeletal rearrangements by activating small GTPases.

In the third model, Gpr125 could play an instructive role in directing the localization of supramolecular complexes (Figure 30C). This model would require polarized distribution or activity of Gpr125. In zebrafish gastrulae, PCP component puncta have been observed to localize preferentially to the anterior or posterior membranes by an unknown mechanism. It is possible that polarized distribution of molecules that can recruit PCP components might serve as a mechanism to initiate asymmetric localization of PCP complexes. The Gpr125 extracellular region contains multiple LRR domains and a hormone-binding domain, which are known to mediate protein-ligand interactions suited to regulate intercellular communication and cell adhesion (de Wit et al 2011; Pal et al 2012). Therefore, upon stimulation with a ligand distributed in a gradient, Gpr125 might relocate to or become active on a particular side of the cell with regard to the source of the gradient. Subsequently, such asymmetrically localized Gpr125 would lead to polarized recruitment of Dvl and formation of supramolecular complexes. Future experiment addressing the localization of Gpr125 and its requirement for asymmetric PCP component localization are needed.

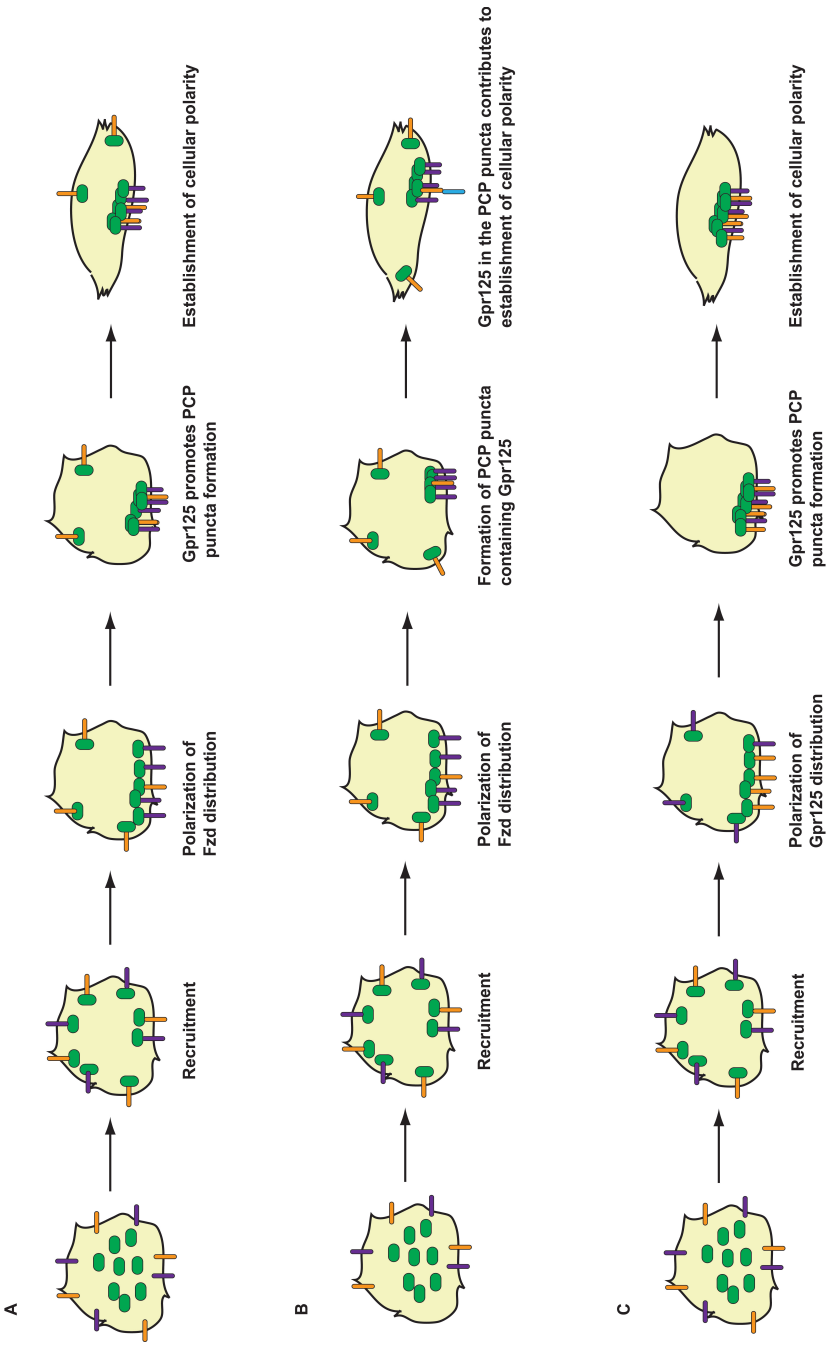

Figure 30. Hypothetical models for the role of Gpr125 in PCP supramolecular complexes and establishment of cellular polarity. (A) Gpr125 promotes polarized Dvl-containing PCP supramolecular complexes formation upon asymmetric distribution of Fzd. (B) Gpr125 proteins in the PCP supramolecular complexes contribute to the establishment of cellular polarity. (C) Asymmetrically localized Gpr125 recruits Dvl-containing PCP complexes and therefore promotes formation of Dvl-containing PCP supramolecular complexes in a polarized manner.

Involvement of PDZBM and PDZ domain in PCP signaling

Dvl proteins possess three conserved domains, an N-terminal DIX (Dishevelled, Axin) domain of 80 amino acids, a central PDZ (Postsynaptic density 95, Discs Large, Zonula occludens-1) domain of about 90 amino acids, and a carboxyl-terminal DEP (Dvl, Egl-10, Pleckstrin) domain of 80 amino acids, plus additional two conserved regions, the basic region and the proline-rich region (Boutros & Mlodzik 1999; Gao & Chen). As Dvl is the signaling hub for both canonical and non-canonical Wnt pathways, the relevance these domains to Wnt signaling has been an area of intensive investigation. The DIX domain can mediate Dvl oligomerization. While it is essential for the canonical Wnt pathway (Boutros et al 1998; Yanagawa et al 1995), the DIX domain is not required for planar cell polarity signaling in the *Drosophila* eye and during zebrafish C&E movements (Axelrod et al 1998; Heisenberg et al 2000). Moreover, Dvl DIX domain deletion mutants only have a very weak effect on PCP signaling in *Drosophila* as well as *Xenopus* (Boutros et al 1998; Wallingford et al 2000). In contrast, the DEP domain seems to be required exclusively for signaling by the PCP pathway. Dvl membrane translocation mediated by DEP domain is the prerequisite for the activation of PCP signaling (Axelrod et al 1998; Boutros et al 1998; Park et al 2005; Yanagawa et al 1995).

The PDZ domain is thought to be involved in Dvl activity in both the canonical and non-canonical Wnt pathways; however, the mechanism and the precise role of this domain in each pathway have not been fully defined. Variation in the types of assays and mutant proteins used has produced confounding

results. Overexpression of a mutant Xdsh (Xdd1) with an internal deletion of the conserved PDZ/DHR domain strongly inhibits induction of secondary axes by WT Xdsh mRNA in *Xenopus* embryos (Sokol 1996). In contrast, a Dvl mutant harboring deletion of the PDZ domain alone showed strong activity in promoting canonical Wnt signaling in *Drosophila* and *Xenopus* (Wallingford et al 2000). With regard to PCP signaling, overexpression of both constructs blocks convergent extension movements in *Xenopus* dorsal marginal zone explants (Sokol 1996; Wallingford et al 2000). The PDZ domain is required for the ability of Dsh to rescue the lethality due to impaired canonical Wnt signaling in *dsh* mutant flies (Boutros et al 1998; Penton et al 2002). On the other hand, this domain seems to be largely dispensable for rescuing the PCP defects in *dsh* mutant flies. Whereas, together with the DEP domain, it is required for the ability of Dvl to suppress the C&E defects of zebrafish *wnt11/slb* mutant embryos (Axelrod et al 1998; Boutros et al 1998; Heisenberg et al 2000; Wallingford et al 2000). Collectively, the data thus far could not lead to a complete understanding of the role of the Dvl PDZ domain in PCP signaling and therefore further studies are needed to answer this question.

The common structure of PDZ domains comprises six β-strands (βA–βF) and two α-helices (αA and αB), which fold to form a six-stranded sandwich (Doyle et al 1996; Fanning & Anderson 1998; Hung & Sheng 2002; Lee & Zheng 2010). Where examined, the PDZ binding motif (PDZBM) found in numerous proteins, binds to the PDZ domain as an antiparallel β-strand inserted into a groove between the βB strand and the αB helix of the PDZ domain (Doyle et al

1996; Hung & Sheng 2002; Morais Cabral et al 1996; Wong et al 2003). Common PDZBMs are composed of the last four amino acids at the C-termini of the proteins. Based on their sequences, PDZ domains can be divided into at least three main classes. Class I PDZ domains recognize in PDZBMs X-S/T-X-Φ-COOH (where Φ is a hydrophobic and X is any amino acid). Class II recognize X-Φ-X-Φ-COOH and class III recognize X-D/E-X-Φ-COOH (Hung & Sheng 2002).

Interestingly, in the PCP signaling system, PDZBM is a common feature of transmembrane components, including the core PCP components Fzd and Vangl2 (Hering & Sheng 2002; Jessen et al 2002; Park & Moon 2002). Moreover, besides Dvl, another intracellular PCP component Scrb also contains multiple PDZ domains (Courbard et al 2009). The prevalence of PDZBM and PDZ domain in the PCP signaling system has elicited many studies on the functional significance of this protein-protein interacting module pair.

The type I PDZB motif has been identified in several Fzd receptors (E-S/T-X-V) and demonstrated to interact with the PDZ domain of PSD95 via the classical PDZBM/PDZ interaction (Hering & Sheng 2002). Although rescue experiments with Fzd lacking the PDZB motif has not been reported, a Fz construct with GFP fused immediately after the PDZBM can rescue wing PCP defects in *fz* mutant flies (Strutt 2001). In the classic binding model, the last amino acid of PDZBM inserts into the groove on the surface of the PDZ domain (Doyle et al 1996). If this is the case for the binding between the PDZBM of Fzd to Dvl, fusion of a fluorescent protein directly to the C-terminus of the PDZBM

might create stochastic hindrance for the last amino acid of PDZBM to insert into the groove and therefore disrupt the binding. Conversely, successful rescue with the Fz-GFP fusion protein suggests that the fluorescent protein does not interfere with binding to Dvl or that Dvl might not bind to PDZMB of Fzd. Consistent with the latter, Dvl does not bind to Fzd PDZBM in *in vitro* studies (Stiffler et al 2007; Tonikian et al 2008). Moreover, Dvl recruitment assays and NMR spectroscopy studies suggest the PDZ domain of Dvl binds to an internal motif of Fzd (KTXXX-W) (Umbhauer et al 2000; Wong et al 2003).

Vangl2 also possesses a Class I PDZBM (ETSV) at its C-terminus (Bastock et al 2003; Jessen et al 2002; Park & Moon 2002). The functional significance of the PDZB motif has been studied *in vivo* in fly, frog and *in vitro* through biochemical studies. In *Drosophila*, Bastock et al. demonstrated that both Vang/Stbm lacking the PDZB motif or tagged with YFP at the C-terminus could rescue the wing PCP defects of *stbm* mutants, suggesting the PDZB motif is not required for Stbm function during PCP (Bastock et al 2003). In *Xenopus*, Park et al. reported that Vangl2/Stbm with PDZBM deletion is not able to inhibit Activin A-induced animal cap explant elongation like full-length Vangl2/Stbm, whereas Goto and Keller reported that Stbm PDZB motif deletion mutants could still block the elongation of dorsal marginal zone but at a lower efficiency than full-length version (Goto & Keller 2002; Park & Moon 2002). In addition, when co-expressed, this deletion mutant was able to attenuate the effects of full-length Vangl2/Stbm to inhibit convergent extension of *Xenopus* dorsal marginal zone explant, suggesting the deletion mutant acts in a dominant negative manner

(Goto & Keller 2002). However, deletion of the PDZBM does not affect Vangl2/Stbm's ability to bind Dvl or recruit it to the membrane, whereas the PDZ domain of Dvl is required for the interaction with Vangl2/Stbm (Park & Moon 2002). Hence, the role of the PDZBM remains enigmatic.

Consistent with the lack of evidence for the interaction between the Class I PDZBMs of Fzd and Vangl2/Stbm with Dvl, structural studies reported that the PDZ domain of Dvl is not a typical Class I PDZ domain. Class I PDZ domains contain a histidine at α2-1 position and its N-3 nitrogen forms a specific hydrogen bond with the hydroxylated side chains of either a serine or threonine residue at the p-2 position of PDZB motif (Doyle et al 1996; Hung & Sheng 2002). However, Dvl lacks this histidine and instead has an asparagine, although, it is intriguing that the oxygen of the Asparagine side chain can also form the hydrogen bond with the S/T and P-2 position. Indeed, in the peptide library mapping experiment done by Tonikian et al, substitution of H for N in Class I PDZ domain only negligibly affected binding to S/T (Tonikian et al 2008).

In contrast to the studies discussed above, a direct interaction has been demonstrated between the PDZ domain of Dvl and the Class I PDZBM of its inhibitor protein, Dpr/Drodo with NMR and co-immunoprecipitation experiments (Cheyette et al 2002; Gloy et al 2002; Wong et al 2003). In this thesis work, the presence of the C-terminal PDZBM in Gpr125 prompted us to investigate whether Gpr125 could interact with Dvl via its PDZ domain. Indeed, the blastula membrane recruitment and pull-down assays both suggested that PDZBM as well as other unidentified motif(s) contribute to direct binding between Gpr125

and Dvl. Interestingly, I found a KTXXW motif adjacent to the PDZBM of Gpr125, reminiscent to the internal KTXXXW motif identified in Fzd that can mediate binding to Dsh (Umbhauer et al 2000; Wong et al 2003). Although in contrast to the three amino acids in Fzd, there are only two amino acids between the conserved T and W in Gpr125. Deletion studies carried out by Umbhauer et al. suggest that removing one of these "spacer" amino acids does not completely abolish the function of this motif (Umbhauer et al 2000). Therefore, future studies investigating whether this KTXXW motif also contributes to the binding between Gpr125 and Dvl are warranted.

In summary, the evidence accumulated thus far indicates that the PDZ domain of Dvl is likely to play an important but not yet fully characterized role in PCP signaling. Specifically, the Dvl PDZ domain has consistently been shown to mediate binding between Dvl and multiple PDZBM-containing transmembrane PCP proteins. Moreover, Dvl has also been shown to interact with multiple intracellular PCP proteins, such as Dgo and Pk via its PDZ domain (Jenny et al 2005). Although the PDZBMs may not be required for Fzd and Vangl2/Stbm to interact with Dvl, they could be involved in interactions with other PDZ proteins in the PCP complex. For example, Vangl2/Sbtm has been reported to interact directly with Scrb via Class I PDZ interaction (Courbard et al 2009; Montcouquiol et al 2003; Montcouquiol et al 2006). In *Drosophila*, the PDZBM of Vang/Stbm is partially responsible for the binding to the third and likely the fourth PDZ domain of Scrb (Courbard et al 2009). Studies in the mouse implicated all but the first PDZ domain of Scrb in the binding to Vangl2, and the PDZBM of Vangl2 seems

to play a pivotal role, as its deletion completely abolishes binding to Scrb (Montcouquiol et al 2003; Montcouquiol et al 2006). Given the observation of PCP protein puncta, likely representing PCP supramolecular complexes, in multiple model systems, one appealing model for the role of the PDZ domain is that Dvl acts as a scaffold protein to assemble supramolecular complexes by interacting with and bridging various proteins via its PDZ domain. Indeed, PDZ domain-containing proteins are known for their roles in clustering submembranous protein complexes (Hung & Sheng 2002; Sheng & Sala 2001). Besides interacting with PDZMB containing proteins, PDZ domains can associate with other PDZ domains to form homo- or hetero-oligomers (Dong et al 1999; Fanning & Anderson 1998; Fanning et al 1998; Fouassier et al 2000; Maudsley et al 2000; Srivastava et al 1998; Xu et al 1998). The PDZ domain has also been reported to interact with other distinct protein motifs, such as the ankyrin repeats, spectrin repeats and LIM domains (Cuppen et al 1998; Maekawa et al 1999; Xia et al 1997). While PDZBMs might not be pivotal for interactions between all PDZBM-containing PCP proteins and Dvl, they might collectively promote or contribute to the formation or stability of PCP supramolecular complexes. In the future, it will be of interest to test the effect of PDZBM deletions of multiple PCP components on formation of PCP supramolecular complexes and various PCP-dependent developmental processes. We showed that Gpr125 PDZBM deletion mutant displayed reduced efficiency in Dvl recruitment and subdomain formation. It will be interesting in the future to examine if this mutant also has reduced ability

to promote recruitment of additional PCP components into Gpr125:Dvl subdomains.

Gpr125 and other Wnt signaling Pathways

Apart from the Wnt/PCP signaling, certain Wnt and Fzd combinations can trigger distinct signal cascades. The best known among all Wnt signaling cascades is the canonical Wnt or Wnt/β-Catenin pathway. As illustrated in Figure 31, in the absence of a Wnt ligand, cytoplasmic β-catenin protein is degraded by the action of the Axin destruction complex, which is composed of the scaffolding protein Axin, the tumor suppressor *adenomatous polyposis coli* gene product (APC), casein kinase 1 (CK1), and glycogen synthase kinase 3β (GSK3β). CK1 and GSK3β sequentially phosphorylate the amino terminal region of β-catenin, resulting in β-catenin recognition by an E3 ubiquitin ligase, β-Trcp, and subsequent β-catenin ubiquitination and proteasomal degradation. When a Wnt ligand binds to a Fzd receptor and a co-receptor low-density lipoprotein receptor related protein 6 (LRP6) or LRP5, Dvl is recruited via interaction with Fz, resulting in LRP5/6 phosphorylation and Axin recruitment. This disrupts Axin-mediated phosphorylation/degradation of β-catenin, allowing β-catenin to accumulate in the nucleus where it serves as a co-activator for TCF to activate Wnt responsive genes (Gao & Chen ; He et al 2004; Logan & Nusse 2004; Macdonald et al 2007; MacDonald et al 2009; Tamai et al 2000).

In the zebrafish embryo, Wnt/β-catenin pathway plays many pivotal roles including DV axis patterning. In DV axis patterning, the role of Wnt/β-catenin

pathway switches at the midblastula transition (MBT). In the pre-MBT phase, maternal β-catenin protein accumulates specifically in the nuclei of dorsal

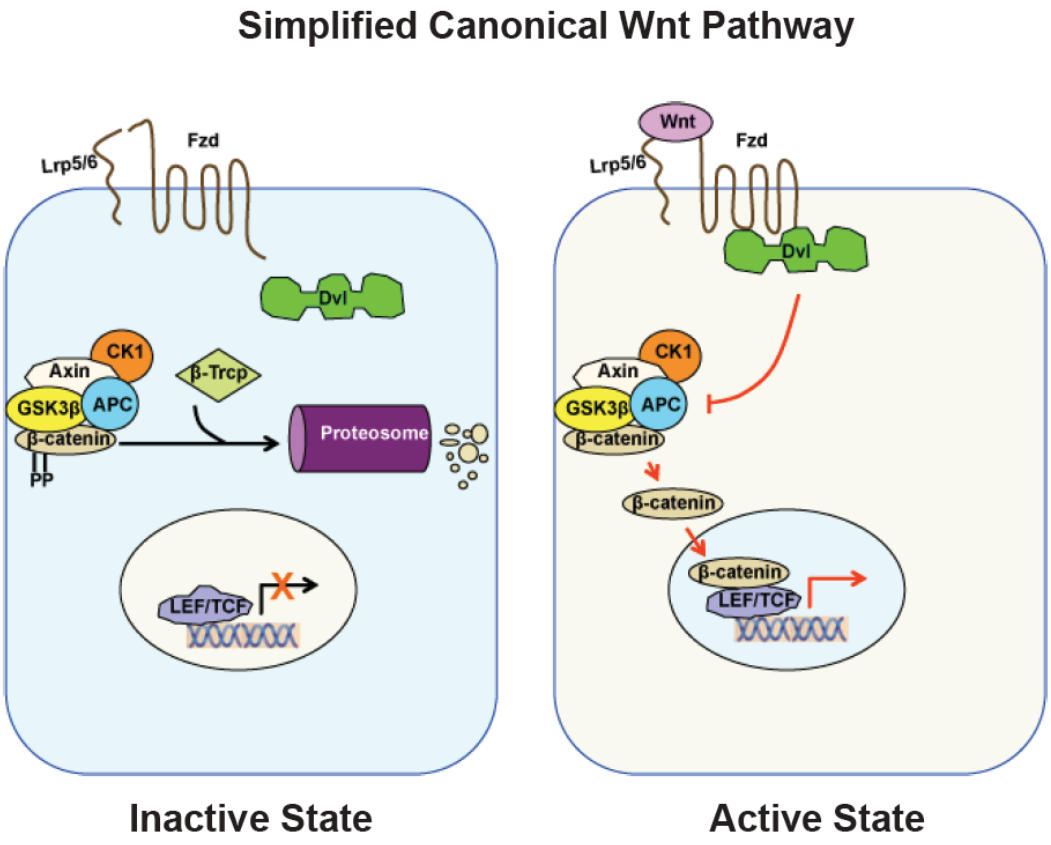

Figure 31. Simplified canonical Wnt pathway. In the absence of Wnt signal, β-catenin is recruited into the Axin destruction complex, and phosphorylated by CK1 and GSK3 at the *N*-terminal 'destruction box'. The phosphorylated β-catenin binds to β-Trcp of the proteosome machinery and is targeted for degradation. As the result, no free β-catenin enters nucleus to form transcriptional complex with LEF/TCF and therefore no transcription of its downstream targets. When Wnt binds to its Fzd receptor and Lrp5/6 co-receptor, Dvl is activated, leading to the inhibition of β-catenin degradation. Stabilized β-catenin enters the nucleus where it forms a transcriptional complex with LEF/TCF and activates the transcription of downstream targets, such as c-Myc.

marginal blastomeres and yolk syncytial layer, where after the onset of the zygotic transcription, it activates the expression of a number of genes, including *bozozok*, *chordin* and *squint*, to establish the dorsal axis and induce the dorsal mesoendodermal fates (Chen & Schier 2001; Feldman et al 2000; Gonzalez et al 2000; Kelly et al 2000). Disruption of the maternal Wnt/β-catenin activity results in embryos with various degrees of ventralized phenotypes (Kelly et al 2000). Conversely, ectopic activation or augmentation of this pathway leads to formation of secondary dorsal axes or dorsalized phenotypes manifest as reduction or lack of ventral structures such as the blood island and ventral tail fin, or posteriorly truncated embryos with a "piggy" tail (Kelly et al 2000; Kelly et al 1995).

During the post-MBT phase, fate mapping and transplantation experiments indicate an activator signal from the Spemann-Mangold organizer acts to induce neural tissue with a broad anterior character. As the germ ring forms, a transformer signal from non-axial germ ring regions modulates the axial character of the nearby neural tissue, resulting in distinct axial forebrain, lateral hindbrain and intervening midbrain territories (Woo & Fraser 1997). In contrast to its role during the pre-MBT phase, Wnt/β-catenin pathway acts in the post-MBT phase to inhibit the role of Spemann-Mangold organizer, resulting in reduction and posteriorization of the neuroectoderm, which is apparent as an expansion of posterior neural fates such as hindbrain at the expense of anterior neural fate, *i.e.* forebrain. (Bellipanni et al 2006; Erter et al 2001; Lekven et al 2001; Momoi et al 2003; Ramel & Lekven 2004). Blocking Wnt/β-catenin activity in the post-MBT phase produces embryos with enlarged heads and reduced tail

structures, reminiscent of dorsalized embryos, resulting from hyperactivation of pre-MBT Wnt/β-catenin activity. Consistent with these dorsalized phenotypes, both excess pre-MBT Wnt/β-catenin signaling and diminished post-MBT Wnt/β-catenin activity lead to expansion of the late dorsal markers *chordin* and *goosecoid* at 50% epiboly. However, to distinguish between these two conditions, only the augmentation of pre-MBT Wnt/β-catenin signaling results in the expansion of the early dorsal marker *bozozok* at 30% epiboly (Bellipanni et al 2006; Momoi et al 2003).

In my *gpr125* GOF studies, a small fraction of embryos injected with high doses of *gpr125* synthetic RNA, such as 400pg, were dorsalized and showed tail truncations. That these morphological phenotypes reflected dorsalization was corroborated by *in situ* hybridization with the dorsal marker, *chordin,* at 50% epiboly, which was expanded in a similar fraction of embryos. These results suggest that besides interfering with C&E movements, *gpr125* can also affect patterning when expressed at high levels. These results raise several interesting questions for future investigations. Firstly, was the dorsalization caused by *gpr125* overexpression a result of augmented pre-MBT or compromised post-MBT Wnt/β-Catenin activity? To address this question it will be interesting to analyze in embryos overexpressing high Gpr125 levels the expression of early dorsal markers such as *bozozok* and *squint* at 3.3 hpf, as these two genes are direct targets of the pre-MBT Wnt/β-catenin activity (Bellipanni et al 2006). Secondly, *gpr125* GOF experiments suggest a role of Gpr125 in both the canonical Wnt and Wnt/PCP signaling pathways. It is intriguing that Gpr125

could mediate a switch between these two signaling cascades at the level of Dvl. Arguing against a role for *gpr125* in DV patterning, *gpr125* morphants did not show any signs of early patterning defects. Therefore, it is possible that the patterning defect caused by overexpression at high levels was an artifact. However, the lack of phenotypes in *gpr125* morphants could also possibly be due to incomplete knockdown or sufficient maternal contribution. Maternal-zygotic and zygotic *gpr125* null mutant embryos are needed to definitively determine the requirement for Gpr125 protein in canonical Wnt signaling and to delineate the underlying mechanism.

Additionally, potential coupling of Gpr125 to heterotrimeric G proteins creates a possible link between Gpr125 and the third Wnt signaling pathway, the Wnt/Ca^{2+} signaling pathway (Figure 32). In both zebrafish and *Xenopus*, binding of *Xenopus* Wnt5a to Rat Fzd2 or *Xenopus* Fzd7 has been shown to activate pertussis toxin-sensitive heterotrimeric G proteins, which subsequently triggers intracellular Ca^{2+} mobilization and activation of calcium-responsive enzymes such as protein kinase C (PKC) and Calmodulin-dependent protein kinase II (Sheldahl et al 2003; Slusarski et al 1997a; Slusarski et al 1997b). As for the other two Wnt pathways discussed in this thesis, the Wnt/Ca^{2+} pathway also requires Dvl, providing another potential interaction with Gpr125 (Sheldahl et al 2003). Wnt/Ca^{2+} signaling has been reported to promote ventral cell fates by antagonizing the pre-MBT Wnt/β-Catenin activity and to regulate gastrulation movements by activating Cdc42 via PKC (Choi & Han 2002; Kuhl et al 2000a; Kuhl et al 2000b). Similarly, in *Drosophila*, Gαo has be shown to function

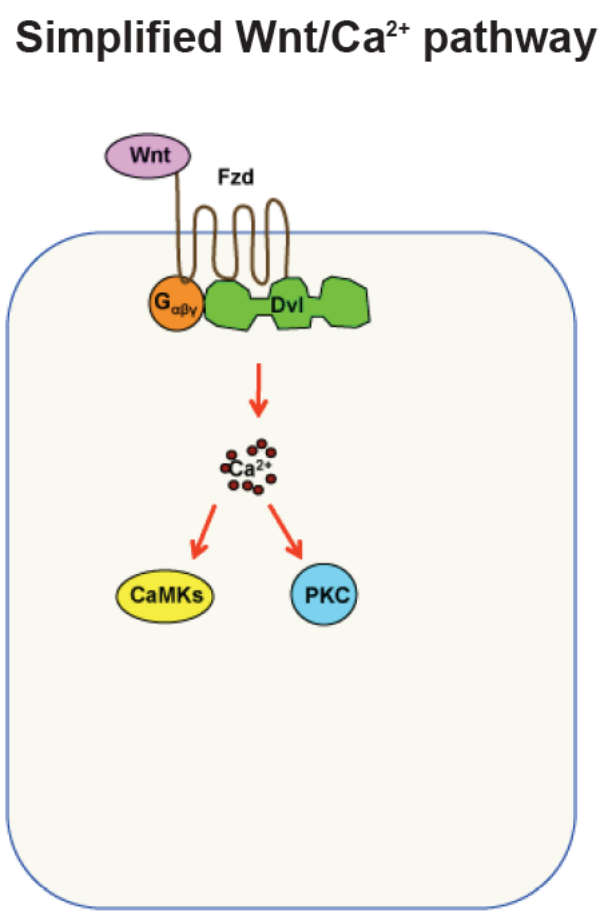

Figure 32. Simplified Wnt/Ca^{2+} pathway. Wnt/Fzd acts via the heterotrimeritc G protein and Dvl to increase the level of intracellular Ca^{2+}. Ca^{2+} then activates PKC, which may activate Cdc42 and regulate cell adhesion and tissue separation during vertebrate gastrulation. Ca2+ also activates CaMKII, which might influence ventral patterning in *Xenopus*.

downstream of Fz and upstream of Dsh to regulate both the canonical and PCP signaling cascades (Katanaev et al 2005). As Gpr125 is a 7TM receptor, it is possible that it couples to heterotrimeric G proteins. However, this remains to be tested. If so, then whether this potential coupling contributes to interactions between Gpr125 and Wnt signaling pathways to regulate C&E movements and patterning becomes an interesting question.

Summary

In this thesis study, I conducted an expression survey of adhesion GPCRs during early stages of zebrafish development. Detailed expression and functional analyses of the Group IV adhesion GPCRs uncovered a role for Gpr125 as a novel modulator of C&E gastrulation movements and FBMN migration. Impairment of planar polarization of cellular properties was identified to underlie C&E defects and associate with loss of asymmetric distribution of Pk in *gpr125* GOF embryo. Based on the results of the molecular-genetic interactions, biochemical interaction and localization studies with PCP signaling components, we propose that Gpr125 acts as a novel component of the Wnt/PCP signaling system and we hypothesize that Gpr125 promotes formation of PCP supramolecular complexes. In addition, examination of the function of Gpr125 protein domains indicated that the GPS domain of Gpr125 is unlikely to mediate proteolytic cleavage of Gpr125, whereas the PDZBM is partially responsible for the direct interaction between Gpr125 and Dvl.

Although this thesis work has provided the first evidence for the biological function of Gpr125 during development, the precise mechanism remains to be uncovered. In addition, whether Gpr125 contributes to other gastrulation movements such as epiboly or other processes including embryonic axis formation or stem cells maintenance remain to be explored. Last but not least, although core PCP pathway components are well conserved between vertebrates and *Drosophila,* vertebrate Wnt/PCP signaling system also employs additional vertebrate specific effectors. Therefore, it will be interesting to test

whether Gpr125 is a vertebrate specific PCP component or has a similar function in regulating planar cell polarity in *Drosophila*.

Although studies from our group and others have furthered our understanding of the cellular and molecular mechanisms contributing to the establishment of planar polarity, numerous questions remain open and new ones have emerged. One key question is how the polarized distribution of PCP signaling components is initiated and maintained across a field of cells, particularly in the context of dynamically moving cells such as those undergoing C&E movements. We also do not understand how PCP signaling cooperates with other signaling pathways to confer polarity to ensure that cells move properly and in an orchestrated manner according to their coordinates relative to the body axes. Gpr125 is an intriguing molecule that could explain formation of asymmetric complexes by linking intracellular signaling components to extracellular environment via its large amino-terminus.

BIBLIOGRAPHY

Adams RJ, Kimmel CB. 2004. *Morphogenetic cellular flows during zebrafish gastrulation.* Cold Spring Harbor, NY: Cold Spring Harbor Lab. Press

Adler PN, Krasnow RE, Liu J. 1997. Tissue polarity points from cells that have higher Frizzled levels towards cells that have lower Frizzled levels. *Current biology : CB* 7:940-9

Ahumada A, Slusarski DC, Liu X, Moon RT, Malbon CC, Wang HY. 2002. Signaling of rat Frizzled-2 through phosphodiesterase and cyclic GMP. *Science* 298:2006-10

Aittaleb M, Boguth CA, Tesmer JJ. 2010. Structure and function of heterotrimeric G protein-regulated Rho guanine nucleotide exchange factors. *Molecular pharmacology* 77:111-25

Antic D, Stubbs JL, Suyama K, Kintner C, Scott MP, Axelrod JD. 2010. Planar cell polarity enables posterior localization of nodal cilia and left-right axis determination during mouse and Xenopus embryogenesis. *PLoS One* 5:e8999

Arac D, Boucard AA, Bolliger MF, Nguyen J, Soltis SM, et al. 2012. A novel evolutionarily conserved domain of cell-adhesion GPCRs mediates autoproteolysis. *Embo J* 31:1364-78

Auman HJ, Yelon D. 2004. Vertebrate organogenesis: getting the heart into shape. *Current biology : CB* 14:R152-3

Axelrod JD. 2001. Unipolar membrane association of Dishevelled mediates Frizzled planar cell polarity signaling. *Genes Dev* 15:1182-7

Axelrod JD, Miller JR, Shulman JM, Moon RT, Perrimon N. 1998. Differential recruitment of Dishevelled provides signaling specificity in the planar cell polarity and Wingless signaling pathways. *Genes Dev* 12:2610-22

Babb SG, Marrs JA. 2004. E-cadherin regulates cell movements and tissue formation in early zebrafish embryos. *Dev Dyn* 230:263-77

Barrallo-Gimeno A, Nieto MA. 2005. The Snail genes as inducers of cell movement and survival: implications in development and cancer. *Development* 132:3151-61

Bastock R, Strutt H, Strutt D. 2003. Strabismus is asymmetrically localised and binds to Prickle and Dishevelled during Drosophila planar polarity patterning. *Development* 130:3007-14

Bedell VM, Wang Y, Campbell JM, Poshusta TL, Starker CG, et al. In vivo genome editing using a high-efficiency TALEN system. *Nature* 491:114-8

Bellipanni G, Varga M, Maegawa S, Imai Y, Kelly C, et al. 2006. Essential and opposing roles of zebrafish beta-catenins in the formation of dorsal axial structures and neurectoderm. *Development* 133:1299-309

Berghmans S, Murphey RD, Wienholds E, Neuberg D, Kutok JL, et al. 2005. tp53 mutant zebrafish develop malignant peripheral nerve sheath tumors. *Proc Natl Acad Sci U S A* 102:407-12

Bingham S, Higashijima S, Okamoto H, Chandrasekhar A. 2002. The Zebrafish trilobite gene is essential for tangential migration of branchiomotor neurons. *Dev Biol* 242:149-60

Bjarnadottir TK, Fredriksson R, Schioth HB. 2007. The adhesion GPCRs: a unique family of G protein-coupled receptors with important roles in both central and peripheral tissues. *Cell Mol Life Sci* 64:2104-19

Boldajipour B, Mahabaleshwar H, Kardash E, Reichman-Fried M, Blaser H, et al. 2008. Control of chemokine-guided cell migration by ligand sequestration. *Cell* 132:463-73

Borovina A, Superina S, Voskas D, Ciruna B. Vangl2 directs the posterior tilting and asymmetric localization of motile primary cilia. *Nat Cell Biol* 12:407-12

Boutros M, Mlodzik M. 1999. Dishevelled: at the crossroads of divergent intracellular signaling pathways. *Mechanisms of development* 83:27-37

Boutros M, Paricio N, Strutt DI, Mlodzik M. 1998. Dishevelled activates JNK and discriminates between JNK pathways in planar polarity and wingless signaling. *Cell* 94:109-18

Branford WW, Yost HJ. 2002. Lefty-dependent inhibition of Nodal- and Wnt-responsive organizer gene expression is essential for normal gastrulation. *Current biology : CB* 12:2136-41

Carmany-Rampey A, Schier AF. 2001. Single-cell internalization during zebrafish gastrulation. *Current biology : CB* 11:1261-5

Carreira-Barbosa F, Concha ML, Takeuchi M, Ueno N, Wilson SW, Tada M. 2003. Prickle 1 regulates cell movements during gastrulation and neuronal migration in zebrafish. *Development* 130:4037-46

Carreira-Barbosa F, Kajita M, Morel V, Wada H, Okamoto H, et al. 2009. Flamingo regulates epiboly and convergence/extension movements through cell cohesive and signalling functions during zebrafish gastrulation. *Development* 136:383-92

Cha YI, Kim SH, Sepich D, Buchanan FG, Solnica-Krezel L, DuBois RN. 2006. Cyclooxygenase-1-derived PGE2 promotes cell motility via the G-protein-coupled EP4 receptor during vertebrate gastrulation. *Genes Dev* 20:77-86

Chandrasekhar A. 2004. Turning heads: development of vertebrate branchiomotor neurons. *Developmental dynamics : an official publication of the American Association of Anatomists* 229:143-61

Chandrasekhar A, Moens CB, Warren JT, Jr., Kimmel CB, Kuwada JY. 1997. Development of branchiomotor neurons in zebrafish. *Development* 124:2633-44

Chen X, Gumbiner BM. 2006. Paraxial protocadherin mediates cell sorting and tissue morphogenesis by regulating C-cadherin adhesion activity. *J Cell Biol* 174:301-13

Chen Y, Schier AF. 2001. The zebrafish Nodal signal Squint functions as a morphogen. *Nature* 411:607-10

Chen Y, Schier AF. 2002. Lefty proteins are long-range inhibitors of squint-mediated nodal signaling. *Current biology : CB* 12:2124-8

Cheyette BN, Waxman JS, Miller JR, Takemaru K, Sheldahl LC, et al. 2002. Dapper, a Dishevelled-associated antagonist of beta-catenin and JNK signaling, is required for notochord formation. *Developmental cell* 2:449-61

Chiang EF, Pai CI, Wyatt M, Yan YL, Postlethwait J, Chung B. 2001. Two sox9 genes on duplicated zebrafish chromosomes: expression of similar transcription activators in distinct sites. *Dev Biol* 231:149-63

Choi SC, Han JK. 2002. Xenopus Cdc42 regulates convergent extension movements during gastrulation through Wnt/Ca2+ signaling pathway. *Dev Biol* 244:342-57

Ciruna B, Jenny A, Lee D, Mlodzik M, Schier AF. 2006. Planar cell polarity signalling couples cell division and morphogenesis during neurulation. *Nature* 439:220-4

Ciruna B, Rossant J. 2001. FGF signaling regulates mesoderm cell fate specification and morphogenetic movement at the primitive streak. *Developmental cell* 1:37-49

Cohen MM, Jr., Shiota K. 2002. Teratogenesis of holoprosencephaly. *Am J Med Genet* 109:1-15

Concha ML, Adams RJ. 1998. Oriented cell divisions and cellular morphogenesis in the zebrafish gastrula and neurula: a time-lapse analysis. *Development* 125:983-94

Couchman JR, Chen L, Woods A. 2001. Syndecans and cell adhesion. *International review of cytology* 207:113-50

Courbard JR, Djiane A, Wu J, Mlodzik M. 2009. The apical/basal-polarity determinant Scribble cooperates with the PCP core factor Stbm/Vang and functions as one of its effectors. *Dev Biol* 333:67-77

Cuppen E, Gerrits H, Pepers B, Wieringa B, Hendriks W. 1998. PDZ motifs in PTP-BL and RIL bind to internal protein segments in the LIM domain protein RIL. *Mol Biol Cell* 9:671-83

Curtin JA, Quint E, Tsipouri V, Arkell RM, Cattanach B, et al. 2003. Mutation of Celsr1 disrupts planar polarity of inner ear hair cells and causes severe neural tube defects in the mouse. *Curr Biol* 13:1129-33

Das G, Jenny A, Klein TJ, Eaton S, Mlodzik M. 2004. Diego interacts with Prickle and Strabismus/Van Gogh to localize planar cell polarity complexes. *Development* 131:4467-76

Davies B, Baumann C, Kirchhoff C, Ivell R, Nubbemeyer R, et al. 2004. Targeted deletion of the epididymal receptor HE6 results in fluid dysregulation and male infertility. *Mol Cell Biol* 24:8642-8

De Robertis EM. 2006. Spemann's organizer and self-regulation in amphibian embryos. *Nature reviews. Molecular cell biology* 7:296-302

De Robertis EM, Kuroda H. 2004. Dorsal-ventral patterning and neural induction in Xenopus embryos. *Annu Rev Cell Dev Biol* 20:285-308

de Wit J, Hong W, Luo L, Ghosh A. 2011. Role of leucine-rich repeat proteins in the development and function of neural circuits. *Annu Rev Cell Dev Biol* 27:697-729

Devreotes P, Janetopoulos C. 2003. Eukaryotic chemotaxis: distinctions between directional sensing and polarization. *The Journal of biological chemistry* 278:20445-8

Diz-Munoz A, Krieg M, Bergert M, Ibarlucea-Benitez I, Muller DJ, et al. 2010. Control of directed cell migration in vivo by membrane-to-cortex attachment. *PLoS Biol* 8:e1000544

Doitsidou M, Reichman-Fried M, Stebler J, Koprunner M, Dorries J, et al. 2002. Guidance of primordial germ cell migration by the chemokine SDF-1. *Cell* 111:647-59

Dong H, Zhang P, Song I, Petralia RS, Liao D, Huganir RL. 1999. Characterization of the glutamate receptor-interacting proteins GRIP1 and GRIP2. *The Journal of neuroscience : the official journal of the Society for Neuroscience* 19:6930-41

Doyle DA, Lee A, Lewis J, Kim E, Sheng M, MacKinnon R. 1996. Crystal structures of a complexed and peptide-free membrane protein-binding domain: molecular basis of peptide recognition by PDZ. *Cell* 85:1067-76

Eaton S, Wepf R, Simons K. 1996. Roles for Rac1 and Cdc42 in planar polarization and hair outgrowth in the wing of Drosophila. *The Journal of cell biology* 135:1277-89

Ebermann I, Phillips JB, Liebau MC, Koenekoop RK, Schermer B, et al. 2010. PDZD7 is a modifier of retinal disease and a contributor to digenic Usher syndrome. *J Clin Invest* 120:1812-23

Erter CE, Solnica-Krezel L, Wright CV. 1998. Zebrafish nodal-related 2 encodes an early mesendodermal inducer signaling from the extraembryonic yolk syncytial layer. *Dev Biol* 204:361-72

Erter CE, Wilm TP, Basler N, Wright CV, Solnica-Krezel L. 2001. Wnt8 is required in lateral mesendodermal precursors for neural posteriorization in vivo. *Development* 128:3571-83

Fanning AS, Anderson JM. 1998. PDZ domains and the formation of protein networks at the plasma membrane. *Curr Top Microbiol Immunol* 228:209-33

Fanning AS, Jameson BJ, Jesaitis LA, Anderson JM. 1998. The tight junction protein ZO-1 establishes a link between the transmembrane protein occludin and the actin cytoskeleton. *The Journal of biological chemistry* 273:29745-53

Feiguin F, Hannus M, Mlodzik M, Eaton S. 2001. The ankyrin repeat protein Diego mediates Frizzled-dependent planar polarization. *Developmental cell* 1:93-101

Feldman B, Concha ML, Saude L, Parsons MJ, Adams RJ, et al. 2002. Lefty antagonism of Squint is essential for normal gastrulation. *Current biology : CB* 12:2129-35

Feldman B, Dougan ST, Schier AF, Talbot WS. 2000. Nodal-related signals establish mesendodermal fate and trunk neural identity in zebrafish. *Current biology : CB* 10:531-4

Feldman B, Gates MA, Egan ES, Dougan ST, Rennebeck G, et al. 1998. Zebrafish organizer development and germ-layer formation require nodal-related signals. *Nature* 395:181-5

Formstone CJ, Mason I. 2005. Combinatorial activity of Flamingo proteins directs convergence and extension within the early zebrafish embryo via the planar cell polarity pathway. *Dev Biol* 282:320-35

Fouassier L, Yun CC, Fitz JG, Doctor RB. 2000. Evidence for ezrin-radixin-moesin-binding phosphoprotein 50 (EBP50) self-association through PDZ-PDZ interactions. *The Journal of biological chemistry* 275:25039-45

Fredriksson R, Lagerstrom MC, Hoglund PJ, Schioth HB. 2002. Novel human G protein-coupled receptors with long N-terminals containing GPS domains and Ser/Thr-rich regions. *FEBS Lett* 531:407-14

Fredriksson R, Lagerstrom MC, Lundin LG, Schioth HB. 2003. The G-protein-coupled receptors in the human genome form five main families. Phylogenetic analysis, paralogon groups, and fingerprints. *Mol Pharmacol* 63:1256-72

Fredriksson R, Schioth HB. 2005. The repertoire of G-protein-coupled receptors in fully sequenced genomes. *Mol Pharmacol* 67:1414-25

Gao C, Chen YG. Dishevelled: The hub of Wnt signaling. *Cell Signal* 22:717-27

Gilland E, Baker R. 2005. Evolutionary patterns of cranial nerve efferent nuclei in vertebrates. *Brain Behav Evol* 66:234-54

Glickman NS, Kimmel CB, Jones MA, Adams RJ. 2003. Shaping the zebrafish notochord. *Development* 130:873-87

Gloy J, Hikasa H, Sokol SY. 2002. Frodo interacts with Dishevelled to transduce Wnt signals. *Nat Cell Biol* 4:351-7

Gonzalez EM, Fekany-Lee K, Carmany-Rampey A, Erter C, Topczewski J, et al. 2000. Head and trunk in zebrafish arise via coinhibition of BMP signaling by bozozok and chordino. *Genes Dev* 14:3087-92

Goodrich LV, Strutt D. 2011. Principles of planar polarity in animal development. *Development* 138:1877-92

Goto T, Davidson L, Asashima M, Keller R. 2005. Planar cell polarity genes regulate polarized extracellular matrix deposition during frog gastrulation. *Current biology : CB* 15:787-93

Goto T, Keller R. 2002. The planar cell polarity gene strabismus regulates convergence and extension and neural fold closure in Xenopus. *Dev Biol* 247:165-81

Goutel C, Kishimoto Y, Schulte-Merker S, Rosa F. 2000. The ventralizing activity of Radar, a maternally expressed bone morphogenetic protein, reveals complex bone morphogenetic protein interactions controlling dorso-ventral patterning in zebrafish. *Mechanisms of development* 99:15-27

Graff JM, Thies RS, Song JJ, Celeste AJ, Melton DA. 1994. Studies with a Xenopus BMP receptor suggest that ventral mesoderm-inducing signals override dorsal signals in vivo. *Cell* 79:169-79

Gray RS, Roszko I, Solnica-Krezel L. 2011. Planar cell polarity: coordinating morphogenetic cell behaviors with embryonic polarity. *Developmental cell* 21:120-33

Green J. 1999. The animal cap assay. *Methods Mol Biol* 127:1-13

Gupte J, Swaminath G, Danao J, Tian H, Li Y, Wu X. 2012. Signaling property study of adhesion G-protein-coupled receptors. *FEBS Lett* 586:1214-9

Habas R, Dawid IB, He X. 2003. Coactivation of Rac and Rho by Wnt/Frizzled signaling is required for vertebrate gastrulation. *Genes Dev* 17:295-309

Habas R, Kato Y, He X. 2001. Wnt/Frizzled activation of Rho regulates vertebrate gastrulation and requires a novel Formin homology protein Daam1. *Cell* 107:843-54

Haitina T, Olsson F, Stephansson O, Alsio J, Roman E, et al. 2008. Expression profile of the entire family of Adhesion G protein-coupled receptors in mouse and rat. *BMC Neurosci* 9:43

Hall A, Nobes CD. 2000. Rho GTPases: molecular switches that control the organization and dynamics of the actin cytoskeleton. *Philos Trans R Soc Lond B Biol Sci* 355:965-70

Hamann J, Vogel B, van Schijndel GM, van Lier RA. 1996. The seven-span transmembrane receptor CD97 has a cellular ligand (CD55, DAF). *J Exp Med* 184:1185-9

Harmar AJ. 2001. Family-B G-protein-coupled receptors. *Genome Biol* 2:REVIEWS3013

Hartman MA, Finan D, Sivaramakrishnan S, Spudich JA. 2011. Principles of unconventional myosin function and targeting. *Annu Rev Cell Dev Biol* 27:133-55

Harumoto T, Ito M, Shimada Y, Kobayashi TJ, Ueda HR, et al. 2010. Atypical cadherins Dachsous and Fat control dynamics of noncentrosomal microtubules in planar cell polarity. *Developmental cell* 19:389-401

He X, Semenov M, Tamai K, Zeng X. 2004. LDL receptor-related proteins 5 and 6 in Wnt/beta-catenin signaling: arrows point the way. *Development* 131:1663-77

Heisenberg CP, Tada M, Rauch GJ, Saude L, Concha ML, et al. 2000. Silberblick/Wnt11 mediates convergent extension movements during zebrafish gastrulation. *Nature* 405:76-81

Hering H, Sheng M. 2002. Direct interaction of Frizzled-1, -2, -4, and -7 with PDZ domains of PSD-95. *FEBS Lett* 521:185-9

Higashijima S, Hotta Y, Okamoto H. 2000. Visualization of cranial motor neurons in live transgenic zebrafish expressing green fluorescent protein under the control of the islet-1 promoter/enhancer. *The Journal of neuroscience : the official journal of the Society for Neuroscience* 20:206-18

Homma S, Shimada T, Hikake T, Yaginuma H. 2008. Expression pattern of LRR and Ig domain-containing protein (LRRIG protein) in the early mouse embryo. *Gene Expr Patterns*

Hung AY, Sheng M. 2002. PDZ domains: structural modules for protein complex assembly. *The Journal of biological chemistry* 277:5699-702

Iguchi T, Sakata K, Yoshizaki K, Tago K, Mizuno N, Itoh H. 2008. Orphan G protein-coupled receptor GPR56 regulates neural progenitor cell migration via a G alpha 12/13 and Rho pathway. *J Biol Chem* 283:14469-78

Jenny A, Darken RS, Wilson PA, Mlodzik M. 2003a. Prickle and Strabismus form a functional complex to generate a correct axis during planar cell polarity signaling. *EMBO J* 22:4409-20

Jenny A, Darken RS, Wilson PA, Mlodzik M. 2003b. Prickle and Strabismus form a functional complex to generate a correct axis during planar cell polarity signaling. *Embo J* 22:4409-20

Jenny A, Reynolds-Kenneally J, Das G, Burnett M, Mlodzik M. 2005. Diego and Prickle regulate Frizzled planar cell polarity signalling by competing for Dishevelled binding. *Nat Cell Biol* 7:691-7

Jessen JR, Topczewski J, Bingham S, Sepich DS, Marlow F, et al. 2002. Zebrafish trilobite identifies new roles for Strabismus in gastrulation and neuronal movements. *Nat Cell Biol* 4:610-5

Jin Z, Tietjen I, Bu L, Liu-Yesucevitz L, Gaur SK, et al. 2007. Disease-associated mutations affect GPR56 protein trafficking and cell surface expression. *Hum Mol Genet* 16:1972-85

Jones CM, Lyons KM, Lapan PM, Wright CV, Hogan BL. 1992. DVR-4 (bone morphogenetic protein-4) as a posterior-ventralizing factor in Xenopus mesoderm induction. *Development* 115:639-47

Kai M, Heisenberg CP, Tada M. 2008. Sphingosine-1-phosphate receptors regulate individual cell behaviours underlying the directed migration of prechordal plate progenitor cells during zebrafish gastrulation. *Development* 135:3043-51

Kaibuchi K, Kuroda S, Amano M. 1999. Regulation of the cytoskeleton and cell adhesion by the Rho family GTPases in mammalian cells. *Annu Rev Biochem* 68:459-86

Kane DA, Hammerschmidt M, Mullins MC, Maischein HM, Brand M, et al. 1996. The zebrafish epiboly mutants. *Development* 123:47-55

Kane DA, McFarland KN, Warga RM. 2005. Mutations in half baked/E-cadherin block cell behaviors that are necessary for teleost epiboly. *Development* 132:1105-16

Katanaev VL, Ponzielli R, Semeriva M, Tomlinson A. 2005. Trimeric G protein-dependent frizzled signaling in Drosophila. *Cell* 120:111-22

Ke N, Ma H, Diedrich G, Chionis J, Liu G, et al. 2008. Biochemical characterization of genetic mutations of GPR56 in patients with bilateral frontoparietal polymicrogyria (BFPP). *Biochem Biophys Res Commun* 366:314-20

Keegan BR, Meyer D, Yelon D. 2004. Organization of cardiac chamber progenitors in the zebrafish blastula. *Development* 131:3081-91

Keller PJ, Schmidt AD, Wittbrodt J, Stelzer EH. 2008. Reconstruction of zebrafish early embryonic development by scanned light sheet microscopy. *Science* 322:1065-9

Keller R, Davidson L, Edlund A, Elul T, Ezin M, et al. 2000a. Mechanisms of convergence and extension by cell intercalation. *Philos Trans R Soc Lond B Biol Sci* 355:897-922

Keller R, Davidson L, Edlund A, Elul T, Ezin M, et al. 2000b. Mechanisms of convergence and extension by cell intercalation. *Philos Trans R Soc Lond B Biol Sci* 355:897-922

Kelly C, Chin AJ, Leatherman JL, Kozlowski DJ, Weinberg ES. 2000. Maternally controlled (beta)-catenin-mediated signaling is required for organizer formation in the zebrafish. *Development* 127:3899-911

Kelly GM, Erezyilmaz DF, Moon RT. 1995. Induction of a secondary embryonic axis in zebrafish occurs following the overexpression of beta-catenin. *Mechanisms of development* 53:261-73

Kilian B, Mansukoski H, Barbosa FC, Ulrich F, Tada M, Heisenberg CP. 2003. The role of Ppt/Wnt5 in regulating cell shape and movement during zebrafish gastrulation. *Mechanisms of development* 120:467-76

Kim HY, Davidson LA. 2011. Punctuated actin contractions during convergent extension and their permissive regulation by the non-canonical Wnt-signaling pathway. *J Cell Sci* 124:635-46

Kim SH, Yamamoto A, Bouwmeester T, Agius E, Robertis EM. 1998. The role of paraxial protocadherin in selective adhesion and cell movements of the mesoderm during Xenopus gastrulation. *Development* 125:4681-90

Kimmel CB, Ballard WW, Kimmel SR, Ullmann B, Schilling TF. 1995a. Stages of embryonic development of the zebrafish. *Dev Dyn* 203:253-310

Kimmel CB, Ballard WW, Kimmel SR, Ullmann B, Schilling TF. 1995b. Stages of embryonic development of the zebrafish. *Dev Dyn* 203:253-310

Kinoshita N, Iioka H, Miyakoshi A, Ueno N. 2003. PKC delta is essential for Dishevelled function in a noncanonical Wnt pathway that regulates Xenopus convergent extension movements. *Genes Dev* 17:1663-76

Klein TJ, Jenny A, Djiane A, Mlodzik M. 2006. CKIepsilon/discs overgrown promotes both Wnt-Fz/beta-catenin and Fz/PCP signaling in Drosophila. *Current biology : CB* 16:1337-43

Kraft B, Berger CD, Wallkamm V, Steinbeisser H, Wedlich D. 2012. Wnt-11 and Fz7 reduce cell adhesion in convergent extension by sequestration of PAPC and C-cadherin. *The Journal of cell biology* 198:695-709

Krasnoperov V, Lu Y, Buryanovsky L, Neubert TA, Ichtchenko K, Petrenko AG. 2002. LEC (CIRL)- Post-translational proteolytic processing of the calcium-independent receptor of alpha-latrotoxin (CIRL), a natural chimera of the cell adhesion protein and the G protein-coupled receptor. Role of the G protein-coupled receptor proteolysis site (GPS) motif. *J Biol Chem* 277:46518-26

Krasnow RE, Adler PN. 1994. A single frizzled protein has a dual function in tissue polarity. *Development* 120:1883-93

Krasnow RE, Wong LL, Adler PN. 1995. Dishevelled is a component of the frizzled signaling pathway in Drosophila. *Development* 121:4095-102

Kuhl M, Sheldahl LC, Malbon CC, Moon RT. 2000a. Ca(2+)/calmodulin-dependent protein kinase II is stimulated by Wnt and Frizzled homologs and promotes ventral cell fates in Xenopus. *The Journal of biological chemistry* 275:12701-11

Kuhl M, Sheldahl LC, Park M, Miller JR, Moon RT. 2000b. The Wnt/Ca2+ pathway: a new vertebrate Wnt signaling pathway takes shape. *Trends Genet* 16:279-83

Kuhnert F, Mancuso MR, Shamloo A, Wang HT, Choksi V, et al. Essential regulation of CNS angiogenesis by the orphan G protein-coupled receptor GPR124. *Science* 330:985-9

Kupperman E, An S, Osborne N, Waldron S, Stainier DY. 2000. A sphingosine-1-phosphate receptor regulates cell migration during vertebrate heart development. *Nature* 406:192-5

Kwakkenbos MJ, Chang GW, Lin HH, Pouwels W, de Jong EC, et al. 2002. The human EGF-TM7 family member EMR2 is a heterodimeric receptor expressed on myeloid cells. *J Leukoc Biol* 71:854-62

Langdon YG, Mullins MC. 2011. Maternal and zygotic control of zebrafish dorsoventral axial patterning. *Annual review of genetics* 45:357-77

Lee HJ, Zheng JJ. 2010. PDZ domains and their binding partners: structure, specificity, and modification. *Cell Commun Signal* 8:8

Lekven AC, Thorpe CJ, Waxman JS, Moon RT. 2001. Zebrafish wnt8 encodes two wnt8 proteins on a bicistronic transcript and is required for mesoderm and neurectoderm patterning. *Developmental cell* 1:103-14

Levin M. 2004. The embryonic origins of left-right asymmetry. *Crit Rev Oral Biol Med* 15:197-206

Li S, Jin Z, Koirala S, Bu L, Xu L, et al. 2008. GPR56 regulates pial basement membrane integrity and cortical lamination. *The Journal of neuroscience : the official journal of the Society for Neuroscience* 28:5817-26

Lin F, Chen S, Sepich DS, Panizzi JR, Clendenon SG, et al. 2009. Galpha12/13 regulate epiboly by inhibiting E-cadherin activity and modulating the actin cytoskeleton. *J Cell Biol* 184:909-21

Lin F, Chen S, Sepich DS, Panizzi JR, Clendenon SG, et al. 2008. Galpha12/13 regulate epiboy by inhibiting E-cadherin activity and modulating the actin cytoskeleton. *J Cell Biol*

Lin F, Sepich DS, Chen S, Topczewski J, Yin C, et al. 2005. Essential roles of G{alpha}12/13 signaling in distinct cell behaviors driving zebrafish convergence and extension gastrulation movements. *J Cell Biol* 169:777-87

Lin HH. 2012. Adhesion family of G protein-coupled receptors and cancer. *Chang Gung Med J* 35:15-27

Lin HH, Chang GW, Davies JQ, Stacey M, Harris J, Gordon S. 2004. Autocatalytic cleavage of the EMR2 receptor occurs at a conserved G protein-coupled receptor proteolytic site motif. *J Biol Chem* 279:31823-32

Lin HH, Stacey M, Saxby C, Knott V, Chaudhry Y, et al. 2001. Molecular analysis of the epidermal growth factor-like short consensus repeat domain-mediated protein-protein interactions: dissection of the CD97-CD55 complex. *The Journal of biological chemistry* 276:24160-9

Lin HH, Stacey M, Yona S, Chang GW. 2010. GPS proteolytic cleavage of adhesion-GPCRs. *Adv Exp Med Biol* 706:49-58

Lin S, Baye LM, Westfall TA, Slusarski DC. Wnt5b-Ryk pathway provides directional signals to regulate gastrulation movement. *J Cell Biol* 190:263-78

Link V, Shevchenko A, Heisenberg CP. 2006. Proteomics of early zebrafish embryos. *BMC Dev Biol* 6:1

Little SC, Mullins MC. 2006. Extracellular modulation of BMP activity in patterning the dorsoventral axis. *Birth Defects Res C Embryo Today* 78:224-42

Liu T, DeCostanzo AJ, Liu X, Wang H, Hallagan S, et al. 2001. G protein signaling from activated rat frizzled-1 to the beta-catenin-Lef-Tcf pathway. *Science* 292:1718-22

Liu T, Liu X, Wang H, Moon RT, Malbon CC. 1999a. Activation of rat frizzled-1 promotes Wnt signaling and differentiation of mouse F9 teratocarcinoma cells via pathways that require Galpha(q) and Galpha(o) function. *The Journal of biological chemistry* 274:33539-44

Liu X, Liu T, Slusarski DC, Yang-Snyder J, Malbon CC, et al. 1999b. Activation of a frizzled-2/beta-adrenergic receptor chimera promotes Wnt signaling and differentiation of mouse F9 teratocarcinoma cells via Galphao and Galphat. *Proc Natl Acad Sci U S A* 96:14383-8

Logan CY, Nusse R. 2004. The Wnt signaling pathway in development and disease. *Annu Rev Cell Dev Biol* 20:781-810

Lu FI, Thisse C, Thisse B. 2011. Identification and mechanism of regulation of the zebrafish dorsal determinant. *Proc Natl Acad Sci U S A* 108:15876-80

Luo R, Jeong SJ, Jin Z, Strokes N, Li S, Piao X. 2011. G protein-coupled receptor 56 and collagen III, a receptor-ligand pair, regulates cortical development and lamination. *Proc Natl Acad Sci U S A* 108:12925-30

Luo R, Jin Z, Deng Y, Strokes N, Piao X. 2012. Disease-associated mutations prevent GPR56-collagen III interaction. *PLoS One* 7:e29818

Macdonald BT, Semenov MV, He X. 2007. SnapShot: Wnt/beta-catenin signaling. *Cell* 131:1204

MacDonald BT, Tamai K, He X. 2009. Wnt/beta-catenin signaling: components, mechanisms, and diseases. *Developmental cell* 17:9-26

Maekawa K, Imagawa N, Naito A, Harada S, Yoshie O, Takagi S. 1999. Association of protein-tyrosine phosphatase PTP-BAS with the transcription-factor-inhibitory protein IkappaBalpha through interaction between the PDZ1 domain and ankyrin repeats. *Biochem J* 337 (Pt 2):179-84

Mapp OM, Walsh GS, Moens CB, Tada M, Prince VE. 2011. Zebrafish Prickle1b mediates facial branchiomotor neuron migration via a farnesylation-dependent nuclear activity. *Development* 138:2121-32

Marlow F, Topczewski J, Sepich D, Solnica-Krezel L. 2002. Zebrafish Rho kinase 2 acts downstream of Wnt11 to mediate cell polarity and effective convergence and extension movements. *Curr Biol* 12:876-84

Marlow F, Zwartkruis F, Malicki J, Neuhauss SC, Abbas L, et al. 1998. Functional interactions of genes mediating convergent extension, knypek and trilobite, during the partitioning of the eye primordium in zebrafish. *Dev Biol* 203:382-99

Marlow FL. 2010. In *Maternal Control of Development in Vertebrates: My Mother Made Me Do It!* San Rafael (CA)

Maudsley S, Zamah AM, Rahman N, Blitzer JT, Luttrell LM, et al. 2000. Platelet-derived growth factor receptor association with Na(+)/H(+) exchanger regulatory factor potentiates receptor activity. *Mol Cell Biol* 20:8352-63

McGee J, Goodyear RJ, McMillan DR, Stauffer EA, Holt JR, et al. 2006. 98-The very large G-protein-coupled receptor VLGR1: a component of the ankle link complex required for the normal development of auditory hair bundles. *J Neurosci* 26:6543-53

McNeill H. 2010. Planar cell polarity: keeping hairs straight is not so simple. *Cold Spring Harb Perspect Biol* 2:a003376

Michalski N, Michel V, Bahloul A, Lefevre G, Barral J, et al. 2007. Molecular characterization of the ankle-link complex in cochlear hair cells and its role in the hair bundle functioning. *The Journal of neuroscience : the official journal of the Society for Neuroscience* 27:6478-88

Miyagi C, Yamashita S, Ohba Y, Yoshizaki H, Matsuda M, Hirano T. 2004. STAT3 noncell-autonomously controls planar cell polarity during zebrafish convergence and extension. *J Cell Biol* 166:975-81

Moeller H, Jenny A, Schaeffer HJ, Schwarz-Romond T, Mlodzik M, et al. 2006. Diversin regulates heart formation and gastrulation movements in development. *Proc Natl Acad Sci U S A* 103:15900-5

Momoi A, Yoda H, Steinbeisser H, Fagotto F, Kondoh H, et al. 2003. Analysis of Wnt8 for neural posteriorizing factor by identifying Frizzled 8c and Frizzled 9 as functional receptors for Wnt8. *Mechanisms of development* 120:477-89

Monk KR, Naylor SG, Glenn TD, Mercurio S, Perlin JR, et al. 2009. A G protein-coupled receptor is essential for Schwann cells to initiate myelination. *Science* 325:1402-5

Monk KR, Oshima K, Jors S, Heller S, Talbot WS. 2011. Gpr126 is essential for peripheral nerve development and myelination in mammals. *Development* 138:2673-80

Montcouquiol M, Rachel RA, Lanford PJ, Copeland NG, Jenkins NA, Kelley MW. 2003. Identification of Vangl2 and Scrb1 as planar polarity genes in mammals. *Nature* 423:173-7

Montcouquiol M, Sans N, Huss D, Kach J, Dickman JD, et al. 2006. Asymmetric localization of Vangl2 and Fz3 indicate novel mechanisms for planar cell polarity in mammals. *The Journal of neuroscience : the official journal of the Society for Neuroscience* 26:5265-75

Montero JA, Carvalho L, Wilsch-Brauninger M, Kilian B, Mustafa C, Heisenberg CP. 2005. Shield formation at the onset of zebrafish gastrulation. *Development* 132:1187-98

Montero JA, Kilian B, Chan J, Bayliss PE, Heisenberg CP. 2003. Phosphoinositide 3-kinase is required for process outgrowth and cell polarization of gastrulating mesendodermal cells. *Current biology : CB* 13:1279-89

Moorman AF, Christoffels VM. 2003. Cardiac chamber formation: development, genes, and evolution. *Physiol Rev* 83:1223-67

Morais Cabral JH, Petosa C, Sutcliffe MJ, Raza S, Byron O, et al. 1996. Crystal structure of a PDZ domain. *Nature* 382:649-52

Moriguchi T, Haraguchi K, Ueda N, Okada M, Furuya T, Akiyama T. 2004. DREG, a developmentally regulated G protein-coupled receptor containing two conserved proteolytic cleavage sites. *Genes Cells* 9:549-60

Muller P, Rogers KW, Jordan BM, Lee JS, Robson D, et al. 2012. Differential diffusivity of Nodal and Lefty underlies a reaction-diffusion patterning system. *Science* 336:721-4

Munoz R, Moreno M, Oliva C, Orbenes C, Larrain J. 2006. Syndecan-4 regulates non-canonical Wnt signalling and is essential for convergent and extension movements in Xenopus embryos. *Nat Cell Biol* 8:492-500

Myers DC, Sepich DS, Solnica-Krezel L. 2002a. Bmp activity gradient regulates convergent extension during zebrafish gastrulation. *Dev Biol* 243:81-98

Myers DC, Sepich DS, Solnica-Krezel L. 2002b. Convergence and extension in vertebrate gastrulae: cell movements according to or in search of identity? *Trends Genet* 18:447-55

Nair S, Schilling TF. 2008. Chemokine signaling controls endodermal migration during zebrafish gastrulation. *Science* 322:89-92

Nishimura T, Honda H, Takeichi M. 2012. Planar cell polarity links axes of spatial dynamics in neural-tube closure. *Cell* 149:1084-97

Nojima H, Rothhamel S, Shimizu T, Kim CH, Yonemura S, et al. 2010. Syntabulin, a motor protein linker, controls dorsal determination. *Development* 137:923-33

Okajima D, Kudo G, Yokota H. 2010. Brain-specific angiogenesis inhibitor 2 (BAI2) may be activated by proteolytic processing. *J Recept Signal Transduct Res* 30:143-53

Oldham WM, Hamm HE. 2008. Heterotrimeric G protein activation by G-protein-coupled receptors. *Nat Rev Mol Cell Biol* 9:60-71

Overington JP, Al-Lazikani B, Hopkins AL. 2006. How many drug targets are there? *Nat Rev Drug Discov* 5:993-6

Paavola KJ, Hall RA. 2012. Adhesion g protein-coupled receptors: signaling, pharmacology, and mechanisms of activation. *Molecular pharmacology* 82:777-83

Pal K, Melcher K, Xu HE. 2012. Structure and mechanism for recognition of peptide hormones by Class B G-protein-coupled receptors. *Acta Pharmacol Sin* 33:300-11

Pan WJ, Pang SZ, Huang T, Guo HY, Wu D, Li L. 2004. Characterization of function of three domains in dishevelled-1: DEP domain is responsible for membrane translocation of dishevelled-1. *Cell Res* 14:324-30

Park M, Moon RT. 2002. The planar cell-polarity gene stbm regulates cell behaviour and cell fate in vertebrate embryos. *Nat Cell Biol* 4:20-5

Park TJ, Gray RS, Sato A, Habas R, Wallingford JB. 2005. Subcellular localization and signaling properties of dishevelled in developing vertebrate embryos. *Current biology : CB* 15:1039-44

Penton A, Wodarz A, Nusse R. 2002. A mutational analysis of dishevelled in Drosophila defines novel domains in the dishevelled protein as well as novel suppressing alleles of axin. *Genetics* 161:747-62

Pezeron G, Mourrain P, Courty S, Ghislain J, Becker TS, et al. 2008. Live analysis of endodermal layer formation identifies random walk as a novel gastrulation movement. *Current biology : CB* 18:276-81

Piao X, Hill RS, Bodell A, Chang BS, Basel-Vanagaite L, et al. 2004. G protein-coupled receptor-dependent development of human frontal cortex. *Science* 303:2033-6

Pickering C, Hagglund M, Szmydynger-Chodobska J, Marques F, Palha JA, et al. 2008. The Adhesion GPCR GPR125 is specifically expressed in the choroid plexus and is upregulated following brain injury. *BMC Neurosci* 9:97

Ponting CP, Hofmann K, Bork P. 1999. A latrophilin/CL-1-like GPS domain in polycystin-1. *Current biology : CB* 9:R585-8

Promel S, Frickenhaus M, Hughes S, Mestek L, Staunton D, et al. 2012. The GPS motif is a molecular switch for bimodal activities of adhesion class G protein-coupled receptors. *Cell Rep* 2:321-31

Ramel MC, Lekven AC. 2004. Repression of the vertebrate organizer by Wnt8 is mediated by Vent and Vox. *Development* 131:3991-4000

Reim G, Brand M. 2006. Maternal control of vertebrate dorsoventral axis formation and epiboly by the POU domain protein Spg/Pou2/Oct4. *Development* 133:2757-70

Reiners J, van Wijk E, Marker T, Zimmermann U, Jurgens K, et al. 2005. Scaffold protein harmonin (USH1C) provides molecular links between Usher syndrome type 1 and type 2. *Hum Mol Genet* 14:3933-43

Rescorla FJ. 2012. Pediatric germ cell tumors. *Semin Pediatr Surg* 21:51-60

Robu ME, Larson JD, Nasevicius A, Beiraghi S, Brenner C, et al. 2007. p53 activation by knockdown technologies. *PLoS Genet* 3:e78

Rohde LA, Heisenberg CP. 2007. Zebrafish gastrulation: cell movements, signals, and mechanisms. *Int Rev Cytol* 261:159-92

Rohrschneider MR, Elsen GE, Prince VE. 2007. Zebrafish Hoxb1a regulates multiple downstream genes including prickle1b. *Dev Biol* 309:358-72

Roszko I, Sawada A, Solnica-Krezel L. 2009. Regulation of convergence and extension movements during vertebrate gastrulation by the Wnt/PCP pathway. *Semin Cell Dev Biol* 20:986-97

Sadler TW. 2010. *Langman's medical embryology*: Lippincott William & Wilkins

Schambony A, Wedlich D. 2007. Wnt-5A/Ror2 regulate expression of XPAPC through an alternative noncanonical signaling pathway. *Developmental cell* 12:779-92

Schier AF, Talbot WS. 2005. Molecular genetics of axis formation in zebrafish. *Annu Rev Genet* 39:561-613

Schindelin J, Arganda-Carreras I, Frise E, Kaynig V, Longair M, et al. 2012. Fiji: an open-source platform for biological-image analysis. *Nat Methods* 9:676-82

Schneider S, Steinbeisser H, Warga RM, Hausen P. 1996. Beta-catenin translocation into nuclei demarcates the dorsalizing centers in frog and fish embryos. *Mechanisms of development* 57:191-8

Scott IC, Masri B, D'Amico LA, Jin SW, Jungblut B, et al. 2007. The g protein-coupled receptor agtrl1b regulates early development of myocardial progenitors. *Developmental cell* 12:403-13

Seandel M, James D, Shmelkov SV, Falciatori I, Kim J, et al. 2007. Generation of functional multipotent adult stem cells from GPR125+ germline progenitors. *Nature* 449:346-50

Sepich DS, Calmelet C, Kiskowski M, Solnica-Krezel L. 2005. Initiation of convergence and extension movements of lateral mesoderm during zebrafish gastrulation. *Developmental dynamics : an official publication of the American Association of Anatomists* 234:279-92

Sepich DS, Solnica-Krezel L. 2005. Analysis of cell movements in zebrafish embryos: morphometrics and measuring movement of labeled cell populations in vivo. *Methods Mol Biol* 294:211-33

Sepich DS, Usmani M, Pawlicki S, Solnica-Krezel L. 2011. Wnt/PCP signaling controls intracellular position of MTOCs during gastrulation convergence and extension movements. *Development* 138:543-52

Sheldahl LC, Slusarski DC, Pandur P, Miller JR, Kuhl M, Moon RT. 2003. Dishevelled activates Ca2+ flux, PKC, and CamKII in vertebrate embryos. *The Journal of cell biology* 161:769-77

Sheng M, Sala C. 2001. PDZ domains and the organization of supramolecular complexes. *Annual review of neuroscience* 24:1-29

Shima Y, Kawaguchi SY, Kosaka K, Nakayama M, Hoshino M, et al. 2007. Opposing roles in neurite growth control by two seven-pass transmembrane cadherins. *Nat Neurosci* 10:963-9

Shima Y, Kengaku M, Hirano T, Takeichi M, Uemura T. 2004. Regulation of dendritic maintenance and growth by a mammalian 7-pass transmembrane cadherin. *Developmental cell* 7:205-16

Shimada Y, Yonemura S, Ohkura H, Strutt D, Uemura T. 2006. Polarized transport of Frizzled along the planar microtubule arrays in Drosophila wing epithelium. *Developmental cell* 10:209-22

Shimizu T, Yabe T, Muraoka O, Yonemura S, Aramaki S, et al. 2005. E-cadherin is required for gastrulation cell movements in zebrafish. *Mech Dev* 122:747-63

Shiratsuchi T, Futamura M, Oda K, Nishimori H, Nakamura Y, Tokino T. 1998. Cloning and characterization of BAI-associated protein 1: a PDZ domain-containing protein that interacts with BAI1. *Biochemical and biophysical research communications* 247:597-604

Silva JP, Lelianova VG, Ermolyuk YS, Vysokov N, Hitchen PG, et al. 2011. Latrophilin 1 and its endogenous ligand Lasso/teneurin-2 form a high-affinity transsynaptic receptor pair with signaling capabilities. *Proc Natl Acad Sci U S A* 108:12113-8

Simons M, Gloy J, Ganner A, Bullerkotte A, Bashkurov M, et al. 2005. Inversin, the gene product mutated in nephronophthisis type II, functions as a molecular switch between Wnt signaling pathways. *Nat Genet* 37:537-43

Simons M, Mlodzik M. 2008. Planar cell polarity signaling: from fly development to human disease. *Annu Rev Genet* 42:517-40

Slusarski DC, Corces VG, Moon RT. 1997a. Interaction of Wnt and a Frizzled homologue triggers G-protein-linked phosphatidylinositol signalling. *Nature* 390:410-3

Slusarski DC, Yang-Snyder J, Busa WB, Moon RT. 1997b. Modulation of embryonic intracellular Ca2+ signaling by Wnt-5A. *Dev Biol* 182:114-20

Sokol SY. 1996. Analysis of Dishevelled signalling pathways during Xenopus development. *Current biology : CB* 6:1456-67

Solnica-Krezel L. 2005. Conserved patterns of cell movements during vertebrate gastrulation. *Current biology : CB* 15:R213-28

Solnica-Krezel L. 2006. Gastrulation in zebrafish -- all just about adhesion? *Curr Opin Genet Dev* 16:433-41

Solnica-Krezel L, Driever W. 1994. Microtubule arrays of the zebrafish yolk cell: organization and function during epiboly. *Development* 120:2443-55

Solnica-Krezel L, Stemple DL, Mountcastle-Shah E, Rangini Z, Neuhauss SC, et al. 1996. Mutations affecting cell fates and cellular rearrangements during gastrulation in zebrafish. *Development* 123:67-80

Song MR. 2007. Moving cell bodies: understanding the migratory mechanism of facial motor neurons. *Arch Pharm Res* 30:1273-82

Speirs CK, Jernigan KK, Kim SH, Cha YI, Lin F, et al. Prostaglandin Gbetagamma signaling stimulates gastrulation movements by limiting cell adhesion through Snai1a stabilization. *Development* 137:1327-37

Srivastava S, Osten P, Vilim FS, Khatri L, Inman G, et al. 1998. Novel anchorage of GluR2/3 to the postsynaptic density by the AMPA receptor-binding protein ABP. *Neuron* 21:581-91

Stacey M, Chang GW, Davies JQ, Kwakkenbos MJ, Sanderson RD, et al. 2003. The epidermal growth factor-like domains of the human EMR2 receptor mediate cell attachment through chondroitin sulfate glycosaminoglycans. *Blood* 102:2916-24

Stacey M, Chang GW, Sanos SL, Chittenden LR, Stubbs L, et al. 2002. EMR4, a novel epidermal growth factor (EGF)-TM7 molecule up-regulated in activated mouse macrophages, binds to a putative cellular ligand on B lymphoma cell line A20. *J Biol Chem* 277:29283-93

Stiffler MA, Chen JR, Grantcharova VP, Lei Y, Fuchs D, et al. 2007. PDZ domain binding selectivity is optimized across the mouse proteome. *Science* 317:364-9

Stockinger P, Maitre JL, Heisenberg CP. 2011. Defective neuroepithelial cell cohesion affects tangential branchiomotor neuron migration in the zebrafish neural tube. *Development* 138:4673-83

Strutt D. 2003. Frizzled signalling and cell polarisation in Drosophila and vertebrates. *Development* 130:4501-13

Strutt D, Johnson R, Cooper K, Bray S. 2002. Asymmetric localization of frizzled and the determination of notch-dependent cell fate in the Drosophila eye. *Current biology : CB* 12:813-24

Strutt DI. 2001. Asymmetric localization of frizzled and the establishment of cell polarity in the Drosophila wing. *Mol Cell* 7:367-75

Strutt DI, Weber U, Mlodzik M. 1997. The role of RhoA in tissue polarity and Frizzled signalling. *Nature* 387:292-5

Strutt H, Strutt D. 2008. Differential stability of flamingo protein complexes underlies the establishment of planar polarity. *Current biology : CB* 18:1555-64

Strutt H, Warrington SJ, Strutt D. 2011. Dynamics of core planar polarity protein turnover and stable assembly into discrete membrane subdomains. *Developmental cell* 20:511-25

Studer M. 2001. Initiation of facial motoneurone migration is dependent on rhombomeres 5 and 6. *Development* 128:3707-16

Sugimura R, He XC, Venkatraman A, Arai F, Box A, et al. 2012. Noncanonical Wnt signaling maintains hematopoietic stem cells in the niche. *Cell* 150:351-65

Sun JP, Li R, Ren HZ, Xu AT, Yu X, Xu ZG. 2012. The Very Large G Protein Coupled Receptor (Vlgr1) in Hair Cells. *J Mol Neurosci*

Tada M, Kai M. 2009. Noncanonical Wnt/PCP signaling during vertebrate gastrulation. *Zebrafish* 6:29-40

Tada M, Smith JC. 2000. Xwnt11 is a target of Xenopus Brachyury: regulation of gastrulation movements via Dishevelled, but not through the canonical Wnt pathway. *Development* 127:2227-38

Tamai K, Semenov M, Kato Y, Spokony R, Liu C, et al. 2000. LDL-receptor-related proteins in Wnt signal transduction. *Nature* 407:530-5

Tang XL, Wang Y, Li DL, Luo J, Liu MY. 2012. Orphan G protein-coupled receptors (GPCRs): biological functions and potential drug targets. *Acta Pharmacol Sin* 33:363-71

Teran E, Branscomb AD, Seeling JM. 2009. Dpr Acts as a molecular switch, inhibiting Wnt signaling when unphosphorylated, but promoting Wnt signaling when phosphorylated by casein kinase Idelta/epsilon. *PLoS One* 4:e5522

Tissir F, Bar I, Jossin Y, De Backer O, Goffinet AM. 2005. Protocadherin Celsr3 is crucial in axonal tract development. *Nat Neurosci* 8:451-7

Tonikian R, Zhang Y, Sazinsky SL, Currell B, Yeh JH, et al. 2008. A specificity map for the PDZ domain family. *PLoS Biol* 6:e239

Topczewski J, Sepich DS, Myers DC, Walker C, Amores A, et al. 2001. The zebrafish glypican knypek controls cell polarity during gastrulation movements of convergent extension. *Developmental cell* 1:251-64

Tree DR, Shulman JM, Rousset R, Scott MP, Gubb D, Axelrod JD. 2002. Prickle mediates feedback amplification to generate asymmetric planar cell polarity signaling. *Cell* 109:371-81

Tucker JA, Mintzer KA, Mullins MC. 2008. The BMP signaling gradient patterns dorsoventral tissues in a temporally progressive manner along the anteroposterior axis. *Developmental cell* 14:108-19

Ulrich F, Concha ML, Heid PJ, Voss E, Witzel S, et al. 2003. Slb/Wnt11 controls hypoblast cell migration and morphogenesis at the onset of zebrafish gastrulation. *Development* 130:5375-84

Umbhauer M, Djiane A, Goisset C, Penzo-Mendez A, Riou JF, et al. 2000. The C-terminal cytoplasmic Lys-thr-X-X-X-Trp motif in frizzled receptors mediates Wnt/beta-catenin signalling. *Embo J* 19:4944-54

Usui T, Shima Y, Shimada Y, Hirano S, Burgess RW, et al. 1999. Flamingo, a seven-pass transmembrane cadherin, regulates planar cell polarity under the control of Frizzled. *Cell* 98:585-95

Van Aelst L, Symons M. 2002. Role of Rho family GTPases in epithelial morphogenesis. *Genes Dev* 16:1032-54

van Wijk E, van der Zwaag B, Peters T, Zimmermann U, Te Brinke H, et al. 2006. The DFNB31 gene product whirlin connects to the Usher protein network in the cochlea and retina by direct association with USH2A and VLGR1. *Hum Mol Genet* 15:751-65

Villefranc JA, Amigo J, Lawson ND. 2007. Gateway compatible vectors for analysis of gene function in the zebrafish. *Developmental dynamics : an official publication of the American Association of Anatomists* 236:3077-87

von der Hardt S, Bakkers J, Inbal A, Carvalho L, Solnica-Krezel L, et al. 2007. The Bmp gradient of the zebrafish gastrula guides migrating lateral cells by regulating cell-cell adhesion. *Curr Biol* 17:475-87

Wada H, Iwasaki M, Sato T, Masai I, Nishiwaki Y, et al. 2005. Dual roles of zygotic and maternal Scribble1 in neural migration and convergent extension movements in zebrafish embryos. *Development* 132:2273-85

Wada H, Okamoto H. 2009. Roles of noncanonical Wnt/PCP pathway genes in neuronal migration and neurulation in zebrafish. *Zebrafish* 6:3-8

Wada H, Tanaka H, Nakayama S, Iwasaki M, Okamoto H. 2006. Frizzled3a and Celsr2 function in the neuroepithelium to regulate migration of facial motor neurons in the developing zebrafish hindbrain. *Development* 133:4749-59

Wallingford JB, Rowning BA, Vogeli KM, Rothbacher U, Fraser SE, Harland RM. 2000. Dishevelled controls cell polarity during Xenopus gastrulation. *Nature* 405:81-5

Walsh GS, Grant PK, Morgan JA, Moens CB. 2011. Planar polarity pathway and Nance-Horan syndrome-like 1b have essential cell-autonomous functions in neuronal migration. *Development* 138:3033-42

Warga RM, Kimmel CB. 1990. Cell movements during epiboly and gastrulation in zebrafish. *Development* 108:569-80

Weiser DC, Pyati UJ, Kimelman D. 2007. Gravin regulates mesodermal cell behavior changes required for axis elongation during zebrafish gastrulation. *Genes Dev* 21:1559-71

Westerfield M. 2000. *The zebrafish book. A guide for the laboratory use of zebrafish (Danio rerio)*. Eugene: Univ. of Oregon Press

Weston MD, Luijendijk MW, Humphrey KD, Moller C, Kimberling WJ. 2004. Mutations in the VLGR1 gene implicate G-protein signaling in the pathogenesis of Usher syndrome type II. *Am J Hum Genet* 74:357-66

Winklbauer R, Medina A, Swain RK, Steinbeisser H. 2001. Frizzled-7 signalling controls tissue separation during Xenopus gastrulation. *Nature* 413:856-60

Winter CG, Wang B, Ballew A, Royou A, Karess R, et al. 2001. Drosophila Rho-associated kinase (Drok) links Frizzled-mediated planar cell polarity signaling to the actin cytoskeleton. *Cell* 105:81-91

Witzel S, Zimyanin V, Carreira-Barbosa F, Tada M, Heisenberg CP. 2006. Wnt11 controls cell contact persistence by local accumulation of Frizzled 7 at the plasma membrane. *J Cell Biol* 175:791-802

Wong HC, Bourdelas A, Krauss A, Lee HJ, Shao Y, et al. 2003. Direct binding of the PDZ domain of Dishevelled to a conserved internal sequence in the C-terminal region of Frizzled. *Mol Cell* 12:1251-60

Woo K, Fraser SE. 1997. Specification of the zebrafish nervous system by nonaxial signals. *Science* 277:254-7

Xia H, Winokur ST, Kuo WL, Altherr MR, Bredt DS. 1997. Actinin-associated LIM protein: identification of a domain interaction between PDZ and spectrin-like repeat motifs. *The Journal of cell biology* 139:507-15

Xu XZ, Choudhury A, Li X, Montell C. 1998. Coordination of an array of signaling proteins through homo- and heteromeric interactions between PDZ domains and target proteins. *The Journal of cell biology* 142:545-55

Yamamoto Y, Irie K, Asada M, Mino A, Mandai K, Takai Y. 2004. Direct binding of the human homologue of the Drosophila disc large tumor suppressor gene to

seven-pass transmembrane proteins, tumor endothelial marker 5 (TEM5), and a novel TEM5-like protein. *Oncogene* 23:3889-97

Yamanaka H, Moriguchi T, Masuyama N, Kusakabe M, Hanafusa H, et al. 2002. JNK functions in the non-canonical Wnt pathway to regulate convergent extension movements in vertebrates. *EMBO Rep* 3:69-75

Yamashita S, Miyagi C, Carmany-Rampey A, Shimizu T, Fujii R, et al. 2002. Stat3 Controls Cell Movements during Zebrafish Gastrulation. *Dev Cell* 2:363-75

Yamashita S, Miyagi C, Fukada T, Kagara N, Che YS, Hirano T. 2004. Zinc transporter LIVI controls epithelial-mesenchymal transition in zebrafish gastrula organizer. *Nature* 429:298-302

Yan YL, Miller CT, Nissen RM, Singer A, Liu D, et al. 2002. A zebrafish sox9 gene required for cartilage morphogenesis. *Development* 129:5065-79

Yan YL, Willoughby J, Liu D, Crump JG, Wilson C, et al. 2005. A pair of Sox: distinct and overlapping functions of zebrafish sox9 co-orthologs in craniofacial and pectoral fin development. *Development* 132:1069-83

Yanagawa S, van Leeuwen F, Wodarz A, Klingensmith J, Nusse R. 1995. The dishevelled protein is modified by wingless signaling in Drosophila. *Genes Dev* 9:1087-97

Yang X, Dormann D, Munsterberg AE, Weijer CJ. 2002. Cell movement patterns during gastrulation in the chick are controlled by positive and negative chemotaxis mediated by FGF4 and FGF8. *Developmental cell* 3:425-37

Yelon D, Horne SA, Stainier DY. 1999. Restricted expression of cardiac myosin genes reveals regulated aspects of heart tube assembly in zebrafish. *Dev Biol* 214:23-37

Yin C, Ciruna B, Solnica-Krezel L. 2009. Convergence and extension movements during vertebrate gastrulation. *Curr Top Dev Biol* 89:163-92

Yin C, Kiskowski M, Pouille PA, Farge E, Solnica-Krezel L. 2008. Cooperation of polarized cell intercalations drives convergence and extension of presomitic mesoderm during zebrafish gastrulation. *J Cell Biol* 180:221-32

Yona S, Lin HH, Siu WO, Gordon S, Stacey M. 2008. Adhesion-GPCRs: emerging roles for novel receptors. *Trends Biochem Sci*

Yu S, Hackmann K, Gao J, He X, Piontek K, et al. 2007. Essential role of cleavage of Polycystin-1 at G protein-coupled receptor proteolytic site for kidney tubular structure. *Proc Natl Acad Sci U S A* 104:18688-93

Zeidler MP, Perrimon N, Strutt DI. 1999. Polarity determination in the Drosophila eye: a novel role for unpaired and JAK/STAT signaling. *Genes Dev* 13:1342-53

Zeng XX, Wilm TP, Sepich DS, Solnica-Krezel L. 2007. Apelin and its receptor control heart field formation during zebrafish gastrulation. *Dev Cell* 12:391-402

Zhu S, Liu L, Korzh V, Gong Z, Low BC. 2006. RhoA acts downstream of Wnt5 and Wnt11 to regulate convergence and extension movements by involving effectors Rho kinase and Diaphanous: use of zebrafish as an in vivo model for GTPase signaling. *Cellular signalling* 18:359-72